University of Strathclyde
Department of Naval Architecture, Ocean and Marine Engineering

Solidification and Storage of Carbon Captured on Ships (CCS)

By

Haibin Wang

A thesis presented in fulfilment of the requirements
for the degree of Doctor of Philosophy

25 January 2017

To my parents

ABSTRACT

In order to meet the IMO's (International Maritime Organisation) target of 14% reduction of CO_2 emissions from marine activities by 2020, the application of Carbon Capture and Storage (CCS) on ships is considered as an effective way to mitigate the CO_2 emission while other low carbon shipping emission technologies are being developed. A comprehensive literature review of onshore CCS applications has indicated that current CCS technologies could not be implemented on-board directly due to the various limitations of ships, such as constraint space and system retrofit. In this thesis, a novel method of chemical CO_2 absorption and solidification for marine applications is analysed and presented. Technical feasibility and cost assessment of this method are carried out by comparison with the conventional method (liquefaction) for a case study ship. The thesis will also present results obtained from laboratory-scale experiments. Theoretical study and lab-scale experiments have shown that the proposed CO_2 absorption and solidification method is a promising, cost-effective and practicable method for CO_2 emissions reduction on ships.

Carbon capture and storage is an excellent solution for reducing the greenhouse gas emissions from applications on shore. A novel method to absorb and solidify CO_2 from the exhaust gases on the ship is proposed and verified. CO_2 gas flow rate, the geometry of the absorption tanks and the concentration of the absorption solution are key factors that affect the reaction efficiency. The experimental results illustrate the impacts of these factors on CO_2 absorption efficiency. Meanwhile, the effects of these key factors on CO_2 absorption rates will also be presented in the CFD simulations of this thesis. Pressure distributions, the concentration of the solution and the velocity of both the gas and the solution during the different processes will be derived from the numerical simulations. The results of the simulations provide fundamental details for the design of a prototype demonstration system on-board a ship. In addition to the key factors discussed above, the effect of atmospheric temperature will be observed and analysed. With a comparison of experimental data and CFD simulation results, it will be demonstrated that the CFD simulations of the effects of

CO_2 gas flow rate, the geometry of the absorption container and the concentration of the absorption solution on absorption rate have a good agreement with the experimental results. Optimised values of these factors are obtained from the comparisons and analyses. The numerical simulations will carried out to test the impact of phase temperature on absorption rate also indicate the optimal temperature for carrying out the absorption process.

As the simulation results match with the experimental results, the simulation model developed is considered to be applicable for a case study ship practical system simulation. Geometry, fluid flow rate, temperature and some other parameters are adjusted to fit a practical system. At this stage, the practical system is designed and the most appropriate absorption process is selected. The designated system is modelled and simulated based on the simulation processes from the lab-scale experiments. The orthogonal design method is applied to optimise the system. Key parameters are varied within a reasonable range so that a large number of trials are initially needed to find the optimal one. With the orthogonal design method, the number of trials is reduced so that computing intensity is reduced and finally the optimised absorption system is derived. The volume required for the precipitation tanks, CaO and $CaCO_3$ storage tanks and the centrifuge separation are derived and the installation and positioning of these tanks, as well as the positioning of the whole system, will be presented.

It is concluded that CCS for marine activities could enable ships to comply with various regional and international CO_2 emissions regulation whilst also maintaining the efficiency of waterborne transportation. The whole design process for the case study ship is presented here and could be applied as a guideline process for new design, analysis and installation.

ACKNOWLEDGMENT

First of all, I would like to thank Professor Peilin Zhou for his supervision and advice. He is one of the most important people who has changed my life. I would not have had this opportunity to pursue my study abroad without his help and guidance. Throughout my entire overseas studies, he has constantly provided me support and invaluable advice on course study, project research and on completing this thesis. He is not just a supervisor who has inspired my research life but also an indeed friend who taught me to enjoy my life abroad. I am full of respect for his expertise, friendliness, patience and modesty and I view him as a person who is a notable professor with vast knowledge, extraordinary character and personality.

Unique thanks are also in order to the administrative team at the Department of Naval Architecture, Ocean and Marine Engineering, with special mention to Mrs Thelma Will and Mrs Carol Georges, for their never-ending assistance and encouragement throughout the different stages of the academic course. I also need to thank my colleagues who have created such a warm atmosphere in the research centre.

The author also wishes to thank the Scottish Environment Network and also ARCHIE-WeST for their support with facilities which made it possible to finish this thesis on time.

This work is dedicated to my family without whom I could not have endured the hardest time of my research. I'm grateful for their understanding, tolerance and encouragement throughout my entire PhD research life.

CONTENTS

LIST OF FIGURES

LIST OF TABLES

ABBREVIATIONS

CCS	Carbon Capture and Storage
CFD	Computing Fluid Dynamic
CPCS	Chemical Processes for Carbon Solidification
D	Diameter
DWT	Deadweight Tonnage
EEDI	Energy Efficiency Design Index
EEOI	Energy Efficiency Operational Indicator
EIGA	European Industrial Gases Association
EOR	Enhanced Oil Recovery
GHG	Greenhouse Gases
H	Height
HSFO	High Sulphur Fuel Oil
ICP	Inductively Coupled Plasma
IMO	International Maritime Organization
IPC	Inductively Coupled Plasma
IPCC	Intergovernmental Panel on Climate Change
ITTC	International Towing Tank Conference

L	Litre
LBP	Length between Perpendiculars
LOA	Length Overall
L/min	Litre per Minute
MCR	Maximum Continuous Rating
SEEMP	Ship Energy Efficiency Management Plan
SFOC	Specific Fuel Oil Consumption
M	Molar mass
m	Mass
mole	Mole number
n	Molar number
P	Power
p	Pressure
ppm	Parts per million
R	Rate
T	Temperature
t	Time
V	Volume

Chemical substances

$Ca(OH)_2$	Calcium hydroxide
$CaCO_3$	Calcium carbonate
CaO	Calcium oxide
CO_2	Carbon dioxide
CO_3^{2-}	Carbonate ion
H_2O	Water
Na_2CO_3	Sodium carbonate
NaOH	Sodium hydroxide
NOx	Nitrous oxides
SOx	Sulphur oxides

Atomic and molar weight

Carbon (C)	12
Hydrogen (H)	1
Oxygen (O)	16
Sodium (Na)	23
Calcium (Ca)	40

$Ca(OH)_2$	74
$CaCO_3$	100
CaO	56
CO_2	44
H_2O	18
Na_2CO_3	106
NaOH	40

Symbols

π	pi
∇	Divergence (vector operator)
∆	Difference
×	Cross product
·	Dot product; scalar product
∧	Unit vector
→	Vector
∑	Sum

CHAPTER 1. INTRODUCTION

1.1. Background and Problem Description

The developments of the global economy have been considerable from the beginning of the Industrial Revolution in Great Britain. It drove not only the country itself but also the entire world to move forwards significantly. From then on, many significant inventions and improvements have emerged which have definitely all had positive effects which have lead the world further towards industrialisation and mechanisation. Since the enormous development in industrial production processes and the global economy, we have become more and more concerned about our living conditions on the planet. This is simply because the side effects (global warming, acid rain etc.) which come along with these developments are significant and are also undeniable, even though the world has greatly changed and advanced. Some changes, like deforesting for industrial utilities, the enormous usage of fossil fuels for power generation, and the emerging and ever growing number of different kinds of vehicles have indeed had a terrible influence on our planet. Due to years of accumulation and disregard for these side effects, the living environment on this planet is being damaged and the consequences are becoming serious.

Nowadays, constructing a more sustainable and "green" world alongside continued economic development has become a global goal. Fortunately, far-sighted researchers have already been considering the possible ways to alleviate the consequences of these side effects. One significant consequence of these side effects, which has already affected our living, is global climate change, also known as global warming. Climate change is one of the most important subjects of this century. Ice caps melting, sea levels rising and the risk of species extinction are extremely harmful results of global warming. The cause of climate change is the huge amounts of greenhouse gases (GHG), including water vapour, carbon dioxide, methane, nitrous oxide, and ozone, which are generated by human activities and emitted into the atmosphere (Houghton, 2004). The greenhouse effects caused by these

GHG's can help prevent heat from radiating into outer space so that the earth is kept warm enough for creatures to survive the cold dark night without sunlight (Greenhouse effect, National Geographic). However, with the growing global economy, large amounts of fossil fuels are being consumed due to energy requirements. As a cumulative result of continuing to burn fossil fuels, the emissions of GHG's (mainly carbon dioxide) are greatly increased. Due to the increase of CO_2 in the atmosphere, the greenhouse effect has been amplified and more radiated heat is reserved than before the Industrial Revolution, leading to an increase in temperature and eventually resulting in global warming.

The IMO is aiming to reduce the emission of CO_2 from marine activities by 14% by the year 2020. According to a report from the IMO, international shipping was estimated to have contributed about 2.2% to the global emissions of CO_2 in 2012 (Third IMO GHG study, 2014). Shipping is still however the most efficient transportation method in terms of carbon emissions per tonne of goods transported. The IMO introduced regulations to increase the energy efficiency of ships so that lower emissions could be achieved for the same transporting load. However, further emissions control is always required to slow down the pace of global warming. Carbon capture and storage (CCS) is a technique which captures the carbon emitted from the use of fossil fuels and transports it to a storage site. There are several active projects applying onshore CCS for power plants and industrial processes (Global CCS Institute 2012). The inspiration for this project is from these onshore applications as they can achieve a high reduction in carbon emissions. Unfortunately, these methods cannot be installed on-board ships directly because of the limitations of ships, such as power demand, constrained volume, and so on. With all these considerations, the objective of this project is to find a reasonable and practical solution for ship carbon emissions control.

1.2. Research Objectives

Considerations and subsequent actions on the mitigation of the global warming effect should be made as soon as possible, in order to prevent the living conditions on our planet from becoming even worse than they already have due to climate change. Otherwise, without control and management, there might be no place to stand on the earth due to the rising of sea levels and we human beings might eventually face the possibility of extinction. Now, more attention and energy should be paid to mitigating the side effects of rapid development, especially climate change. In order to sustain the environment and indeed the world, more and more research and development should be made and the mitigation of the global warming effect will be a great contributor and one of the most significant solutions.

Nowadays, a considerable number of methods for climate change mitigation are under research and development. Energy saving through improving energy efficiency and emissions reduction, especially of GHG's, are the mainstream of climate change mitigation methods. As a matter of fact, even saving every single piece of paper are helpful and meaningful to the abatement of the impact on the climate as deforestation will be slow down, which also has an impact on CO_2 absorption. However, it is even more difficult to bring temperature levels back to the pre-industrial level so any possible helpful methods should be considered, regardless of whether they are already under research or have already been applied.

According to Figure 1-1, CO_2 makes the most of contribution to climate change among all GHGs. This is simply because fossil fuel consumption is considerable. According to a report from the Intergovernmental Panel on Climate Change (IPCC, 2007), the CO_2 in the atmosphere has increased by 100 parts per million (ppm) compared with pre-industrial levels. It may also have terrible effects on food production and economic development as a result of global warming. Therefore, a feasible method for mitigating the emission of CO_2 is urgent. Carbon capture and storage (CCS) is one of the reasonable and feasible methods

under consideration, which has lately and widely been applied in onshore power plants and industrial processes and a particular literature review will be shown in this thesis. CCS could capture the carbon content from the use of the fossil fuels and transport the captured carbon for storage. Usually, separation methods are applied for the capture processes. Pipeline transportation is a preferred method for carbon transportation and enhanced oil recovery (EOR) is applied for CO_2 storage. EOR was developed and applied for oil recovery and now also helps on carbon storage.

As climate change should be considered and treated in great detail and scope, impacts from marine activities should be considered as well, which will be greatly beneficial for the mitigation of climate change. However, there are many factors that should be considered when focusing on the control of maritime GHG emissions. This thesis will present a CCS review as well as the possibilities and obstacles of CCS as applied on ships. One of the objective is to achieve GHG emissions reduction on ships using a feasible and practical method and with few impacts on overall transportation performance. This thesis aims to make a contribution towards capture technology research and development for marine vessels. This research also aims to evaluate the feasibility of maritime CCS through laboratory experiment and numerical simulations.

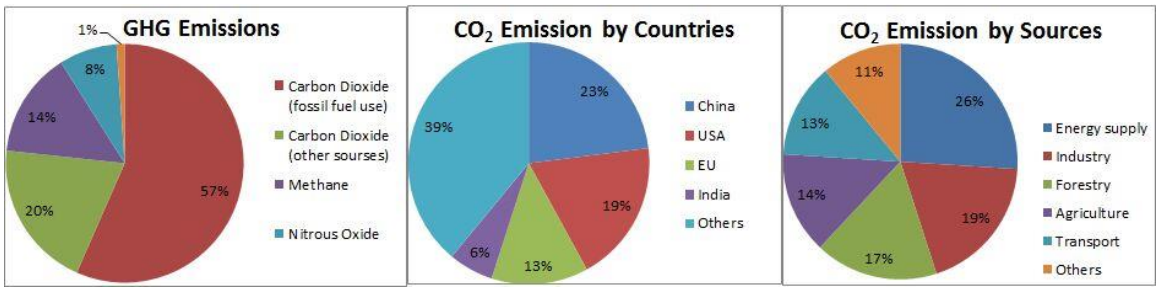

A B C

Figure 1-1 GHG emissions by gas type, countries and sources.
Data source: Carbon Dioxide Information Analysis Centre (Boden et al., 2010)

1.3. Outline of the Thesis

- Chapter 2 presents a review of literature in the field of climate change mitigation. The current situation regarding CO_2 and future predictions are illustrated. Literature reviews on carbon capture and storage are given in this chapter. This chapter also indicates the current situation in maritime CCS applications. Finally, literature reviews on CFD modelling and simulation are carried out.
- Chapter 3 proposes a novel carbon emissions reduction method for ships and describes the capture and storage processes. Some safety issues of handling chemicals are also illustrated.
- Chapter 4 gives a list of experimental apparatus and also the setup of the experimental rigs used. Chemical materials and experimental processes are introduced in this chapter. Experimental data will be presented in this part as well as the error and accuracy analysis.
- CFD simulations of the absorption process are achieved and shown in Chapter 5. The methodology using the simulation software, and the modelling and simulation processes are introduced. The comparisons of experimental and simulation results are also presented in this chapter.
- In Chapter 6, with the experimental results from the previous chapter, a case study is carried out on a ship to prove the economic feasibility of the proposed method. A suitable case study ship is selected and a comparison of economic effectiveness between the proposed chemical method and a known liquefaction method is also presented for this selected ship. Chapter 6 also illustrates an extensive simulation of the model presented in the previous chapter for a practical system. A case study ship is presented including vessel modelling, system design, tank design and positioning on a selected ship.
- Conclusions of this study and recommendations for further research are given in Chapter 7.

In order to indicate the relationships between chapters, a flow chart is presented in the following Figure 1-2.

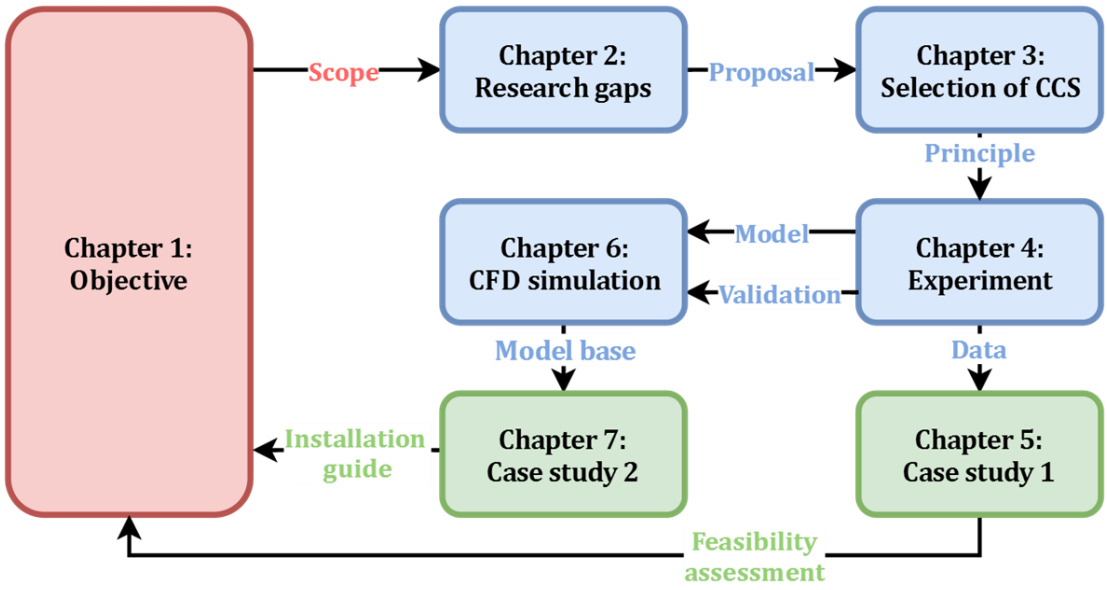

Figure 1-2 Interconnections between chapters.

1.4. Innovation and Contribution

Carbon capture and storage technology has been an effective option for CO_2 emissions reduction mainly for power plants and industrial processes. This thesis indicates that CCS is able to help maritime activities reduce their carbon emissions, specifically from ship engine exhausts. The feasibilities of CCS for ships are verified from two different angles: experimental scale tests and practical installations.

Together with a case study on economic feasibility assessment, the proposed method is verified to be suitable for carbon emission absorption on ships. The following are the most significant developments described and presented in the experimental part:

- A feasible method for solidifying carbon dioxide captured from marine engine exhaust gas for easy, safe and economical storage on-board ship is proposed.
- A series of laboratory experiments is carried out to examine the feasibility of the chemical absorption process which provides a possible guideline and procedure for future research using the process.
- The effects of various parameters, such as gas input flow rate, solution height, solution volume and diameter of the measuring cylinder on the absorption rate are examined.
- Operational costs of the proposed method are assessed and compared with the more common CO_2 liquefaction method.

For practical installation of the system, a CFD simulation model is built, assessed and optimized based on the results from the experiments. After analysing the lab-scale CFD model, a new full scale model is designed and optimized. The following points present the main contribution from the practical design part:

- CFD simulation and laboratory scale experiment of the CO_2 absorption process are presented, compared and analysed. This phase gives a method for applying CFD

software to the assessment of chemical absorption processes. The validity of the simulation model is proved as comparisons between the experimental and simulation results indicate a good agreement.

- The effect of many significant parameters, such as NaOH solution concentration, gas input flow rate, solution column height, solution volume and diameter of the reaction tanks on the absorption rate and reaction rate are examined. Optimised parameters are derived and discussed based on the analysis of the results.
- A guideline procedure for design and installation of the system on ships is presented. The design processes include system selection, modelling and optimisation. The installation includes the system positioning, fitting and process demonstration.

CHAPTER 2. LITERATURE REVIEW

2.1. Current CO_2 Situations

Over centuries of consuming fossil fuels, the concentration of CO_2 in the atmosphere has increased by 100 ppm according to a report from the IPCC (IPCC, 2007). The increase of CO_2 in the atmosphere, as is the nature of GHG's, leads directly to global warming and poses a risk to every single creature on our planet. This situation is urgent and a solution is required to sustain the environment in a good condition. This section will elaborate on the current situation regarding CO_2 emissions from different perspectives, and the prediction of future conditions will also be presented.

2.1.1. Emissions of Carbon Dioxide

First of all, from the angle of emissions gas types, the first pie chart in Figure 1-1 indicates the amount of different gases emitted by percentage. The pie chart, which is from the Carbon Dioxide Information Analysis Centre, illustrates that the emission of CO_2 is much more than any other gases as it comprises 77% of the total GHG emissions. Among all CO_2 emissions, 74% of CO_2 emissions are attributed to fossil fuel combustion and only 22% is due to deforestation and biomass decay. Hence, more consideration on CO_2 emissions from fossil fuel utilisation is necessary in order to achieve the required mitigation of climate change.

The second pie chart in Figure 1-1 indicates that the increase of CO_2 content in the atmosphere is not a result from a single country or community. Global emissions are no longer a regional problem but an international one because the global economy is growing rapidly and countries are increasingly relying on each other. According to the chart, it is obvious that China has the highest CO_2 emissions in the world and the USA and the EU follow. Certainly, these countries and unions should be aware of the serious effects of GHG emissions and should be responsible for taking actions as soon as possible. In fact, all the

countries should develop and carry out a suitable and reasonable policy for GHG control based on their specific situations.

Since policies for GHG reduction are necessary, we should think about what exactly we can do towards emissions reduction. It appears to be the most practical question but answering it requires a feasible solution. Nowadays, the emission of CO_2 is generally from energy supply, industry, forestry, agriculture, transportation, residential and commercial buildings, and waste. The percentages of these emission sources are shown in the last pie chart in Figure 1-1. The chart reveals that there are many emission sources and clearly they are all equally serious as the percentages they account for are quite similar. Improvements solely on one source may not be of great help but efforts focusing on all these sources will make a significant difference. Hence, it is reasonable to make any possible efforts towards emissions reduction from all sources.

2.1.2. Prediction

Currently, climate change is an ongoing issue because the quantity of carbon dioxide being emitted is still growing. Figure 2-1 presents a chart with a trend line of world carbon emissions from fossil fuels from the year 2000 to 2013, which is according to data from the Carbon Dioxide Information Analysis Centre (Boden et al., 2016). The trends illustrate a rapid increase in emissions and further trends can be predicted easily. According to the curve, although there is a slight decline in 2009, the emissions will keep increasing if no further policies and actions are adopted. It is obvious from this data that the rate of increase in carbon emissions is rapid. It is a fact that global warming has already influenced the environment and the climate all over the world. According to NASA, snowpack is decreasing in North America and grasslands are replacing forests in Latin America. Frequent flooding occurs in Europe and unfortunately, Africa still faces the problem of water shortage. Also, in Asia, portable fresh water is now less easily available (NASA, 2016). The mitigation of the greenhouse effect is now so necessary that the approach for

GHG reduction should be implemented as soon as possible. Fortunately, there is still time to make some changes for the future in order to slow or even reverse these negative impacts.

As indicated previously, the huge amount of CO_2 emissions should be attributed to all nations or groups and all the emission sources should be seriously considered as well. Having CO_2 emissions reduced in every field or industry is the key to climate change mitigation. For the shipping industry, it is the responsibility of the whole sector to make contributions to the preservation of our environment. Fortunately, EEDI and EEOI are in forced by the IMO towards an eventual goal of climate change mitigation.

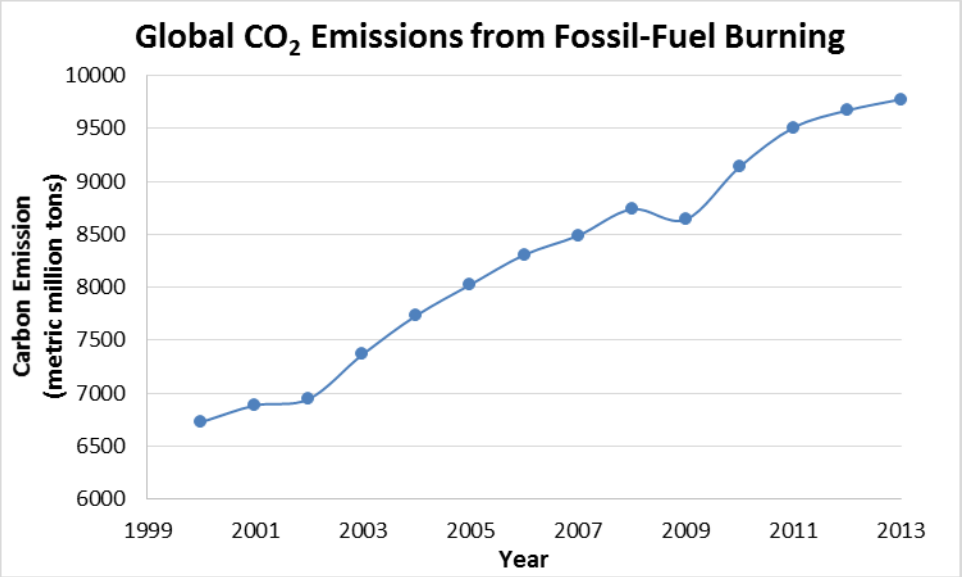

Figure 2-1 Trends in CO_2 emissions from 2000 to 2013

2.1.3. IMO Solutions

In this section, the GHG emissions control methods suggested by the IMO will be introduced. The aim of the IMO's regulations is to reduce the carbon emissions of ships by increasing the energy efficiency of marine activities. The amount of carbon dioxide emitted from fossil fuels used is fixed and can be calculated by applying conversion factors for different fuel types. For example, the quantity of carbon dioxide emitted from high sulphur

fuel oils (HSFO) is 3.075 times the quantity of fuel used. The conversion factors of several fuels are listed in Table 2-1 (MEPC, 2010). These factors are derived as the chemical formula of fossil fuel are known: for CH_4 as an example, for 1 ton of CH_4 there will be 0.75 ton of carbon so the carbon dioxide is 2.75 ton of CO_2. Therefore, if the energy efficiency is increased, the actual work done in a fixed time will increase for the same amount of carbon emitted.

Table 2-1 Conversion factors of several common fossil fuels (MEPC, 2010)

	Fuel type	*Conversion factor (t CO_2 / t Fuel)*
1	Marine Diesel And Marine Gas Oils (MDO/MGO)	3.082
2	Low Sulphur Fuel Oils (LSFO)	3.075
3	High Sulphur Fuel Oils (HSFO)	3.021
4	Liquefied Natural Gas (LNG)	2.750
5	Liquid Petroleum Gas (LPG): Propane	3.000
6	Liquid Petroleum Gas (LPG): Butane	3.030

In order to try to improve the energy efficiency of international shipping, new regulations entered into force on 1st January 2013. The IMO adopted a series of amendments and added them into the International Convention for the Prevention of Pollution from Ships (MARPOL) in July 2011. A new chapter was added into MARPOL Annex VI to make mandatory regulations for different kinds of ships, such as the Energy Efficient Design Index (EEDI) for new ships, the Energy Efficiency Operation Index (EEOI) for existing ships and the Ship Energy Efficiency Management Plan (SEEMP) for all ships. These regulations are targeting at all ships with a capacity of 400 gross tonnes and above. For these energy efficiency improvement methods, their calculations are based on the ratio between CO_2 emissions and transport work. For example, the carbon emissions for a new vessel (applying EEDI) are indirectly obtained by multiplying power output with fuel consumption of all engines, taking into consideration the fuel carbon factors. The transport work is derived from multiplying capacity with a reference speed for the selected vessel. The ratio between carbon emissions and transport work presents the EEDI of the vessel. Then the comparison between designed EEDI with the target value in the IMO regulations indicates whether further carbon emission reduction techniques are required. However,

these regulations are based on increasing the energy efficiency and there is another type of technologies which store carbon captured for industrial utilisation. Further review on CCS technologies will be carried out in the next section.

2.2. Onshore CCS Methods Reviews

Carbon Capture and Storage (CCS) is the terminology used to describe a series of techniques applied on emissions sources, like power plants and industrial processes, for separating off the CO_2 from fossil fuels or exhaust gases, transportation of the CO_2 with pipelines or ships, and storage underground or in the oceans. CCS is applied to mitigate climate change and to finally achieve a sustainable way of living. Now, carbon capture technologies are interesting to researchers all over the world because there are still many improvements and development that can be and should be made on emissions reduction, energy consumption and cost efficiency. As of the end of 2012, there have been 14 active CCS industrial projects onshore (Global CCS Institute 2012). Application of CCS is one of many ways to achieve emissions reduction from the burning of fossil fuels (Global Trends in Carbon and Sulphur Emissions, 2011). The Boundary Dam Integrated Carbon Capture and Sequestration Demonstration Project is an active CCS project launched in 2014 in Canada (Boundary Dam Integrated Carbon Capture and Storage Demonstration Project, 2014). The target is a power station. An amine-based post-combustion capture method is applied for the capture of CO_2. A pipeline is used as the transportation method and EOR is used for carbon storage. The Gorgon Carbon Dioxide Injection Project is an Australian project currently on progress, which will go into operation in 2016. The target is in natural gas processing and this CCS project will apply a pre-combustion capture method (natural gas processing), use pipeline transportation and EOR storage (Gorgon Carbon Dioxide Injection Project, 2015). The FutureGen 2.0 Project is still in the definition stage and is a CCS project which will apply an oxy-fuel combustion capture method on a power station in the USA. The compression method will be applied for separation. Pipeline and dedicated geological storage will be utilised for CO_2 transportation and storage (FutureGen 2.0 Project, 2013). All of the capture methods mentioned above will be discussed in the next section. During the review, most of the focus is on the capture and storage parts, as the objective of this thesis is to make a contribution towards capture technology research and development for marine vessels.

2.2.1. Capture Methods

Capturing carbon from fossil fuels ensures that the GHG's (especially CO_2) will not be emitted into the atmosphere. Without the emission of GHG's, the ongoing process of climate change (global warming) will be alleviated and eventually halted. There are currently three main methods that are widely used and applied on power plants: pre-combustion capture, oxy-fuel capture, and post-combustion capture. These methods are based on different principles so their applications may vary. The following sections will introduce these capture methods in detail so that the selection of capture methods for marine applications can be based on a knowledge of the characteristics of these different methods.

2.2.1.1. Pre-Combustion Capture

The first capture method introduced will be the pre-combustion capture method. The main principle of this method is to remove CO_2 from the fossil fuel prior to burning it. There are some chemical reactions that take place before the combustion in the engine to transfer the fossil fuel into a hydrogen fuel. As shown in the first schematic in Figure 2-2 the fossil fuel for the power plant is reformed with steam, and a mixture gas of CO_2 and H_2 (hydrogen) is produced. There are two reactions involved in the reforming processes: the steam-reforming reaction generates synthesis gas (a mixture of CO and H_2, also known as syngas) and the water-gas shift reaction transfers CO to CO_2. Both of the reactions generate H_2 which can be used as a fuel by hydrogen gas turbines. The final products are CO_2 and H_2. The CO_2 can be captured through suitable methods and the H_2 is separated as a fuel for the power plant which generate no CO_2 at all. The most popular methods used for CO_2 capture are the chemical absorption method with an absorbent and the condensation method.

This pre-combustion method is applicable to Integrated Gasification Combined Cycle (IGCC) or Natural Gas Combined Cycle (NGCC) power stations. It is a high-efficiency technique with low risk and it can capture 90-95% of the CO_2 from fuel oil. However, as

the installation of the system needs to be coupled with a chemical plant for reforming and capture, it requires a large amount of initial investment on designing, building and integrating the system. This method can be used for ships because using hydrogen fuel is mature for internal combustion engine. However, using H_2 as fuel can eliminate carbon emission directly and easily so it makes the carbon reduction complex when applying pre-combustion method. Hence, this method will not be considered for traditional engine and will not be considered further in this research. The gas turbine with hydrogen fuel also poses high nitrogen emissions, especially NO_2, which is also harmful to the environment.

2.2.1.2. Oxy-Fuel Capture

The oxy-fuel capture method combusts the fossil fuel within pure oxygen rather than within air. The oxygen will first be separated from the air using separation devices. After the combustion, the emission gases will have a high concentration of CO_2 (around 90%) due to a relatively complete combustion and few impurities in the oxygen. Hence, it is easy to achieve CO_2 separation under these conditions. As shown in the second flow chart in Figure 2-2, after the combustion processes, only condensation or compression is required for the separation between CO_2 and water.

Regardless of the energy consumed, a potential 100% of CO_2 can be captured with this method. The emission of other gases, like NOx and SOx, are also directly and greatly reduced due to the occurrence of complete combustion. The system of oxy-fuel capture can be retrofitted to existing power plants as it doesn't affect the power plant system greatly. One thing that matters to existing plants is that with high oxygen concentration, the combustion temperature is higher than it would be if only air was used. A higher material quality for the combustion chambers may be required and a high power penalty is another big drawback of this method. Currently, there are only a few power plants installed with this method because it is still under research and development.

2.2.1.3. Post-Combustion Capture

In this method, the CO_2 is captured from the exhaust gases after combustion of the fossil fuels has taken place. Usually, power stations with this method for carbon capture are retrofitted with an exhaust gas treatment system as illustrated in the third chart in Figure 2-2. One typical method of capture is to use chemical sorbents to absorb the CO_2 and then apply heating or increase the pressure to have the CO_2 released from the absorbent and transported for further storage. Nowadays, amine and quicklime are commonly used as sorbents due to their high capability of absorption and characteristics of releasing the gas when heat and pressure are applied. There are some other methods for CO_2 separation that are currently under research and development, such as the application of active carbon or utilisation of a membrane.

As the system is based on processes of exhaust gas treatment, the retrofitting is the easiest amongst the three capture methods discussed. This method requires the least changes on the target plants. It is also the most mature approach as it has been used for at least half a century. Despite these merits, it also requires some improvements in reducing the inherent running costs, such as the recycling and replacement of absorbents. There are many experiences gathered to date on large scale power plants but it is still not applicable for ships so that further research and development are required.

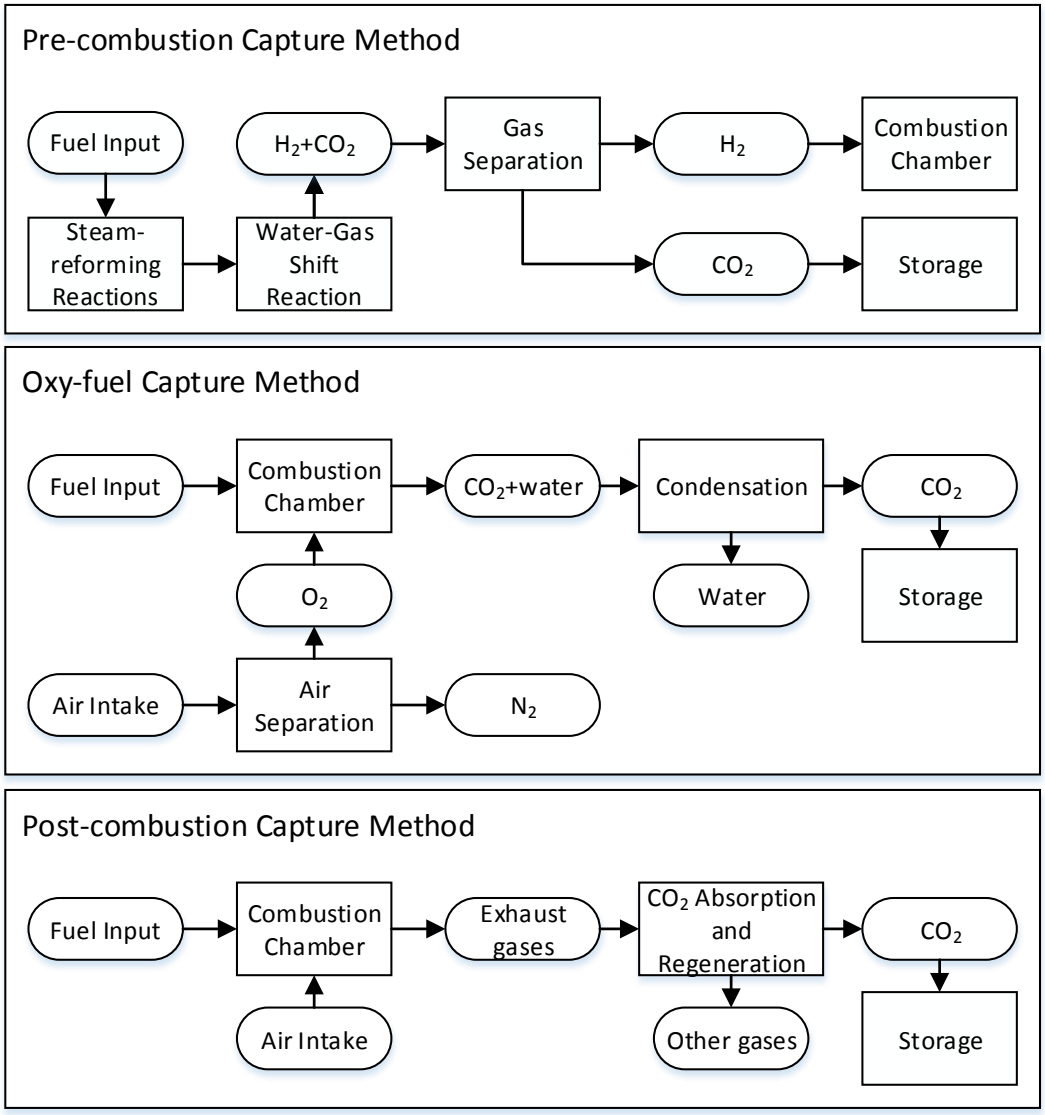

Figure 2-2 Schematics of general carbon capture methods

Table 2-2 from the report of the IPCC indicates the methods and technologies which are currently available and under development for all three aforementioned capture methods. Basically, these capture technologies can be applied to different capture methods.

For transportation, the CO_2 captured will usually be transported in either gaseous or liquid form. Currently, liquefied CO_2 transportation is more popular. This is because CO_2 in its dense liquid phase has a high density and a low viscosity. CO_2 is usually compressed with

multistage compressions into a dense liquid state. Under these conditions, low storage volumes and low transportation pressures are required so that it is very convenient and efficient for transportation using both pipelines and ships.

Table 2-2 Carbon Capture Methods and Technologies

Separation task	**Pre-combustion Capture**	**Oxy-fuel Capture**	**Post-combustion Capture**
Capture Techniques	CO_2/H_2	O_2/N_2	CO_2/N_2
Solvents	Physical solvents Chemical solvents	N.A.	Chemical solvents
Membranes	Polymeric	Polymeric	Polymeric
Solid Sorbents	Zeolites Activated carbon Alumina	Zeolites Activated carbon	Zeolites Activated carbon
Cryogenic	Liquefaction	Distillation	Liquefaction

To find out a suitable technology, some researchers investigated different methods and techniques are reviewed. Research carried out by Yu et al. indicated the efficiencies of carbon capture by absorption and adsorption and absorption is preferred (Yu et al., 2012). Ethan and his colleagues investigated two different absorption methods, using ammonia and organic solvents (Ethan et al., 2016). Joshuah and his team tested the absorption efficiency of using NaOH capture carbon dioxide from air (Joshuah et al., 2008) and Lin and Chen apply cross-flow packed bed to test the carbon absorption rate of NaOH solution (Lin and Chen, 2007). Comparing their results and considering the constraints on ships, using NaOH solution is preferred. As this method has not been used for ships yet, it is significant to test and investigate it for maritime application. The next section will review literatures for maritime CCS in order to find out the importance of this research.

2.3. Maritime CCS

According to working paper from European Commission, the European Union (EU) is aiming to reduce GHG emissions by at least 20% compared with 1990 levels by the year 2020 (European Commission, 2012). The US is also trying to cut off its GHG emissions with a tough target (WRI, 2002). A 20% reduction of carbon emissions from ships is also set up as a global target by the United Nations, to be achieved by 2020 (Shipping, World Trade and the Reduction of CO_2 Emissions, 2014). Apparently, GHG emissions reduction is becoming a mainstream topic in environment protection. From the previous chapter, the significance of actions and policies for CO_2 reduction is clear and there are also many different methods available to help achieve it. The 450 Scenario, prepared and adopted by European Union climate change expert group 'EG Science' in 2008, says that global temperatures have to be stabilised within 2 degrees compared with pre-industrial levels (Information Reference Document, 2008). Otherwise, changes like heat waves, droughts, and extreme precipitation events will greatly impact future climate. According to the IPCC Assessment Report 4 (IPCC, 2007), carbon emissions need to start declining before 2015 and should be further reduced to less than 50% of today's emissions by 2050. All these requirements indicate how urgent it is to have carbon emissions reduction.

A report from the IMO, 'Second IMO GHG Study 2007', indicates that shipping was estimated to have emitted 1046 million tonnes of CO_2 in 2007 which is about 3.3% of the total global emissions (Second IMO GHG study, 2007). It is a relatively small quantity of GHG emission from the marine engineering field but it is still the responsibility of marine engineers to make a contribution to global reduction effort. The IMO has already set up regulations and proposed measures for marine emissions reduction in order to help construct a more sustainable environment. According to the 'Third IMO GHG Study 2014" about 938 million tonnes of CO_2 emissions were estimated to have originated from shipping in 2014. 796 million tonnes were contributed by international shipping in 2012 (Third IMO GHG study, 2014). This means that a reduction has already been achieved through recent work on carbon emissions reduction.

2.3.1. Maritime Regulations

New measures from the IMO relating to energy efficiency entered into force on 1st January 2013which could help ship operators save $34 to 60 billion in fuel costs in 2020. The regulations should bring significant emissions reductions: by 2020 about 150 million tonnes of annual CO_2 reductions are estimated and by 2030 the amount is projected to increase to 330 million tonnes of CO_2 annually. From the angle of a reduction ratio, the average reduction will be approximately 14% in 2020 and approximately 23% in 2030 comparing to current figures, as this also takes into account the expected increases in global shipping fleets.

The measures proposed are mainly applications of methods for increasing energy efficiency through improved designs and effective operations. The resulting reduction in GHG emissions can be found by comparing the second and third IMO GHG studies. The Energy Efficiency Design Index (EEDI) for new builds and the Energy Efficiency Operation Index (EEOI) and Ship Energy Efficiency Plan (SEEMP) for all ships are predominant methods which can be performed at both ship design and operation stages. It is reasonable to expect a reduction in GHG emissions by reducing fuel consumption. The cost of fuel is reduced and the emissions of carbon dioxide decline as well. Most of the emissions reduction applications are already utilised on ships at the requirements of ship yards and customers, such as hull coatings and engine optimisation.

2.3.2. Previous Research on Maritime CCS

Although the IMO carbon emissions reduction target mentioned above could be achieved through energy efficiency improvement methods (using the EEDI, EEOI and SEEMP), CCS is still a reasonable and feasible way to mitigate climate change. The objective of the application of CCS methods is to provide a feasible and suitable way for controlling emissions as well as an optional way to enhance the decrement. Currently, CCS is relatively more mature on power plants and industrial processes than maritime applications. It is a

fact that there are only a few CCS applications found on board ships today. There is one project ongoing in Europe which is a collaboration between Process Systems Enterprise (PSE) and the classification society DNV-GL, which is working on an on-ship carbon capture system in order to reduce the marine GHG emissions and meet the regulations. Approaches considered are amine absorption, pressure-swing absorption, heat-integrated distillation and membrane processes. A DNV-GL report has indicated that, by applying CCS on ships, CO_2 emissions from ship operation can be reduced by 65% (DNV-GL and PSE report, 2013). According to their project, application of CCS is a suitable and reasonable choice so more research and development will help greatly in the development of maritime CCS.

2.3.3. Challenges of Application on Ships

Generally, there are many capture techniques available for all the three capture methods but with different conditions and efficiencies. These methods for industrial uses and power plants aim to capture CO_2 from emissions and then transport and store it in suitable and profitable locations, such active or depleted oil fields for enhanced oil recovery (EOR). Sometimes, CO_2 is stored in the CO_2 lakes in the ocean. Some projects try to trap CO_2 in the layer of saline aquifers underground. As mentioned in the previous section, there are basically two ways to transport CO_2: in gaseous phase and in dense liquid phase. Conversion of CO_2 into the dense phase is not only popular for onshore transportation but also preferred for ship applications (IPCC, 2005). In gaseous form, the volume occupied by CO_2 is considerable. These onshore capture methods will apply a compression process for convenient and efficient transportation and storage. However, if applying these methods on-board the ship mechanically, serious problems arise such as power penalties, space requirements for storage and safety issue from carrying liquid cargo.

Liquefaction or compression of CO_2 requires considerable energy which will lead to high energy demand. This is because a large amount of power is required for compression while changing from gas to dense liquid phase. The space requirements arise from the installation

of new equipment and storage tanks. As the space on-board is limited, these spaces for CCS should ideally be small so that there is no need to detract from cargo carrying spaces. Otherwise, the storage of CO_2 on the ship will have a severe impact on the ship's transportation performance. Another problem of CO_2 compression is that the state of CO_2 is very complicated (Barthelemy et al., 2010) and any little change in temperature or pressure may lead to density and volume changes and even may result in phase changes. While the liquid CO_2 is turning into gas, high pressure occurs and may lead to a risk of leakage or even explosion. Since the storage conditions for liquefied CO_2 are so strict, the requirements for the storage tank materials are also high. As the ship is running, the CO_2 will be captured and stored as liquid in tanks which might lead to a sloshing effect in these partially filled storage tanks. The stability of the ship might then be affected. These adverse effects will definitely have a serious influence on the performance of the vessel.

In order to try and eliminate these problems, this thesis aims to find an efficient method to have carbon easily and safely stored on the ship. Other than typical CO_2 compression methods, another candidate is the combination reaction between CO_2 and a metallic oxide. This can be considered because the requirements of the reaction are simple and the final products are convenient for storage. Hence, this thesis will present this method in detail and will try to highlight the feasibility of capturing CO_2 by alkaline solution and keeping it in solid form. The following chapter will present a detailed introduction and description of the processes involved.

2.4. CFD Modelling and Simulation

The feasibility of the proposed carbon capture and storage method is tested by lab-scale experiments which are carried out in a chemical laboratory. Many data are derived from these experiments and could be applied for CFD modelling. CFD software is applied for setting up and optimising the model. The optimised model can be used for the design of the practical system to be installed on the ship.

In order to design a reasonable and feasible CFD model, a series of literatures are reviewed. Horvath and his research group have successfully modelled and simulated a cuboid bubble column using the Volume of Fluid (VOF) model. The VOF model is suitable for capture free surface between phases to present immiscible phase interaction and the computation cost of this model is low. Their simulation results are close to the experimental data (Horvath et al., 2009). Another investigation tests both mixture and Eulerian approaches on a bubble column reactor under unsteady state conditions and low gas flow rates. The results from the simulation show a good consistency with experimental data (Mohammad, I. and Mohammad, A.K., 2011). It also indicates that similar outputs can be derived from both the mixture and the Eulerian model, but the Eulerian model demonstrates a better convergence and stability. Asendrych and his colleagues applied a two-fluid Eulerian model for an amine-based carbon capture system. A 2D axisymmetric CFD model was designed and analysed. The results illustrate that the ratio of solution to gas has a significant impact on the reaction efficiency. They also achieved a good agreement between numerical results and experimental data (Asendrych et al., 2013).

Therefore, considering the absorption reaction between the gas (CO_2) and the fluid (NaOH solution), the Eulerian model is an option for the multiphase reaction simulation. In this thesis, the simulation of the experiments will be presented and the subsequent optimisation of the simulation model will give fundamental details for the full scale practical system simulation. After the simulation model for the practical system is designed and optimised, the whole system on-board the ship can be designed so that the practical installation of a carbon solidification system can be achieved.

CHAPTER 3. CAPTURE AND SOLIDIFICATION PROCESSES OF CO_2 ON SHIPS

3.1. Objective

International shipping is estimated to have emitted 796 million tonnes of CO_2 in 2012 which is about 2.2% of total global emissions (Third IMO GHG study, 2014,). Although the emission amount of GHG from shipping transportation is not so significant, it is still considered to be responsible and essential to address this in order to help alleviate the effects of climate change. If left without any regulations and actions, the emissions from shipping might be tripled by 2050. It is therefore necessary to take precautions on CO_2 emissions from marine activities. Since precautions are necessary for ships currently, this section makes a proposal for a method of capturing CO_2 on marine vessels.

On-board ships, as a matter of fact, there are several severe limitations to be considered, such as limited power output, very valuable volumes and weights, and safety issues due to installation. Retrofit conditions for existing ships also require further consideration. A carbon capture method will be illustrated with discussions on its merits and drawbacks. This chapter will also present the comparison of this proposed method and another candidate, comparing their viability and their effects on shipping performance.

3.2. Methods Consideration

To date, the IMO has concentrated on energy efficiency improvements of vessels. The EEDI, EEOI and SEEMP are typically highlighted and focused on in recent research work. Certainly, energy efficiency can be improved at the design and operation stages and it can lead to the reduction of fuel consumption and therefore decrease CO_2 emissions indirectly. In this thesis, CCS on-board ships will be studied as this has previously been shown to be a promising way to reduce CO_2 emissions from the exhaust gases directly (Lin and Chen, 2007). There are many carbon capture methods that can be applied to power plants and

industrial processes. However, there are a few applications of CCS on ships at present. Currently, there is an on progress project from DNV GL and PSE, aiming to apply onshore CCS for a VLCC which has relative abundance of deck space (DNV GL, 2013). Previously, three types of CCS methods were mentioned: pre-combustion capture, oxy-fuel combustion capture and post-combustion capture. According to Table 2-2, the purpose of pre-combustion capture is to separate CO_2 from hydrogen gas (can also be applied to natural gas), oxy-fuel combustion capture aims to separate O_2 from N_2. Post-combustion capture is where CO_2 is separated from N_2. The following paragraphs will discuss the shortcomings and merits of these capture methods in order to have a general view about their viability for installation on ships.

3.2.1. Oxy-Fuel Combustion Capture

The oxy-fuel combustion capture method comprises of burning fuel in high purity oxygen instead of air. The system could be retrofitted to the engine as only air separation equipment is required before the air inlet to a normal marine engine. The available air separation systems are based on industrial oxygen production technologies, such as air separation comprising of cryogenic distillation, absorption using multi-bed pressure swing units and polymeric membranes. A flue gas circle is necessary to mix the flue gas with the input oxygen in order to reach high combustion temperatures. Therefore, as the conditions of the emissions are changed from the initial ones, it is expected that the NOx emissions will grow which should be carefully considered. Another issue is due to the too violate combustion which may damage the engine. Considering the cost of this method, it is primarily due to the power requirements of the air separation and feeding system. It means that consideration and improvement on this angle will optimise the capital and running costs.

Certainly, combustion with pure oxygen has a range of good effects but this method is not ready at present for commercial use and is currently only used in the metal smelting industry. Hence further research and development would be necessary and many

constraints should be considered when applying oxy-fuel combustion to a CCS system. Also, if installed on a ship, the new equipment can only be installed within restrict space which may cause problems for the ship owners.

3.2.2. Post-Combustion Capture

As a relatively mature method, the post-combustion capture method is more widely used in power plants and industrial processes than the other two approaches presented above. Another reason for widespread utilisation is that in large scale processes, direct firing of fossil fuels in air is the most economic approach. As a retrofitted capture system, it can be coupled with an existing system. The difference is that the post-combustion capture system is installed after the combustion chamber. It could be coupled with the exhaust gas emission system directly and use various separation systems to then capture the CO_2. The main costs are due to initial investment and power costs associated with the capture system. Absorption processes based on chemical solutions are currently a preferred option for post-combustion CO_2 capture. The power costs for these processes are due to feeding gas into the absorbent for absorption and to heating for absorbent regeneration. An obvious drawback is that a large scale absorption system will be required due to tonnes of exhaust gases generated. Another disadvantage is that the concentration and purity of CO_2 in the exhaust gas is low because there are many other gases present as well, which need to be separated from the CO_2. Some gases may affect and degrade the absorption solution, such as SO_2 and SO_3. These gases are acid gas pollutants that can react with alkaline solutions. Usually, low sulphur fuel is the preferred solution and also a scrubber or SCR can be installed for further exhaust gas desulphurisation. As these methods could not eliminate all other acid gas, the degradation of the absorbent is still unavoidable. From the point of view of capturing the CO_2, all these three methods could use the same techniques but the capture rates will vary. Since the carbon capture system will be installed on ships, the constraints of installation should also be carefully considered. The advantages of post-combustion methods are easy retrofit, low costs, fewer changes on-board and relative independence from other systems.

3.3. Chemical Processes Description

The proposed method aims to use chemical substances which can react with and absorb carbon dioxide at atmospheric temperature. The processes produce a solid compound which is easy to store on ships. The chemical processes for carbon solidification will be referred to as CPCS in the following sections. The processes are basically three procedures: absorption, precipitation (causticisation) and filtration. The two chemical reactions are presented below (Pflug et al., 1957; Mahmoudkhani and Keith, 2009):

$$CO_2 + 2NaOH \rightarrow Na_2CO_3 + H_2O \quad (1)$$

$$Na_2CO_3 + CaO + H_2O \rightarrow CaCO_3\downarrow + NaOH \quad (2)$$

$$CaO + H_2O \rightarrow Ca(OH)_2 \quad (3)$$

In the first reaction, the carbon dioxide is absorbed by sodium hydroxide (NaOH, caustic soda). This is a natural characteristic of sodium hydroxide as it is a strong alkali. One product from the absorption reaction is sodium carbonate (Na_2CO_3, washing soda) which is a relatively stable compound. Then the product solution is transported to react with calcium oxide (CaO, quicklime) and water through which a precipitate, calcium carbonate ($CaCO_3$, limestone), is produced, as shown in reaction 2. This reaction is the causticisation process and has been previously used in the industrial production of caustic soda (Littman and Gaspari, 1956). After the filtering, washing and drying processes, the limestone powders will be stored in tanks and unloaded at the final destination.

The advantage of using NaOH than $Ca(OH)_2$ directly is that the solubility of $Ca(OH)_2$ in water is much lower that NaOH at atmosphere temperature. It will slow down the absorption process because only dissolved $Ca(OH)_2$ can absorb CO_2. Due to constantly generating and feeding of the exhaust gases into the absorption system, the absorption reaction should be rapid enough to make sure the releasing of exhaust gases from engine. Therefore, NaOH is selected for carbon absorption.

As masses are related to molecular masses and molar numbers, the relationships between the different substances are shown in the following equation:

$$m_1/m_2 = (n_1 M_1) / (n_2 M_2) \quad (4)$$

Where:

m_1 = total mass of substance 1 (ton);

m_2 = total mass of substance 2 (ton);

n_1 = molar number of substance 1 (mole);

n_2 = molar number of substance 2 (mole);

M_1 = molar mass of substance 1 (kg/mole);

M_2 = molar mass of substance 2 (kg/mole).

This relationship will be used to derive the masses of the different chemical substances involved in the reactions.

The absorption reaction is an exothermic reaction from which the heat released can be recovered so that the reaction is not too drastic, and also the energy efficiency of the system can be increased. One internal reaction, integrated into reaction 2, is the generation of calcium hydroxide ($Ca(OH)_2$, hydrate lime) (Souto et al., 2008). This is also an exothermic reaction where the reaction heat released can also be recovered and reused. The heat release rates from the three reactions are 109.4, 5.3 and 65 kJ per mole of CO_2 respectively (Mahmoudkhani and Keith, 2009). While dissolving NaOH into water, heat is also released, around 35.82 kJ per mole NaOH (Japan Soda Industry Association, 2006). Based on these reactions and processes, the CO_2 from the exhaust gas can then be captured and stored in a solid form on-board the ship.

The reason why NaOH is used for absorption is due to the absorption rate of CO_2. As the continuously generation of exhaust gas, the reaction should be prompt. According to Lin and Chen's research, the CO_2 removal rate grows with an increase in NaOH concentration (Lin and Chen, 2007). Compared with $Ca(OH)_2$, the solubility of NaOH in water is much higher. As the maximum concentration of $Ca(OH)_2$ is limited by its solubility, the absorption rate is constrained indirectly. Another reason for the selection of NaOH is that the sediment generated ($CaCO_3$) may cover the undissolved $Ca(OH)_2$ and prevent it from dissolving into water. Although this undissolved effect can be reduced by centrifugal stirring, it is still difficult to eliminate and require greater investment in terms of the power supply and the stirring system. Therefore, considering these reasons, it is preferable to apply NaOH solution for the absorption process.

3.4. System Design and Components

The design of the system and selection of the components is based on the processes involved in the capture and storage, for example the process during reaction 1 is feeding CO_2 into a sodium hydroxide solution for absorption therefore a gas feeding system and reaction tank are required. Due to the presence of a strong alkali, anti-corrosion materials should be applied to the system for safety reasons. After the absorption process, the precipitation reaction starts to generate sediment $CaCO_3$. Precipitation tanks with stirring devices are required here in order to accelerate the mixing and reaction. Then the filtration of the sediment and solution will be carried out in a centrifuge. The separated sediment will be stored in storage tanks and the solution will be recycled back into the absorption process. With considerations for all these steps of the capture processes, the following system is presented in Figure 3-1. This figure is shown to make it easier to understand the processes presented in the following sections.

3.4.1. Capture Processes

The exhaust gases first go through a water scrubber in order to remove the SOx emissions as well as to cool down the exhaust gases. The scrubber system is a relatively more mature system than the capture system for ship applications so it will not be introduced and analysed in detail here. The reduction target of the carbon capture system is based on the regulations from the IMO, which is a 20% reduction of CO_2 emissions by 2020. Therefore, a target of 20% reduction on CO_2 emission is selected for this project. A certain amount of exhaust gases will be extracted, fed through a by-pass system and then fed into the absorption system. Apart from regulation, another reason of 20% carbon reduction is considering the impact on cargo transportation performance. The by-pass system is equipped with a gas separation facility in order to remove the impurities in the gas, such as NOx, soot and water vapour. This is important because the purity of the CO_2 will affect its reaction rate with the alkaline solution. The CO_2 rich gas is then fed into the absorption reaction tank and the absorption process starts.

The following step is to transfer the product from reaction 1 to the precipitation tank for the double replacement reaction. A transferring pump with flow control units is installed between the two tanks. As long as calcium oxide is fed into the precipitation tank, reaction 2 will begin. The product from reaction 2 is a mixture of calcium carbonate and sodium hydroxide solution. The mixture is pumped into a centrifuge to separate the sediment from the solution. After filtering, washing and drying, the sediment will be finally stored in storage tanks. The NaOH produced in reaction 2 is recycled and pumped back into the absorption reaction tank. Then the new cycle repeats the same processes so that the system can work continuously.

3.4.2. Components

The components in the system should be carefully considered as there are many corrosive materials involved, such as acid gas (CO_2) and alkali solutions (NaOH). Figure 3-2 presents a list of materials selected and their functions and principles for all the devices used in the processes. The system concept is already presented above in Figure 3-1.

3.1. Safety Issues

Considerations on safe operation of the new system are necessary because there are many chemical substances involved in the different processes. CO_2 is an acid gas and NaOH and $Ca(OH)_2$ are two alkaline solutions involved in the reactions. The safe handling of these materials is essential because they can cause harm to both the ship and the crew. This section illustrates the possible risks due to these materials and the safety requirements for avoiding these hazards.

3.1.1. Risks of CO_2

When the concentration of CO_2 in the air rises above 15%, it is lethal to human beings as it can cause asphyxia (The International Volcanic Health Hazard Network-Carbon Dioxide, 2016). It is therefore important to prevent CO_2 in the pipes and tanks from leaking. As CO_2 is denser than air, the leaked gas will accumulate and finally reach a hazardous and fatal concentration. Hence, the seals of pipe connections and tanks should be well treated. Also, ventilation in nearby compartments is required to reduce the possibility of accumulations.

As an acid gas, CO_2 can be corrosive when in contact with water. It can clog and damage the pipes and tanks in the system. Therefore, water removal devices are necessary to help reduce the maintenance costs for pipes and tanks.

3.1.2. Risks of Alkaline Solutions

Both sodium hydroxide and calcium hydroxide are strong alkaline solutions and they are highly corrosive substances. They are able to corrode the decks and tanks on the ship. It is vital to keep the solutions from leaking. The materials used for the tanks and pipes should be anti-corrosive to keep them from cauterising and being damaged by alkaline solutions. These alkaline solutions are extremely harmful to human eyes and skin as well. When handling these solutions, goggles, gloves and coats should be worn for safety reasons. Suitable and immediate treatments should be locally available and on standby at all times. When accidently touched, cleaning and washing the skin with a lot of water and applying boric acid to neutralise the alkalinity is recommended. If the alkaline solutions come into contact with eyes, they should be washed with water immediately and medical attention should be sought as soon as possible.

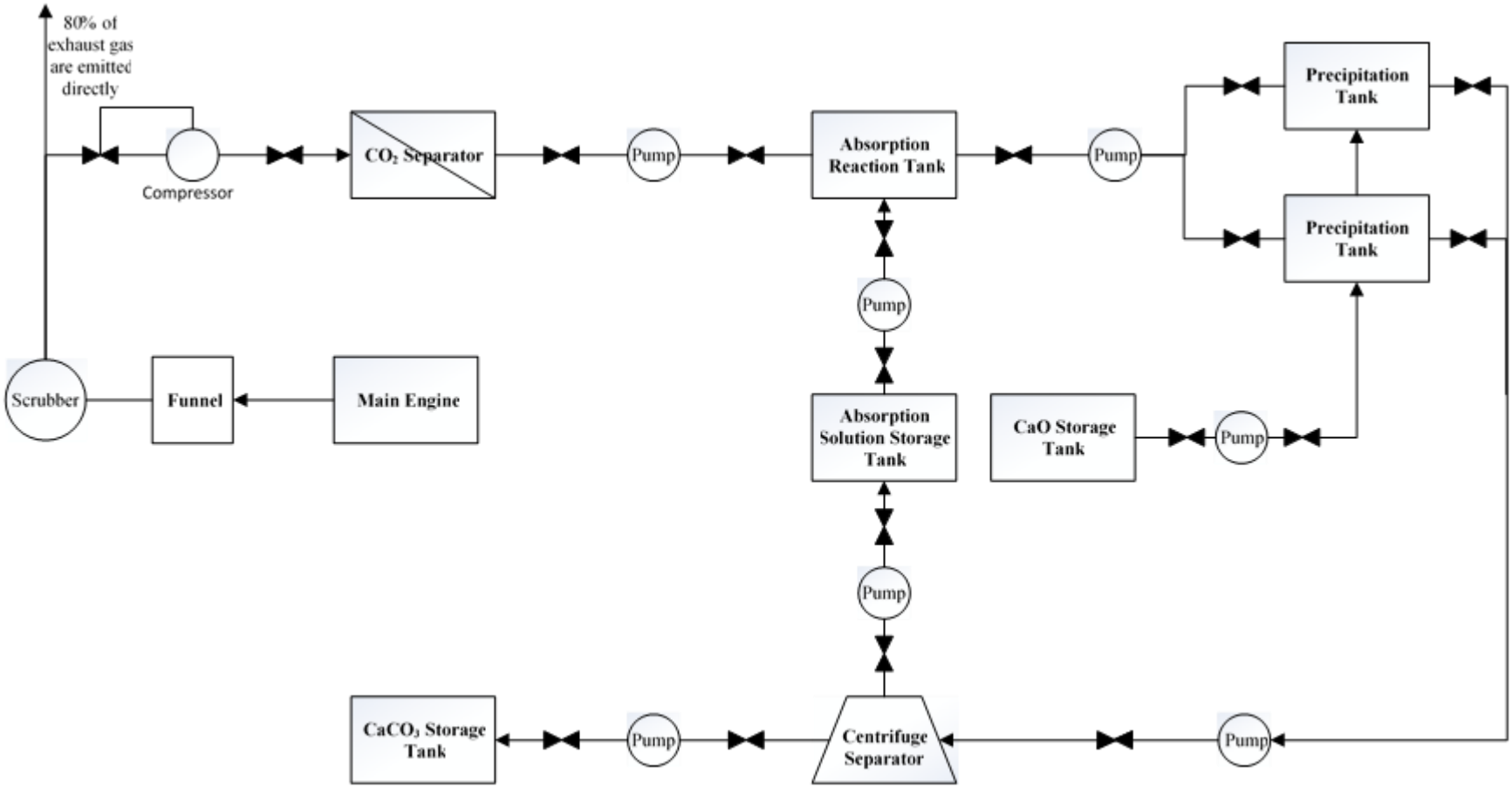

Figure 3-1 Design of carbon capture and storage system

Components of CCS system					
Devices		**Code**	**Material**	**Function**	**Principles**
Exhaust gas treatment	Exhaust gas flow divided device	G	Same as funnels	Distract 20% of flue gas into the CCS devices	A new structure of funnels will divide the gas into two parts: one will be emitted to atmesphere and the other will be pump into system.
	Pump for flue gas	P1	Anti-Corrosion Materials	Provide pressure for transporting gas	Pump principle
CO2 separation	Valve for two filter or adsoption devices	Vm	Electrical valve with thermal resistance	Control the direction of gas: to M1 or to M2	A electrical valve that controled by computer with a switch frequency based on adsorption rate.
	Filter or adsoption devices	M1	Heat resistance material	Filter or adsorb CO2 and release it after flue gas emitted	Membrane could selective filter CO2.
		M2			
CO2 absoption	Valves for absorption devices	Vn1	Normal CO2 transport pipeline	Monitor M1 and M2 and releaseto and isolate CO2 from absorption devices in time	Valves with sensors that monitoring the working of M1 and M2. when Mi releasing CO2, Vni will open.
		Vn2			
	Absorption devices	N1	Anti-Corrosion Materials	Applying of alkaline solution to absorb CO2	Containers for reaction 1.
		N2			
	Valves for Salt metathesis reaction	Vs0	Anti-Corrosion Materials	Control the feeding of Na2CO3 solution into next reaction stage	Valves with sensors that monitoring the working of N1 and N2. When Ni has done absoption, Vsi will open and feed Na2CO3 to Device T1.
		Vs1			
		Vs2			
CO2 solidification	Pumps for water, solution and solid	P2,P3, P4	Anti-Corrosion Materials	Pump Na2CO3 solution, water and Lime into T1	Pump principle
	Salt metathesis reaction container	T1	Anti-Corrosion Materials; Heat resistance material	Carbon solidification and transportation tank	Feeding CaO in the Na2CO3 solution and reacting as reaction 2.
	Tray plate	L	Anti-Corrosion Materials; Heat resistance material	Lift the stone generated in T1	The tray plate is installed in T1. While enough limestone is generated or after a regular time, the tray will lift the stones and transport them to next device.
Material and heat recovery	Pump for NaOH recycling	P6	Anti-Corrosion Materials	Pump the NaOH yield in reaction 2 back to T1	Pump principle
	Valves for alkali recyling	Vr1	Anti-Corrosion Materials	Recycled the alkaline solution.	Pumping the solution back to device N1 or N2.
		Vr2			
	Valves for heat recovery	Vr3	Heat resistance material	Heat generated during reaction 2 will be recovered	Feeding water and absorbing heat outside the device.
		Vr4			
Limestone treatment and storage	Pump for Limestone transfer	P5	Anti-Corrosion Materials	Transfer limestone to T2	Pump principle
	Valves for limestone treatment (inlet and outlet)	Vt1	Anti-Corrosion Materials	Transport stones in time from device T1	Monitering T1 and opening for transport while tray is lifted.
		Vt2		Recycle waste liquid	After treatment, the waste liquid will be drained back to T1.
	Limestone treatment tank	T2	Heat resistance material	Clean limestone for storage and recycle the solution back to device T1	Washing, drying and filtering.
	Limestone storage tank	T3	No requirements	Storage and unload limestone	A tank with load and unload equipment for storaging and unloading limestone.

Figure 3-2 Materials selections, function and principles of devices.

CHAPTER 4. EXPERIMENTAL SETUP, MATERIALS AND PROCEDURES

4.1. Introduction

The principles behind the chemical absorption and solidification processes are presented in the last chapter. In this chapter, experiments of these processes will be illustrated, including rig construction, introduction of the apparatus, processes and operation descriptions, and error and accuracy analysis. The aim of carrying out the experiments is to test and verify the feasibility of the proposed processes. During the experiments, many factors that could impact on the process efficiencies will be observed. This information will be useful for designing a practical system for installation on a ship in the later stages of this work.

This chapter first introduces how the experimental rigs are constructed and also presents the apparatus involved. Then the processes and operation of the experiments will be outlined. All the applications of the apparatus will be described in the following sections. Then the possible errors and the overall accuracy of the experiment will be discussed. Finally, this chapter will present the results obtained from these experiments, including gas absorption rate and NaOH solution recycling rate.

4.2. Experimental Rigs and Apparatus

4.2.1. Experimental Rigs

The construction of these experimental rigs is for testing the processes of carbon absorption and solidification. A CO_2 tank is applied for constant feeding of CO_2 gas for the absorption process. The gas will be released into the NaOH solution so a container for the solution is also required. A measuring cylinder is selected as a suitable container so phenomena from the reactions can be observed directly through the glass sides. To feed the gas in, one flow

pressure regulator and one flow meter are used in order to control the flow pressure and flow rate. A rubber pipe is connected to the flow meter. A diffuser is attached to the outlet of the delivery pipe so that the gas can be evenly distributed into the alkaline solution. A lab stand with a clamp is used to keep the rubber pipe in position. Two scales are located under the CO_2 bottle and the measuring cylinder to display their weights. The experimental rigs for the absorption process are presented in Figure 4-1 along with a schematic chart.

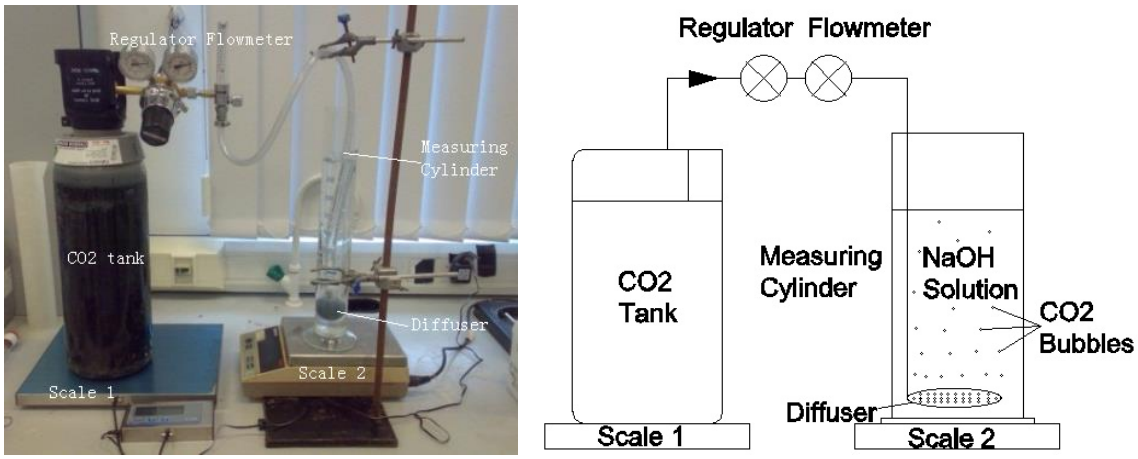

A B

Figure 4-1 Experiment rigs (A) and schematic chart (B) of absorption processes

Before the filtration experiment is carried out, the mixture of $CaCO_3$ sediment with the solution should be prepared first. This mixture is the product of the reaction between the Na_2CO_3 solution (from the absorption reaction) and CaO. To obtain this mixture, a sample of the Na_2CO_3 solution is taken with a test tube and a specific amount of CaO is added based on calculation. It usually takes 20 minutes at most to complete the reaction however shaking the test tube can help increase the reaction rate and hence reduce the reaction time.

The filtration experiment is designed to remove the $CaCO_3$ sediment from the mixture. A simple filtration experiment rig is constructed using a funnel and an Erlenmeyer flask. A layer of filter paper is attached to the funnel which will prevent the sediment from moving

down into the funnel. Due to the small pore size of the selected filter paper, the filtration process is extremely slow. To increase the speed of the filtration process, a pump is utilised to extract the air from the Erlenmeyer flask. This creates a pressure difference between top and bottom of the funnel so that the solution can move downwards to counteract the air movement. During the filtration process, fresh water is also fed into the funnel to make sure that all of the solution is dissolved and moved down into the flask. The experimental rig for the filtration process is shown in Figure 4-2 along with a schematic chart.

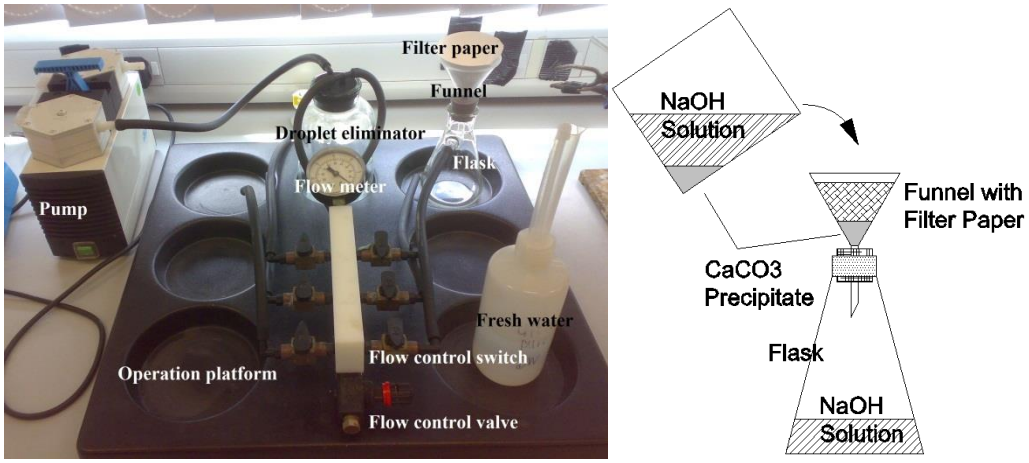

A B

Figure 4-2 Experimental rig (A) and schematic chart (B) of filtration processes

4.2.2. Apparatus

The objective of this section is to introduce the key apparatus involved in the experiments and to explain their function and operation during the experiments.

- CO_2 tank (bottle)

The CO_2 bottle is a container filled with high purity pressured CO_2 gas. It is supplied by the company BOC and the bottle is a vapour withdraw cylinder borrowed from the same company. The gas from the bottle is used for the absorption reaction process. In a practical

process, the gas will be provided by the engine exhaust gas which will have been purified by the gas separator as was discussed in the previous chapter.

- Regulator

A regulator is applied to control the gas inlet pressure. The regulator is compatible with the CO_2 bottle and it is also made by BOC. There are two meters on the regulator as presented in Figure 4-3. The left one is the outlet pressure meter and the right one is the inlet pressure meter. The pressure from the bottle cannot be controlled but it is within the measurement range of the inlet pressure meter. The gas pressure from the bottle can be displayed by the meter on the right. The outlet pressure of the regulator can be controlled and measured with the other meter. Because the system on a ship is under atmospheric conditions, the outlet pressure is selected and controlled to be 1 bar.

Figure 4-3 Flow meter and regulator used in the experiment

- Flow meter

After the regulator, a flow meter is attached to control the gas flow rate, which is one of the significant factors that can affect the experiment. The maximum flow rate which can

be measured by the meter is 15 L/min and the minimum rate is 1L/min. There is also a valve controller on the flow meter, thus the exact flow rate required can be obtained by adjusting the controller.

- Diffuser

The use of diffuser is to distribute the CO_2 gas evenly into the absorption reaction tank. It is coupled to the pipe with a connector. It is made from ceramic which can resist the corrosion of strong alkalis. The applied gas diffuser is shown in Figure 4-4.

Figure 4-4 Gas diffuser applied in the experiment.

- Measuring cylinders and beakers

Two different sizes of measuring cylinders, and a beaker, are selected to act as the absorption reaction tanks. Two measuring cylinders with maximum volumes of 1 L and a 2 L are selected and another beaker with maximum volume of 2 L is also used in the experiment. The diameters of the three containers are different so that the impact of the shape of the containers on the absorption rates can be analysed. Furthermore, 3 more plastic beakers are used during the solution preparation. Attention should be paid when preparing

the solutions. A large amount of heat will be generated during preparation. To avoid water from boiling, water should not be added into the solid NaOH. This is extremely dangerous as the water vapour will now contain NaOH which is highly corrosive. The operation should be that add the solid NaOH into the water and the heat generated during the dissolving process will be absorbed by the water, which can also increase the dissolving process. Then more water is added to the beaker so that the required concentration of the solution can be reached.

- Scales

There are three scales used in the experiments. Two of them are presented in the experimental rigs in Figure 4-1 and another one is used for measuring the weight of the chemicals. All measurements are accurate to two digits as the data collected from the scales will be used in later calculations.

- Test tube

A test tube is often used for collecting samples. In this case, after the absorption, a sample of Na_2CO_3 solution is taken using a test tube and then CaO will be added into it to generate sediment $CaCO_3$. It also makes it easy to generate sediment by shaking the test tube.

- Filter paper

Whatman grade 589/3 qualitative filtration paper is used for the separation of the NaOH solution and sediment $CaCO_3$ in the experiment. This type of filter paper is suitable for high retention of fine particles and has an excellent resistance to strong alkali solutions. The filter paper is selected also due to the size of the funnel used. The particle size of $CaCO_3$ ranges from 1 to 3 μm and the pore size of the filter paper is less than 2 μm which is the smallest one available for laboratory use. The small pore size leads to a slow filtration process, but also results in a very small amount of $CaCO_3$ slipping through the filter.

- Funnel and Erlenmeyer flask

Glass funnels and Erlenmeyer flasks are used in the filtration process. They are coupled to each other. Solutions from the precipitation reaction are poured into the funnel lined with filter paper and the clear solution left in the Erlenmeyer flask is the regenerated NaOH solution. The glass apparatus are selected to make it easy to observe the filtration process and the clear solution. If the solution is cloudy, it indicates that the sediment has leaked into the flask so filter paper with a smaller pore size should be applied.

- Pump

Due to a very small pore size in the selected filter paper, the filtration process is slow. Hence, an air pump is utilised to accelerate the process. The pump is connected to an operation platform with a gas control switchboard, gas control valve, flow meter and droplet eliminator. The gas control switch should be turned on or off in order to start or stop pumping. The gas control valve can control the gas flow rate through the filtration system. The total flow rate through the pump can be observed from the flow meter. A droplet eliminator is applied to make sure no liquid is drained into the pump. Otherwise, there is a risk of damaging the pump.

- Inductively Coupled Plasma (ICP)

An ICP system is applied to detect the concentration of metal elements (Na and Ca) in the solution. If the concentration of these elements is derived, the concentration of the related compounds (NaOH, Na_2CO_3, $Ca(OH)_2$) can be obtained. It is a powerful tool which can be accurate to 0.0001mg/L. Data from the ICP will be applied in later calculations as well.

As the experiment rig is completed with all these apparatus, the experiments can be conducted and will be described in the following section.

4.3. Experiment Processes and Operations

In this section, the processes and operations of the experiments will be illustrated. The processes include preparation, the absorption reaction process, the precipitation process, the filtration process and the product testing process. This section will introduce all the operations in these processes, including preparation, reaction, measurement, filtration and so on. The product testing process is the application of an indicator and of the ICP to examine the composition and also the concentrations of ions of the final products. It will be carried out once the other reaction processes are completed.

The NaOH solution is prepared in the preparation process. For example, if preparing 1 litre of NaOH solution with a molar concentration of 4 mole/L, the quantity of NaOH solute in the solution is first calculated, to give 1 L*4 mole/L = 4 mole. Then the mass of the NaOH solute can be derived from the molar mass of NaOH which is 40 g/mole. The mass of NaOH solute is found to be 4 mole * 40 g/mole = 160 g. After weighing out the exact amount of NaOH using the scales, the solute will be added into water in a beaker. When all of the solute is dissolved into the water, the solution is poured into a measuring cylinder. The beaker is then washed with fresh water and also poured into the measuring cylinder. Then fresh water is added into the measuring cylinder until it reaches the required volume, in this case 1 litre. The prepared solution will be used for absorbing the CO_2 in the absorption reaction process.

In the absorption reaction process, the gas will be provided by the CO_2 tank, controlled by the regulator and the flow meter and then fed into the measuring cylinder, which now contains the NaOH solution. Two scales are utilised for observing the instantaneous weights of the measuring cylinder and the CO_2 bottle. Their weights are recorded regularly (usually every 5 minutes) and also at the end of the absorption process. The difference between two different measurements in the measuring cylinder is the amount of CO_2 absorbed. The amount of CO_2 released from the CO_2 bottle can also be derived from the

weight changes displayed on this scale. As the total gas fed in and absorbed is calculated, the absorption rate of this process can be obtained.

Three samples are collected in test tubes from the product solution of the absorption process and used for the precipitation process. The average results are derived for these sample tests. A PH indicator, Phenolphthalein, is used to indicate the complete of reaction. It is added to each sample and the colour change of the solution can be observed. If the colour turns pink, it means there is still some NaOH left in the solution. Otherwise, the NaOH solute has been used up for absorption.

The required amount of CaO for a full reaction is derived based on the relationship in the precipitation reaction in Equation (2). Since all of the NaOH may not be used up during the absorption process, the CaO provided can be sufficient or even excessive. This means that all of the absorbed CO_2 will be precipitated as sediment $CaCO_3$. The precipitation efficiency can be improved by increasing the contact between the CaO and the solution. Shaking the test tube is applied. For a practical system on a ship, this can be achieved by installing a stirring device. The mixture of $CaCO_3$ sediment and NaOH solution will be treated and separated in the following filtration process.

The filtration starts with the mixture of $CaCO_3$ sediment and NaOH solution which is poured into the funnel lined with filter paper. To increase the speed of the filtration process, a pump is used as discussed previously in Figure 4-2 (A). Without the pump working, the filtration can also proceed however the flow rate of the solution going through the funnel is slow. With the pump working, a pressure difference is generated between the inside and the outside of the flask. Fresh water will be added in order to dissolve any residual NaOH left on the filter paper. The clear solution in the flask will be tested using the ICP so that its ingredients can be identified. The sediment will be dried in a lab oven and then weighed using scales. Thus the NaOH regeneration rate and $CaCO_3$ production rate can be derived. The flowchart of designed experiments is presented in Appendix 1.

4.4. Experimental Results and Analysis

Table 4-1 presents the experimental results which have been obtained for the gas absorption rate, the NaOH regeneration rate and the $CaCO_3$ filtration efficiency. The surrounding conditions in the laboratory are atmosphere conditions. The CO_2 absorption rate is a ratio between the gas absorbed and the gas fed into the cylinder. The regeneration rate of NaOH is defined as the ratio of NaOH regenerated to that initially supplied. The $CaCO_3$ filtration efficiency is determined by the ratio of $CaCO_3$ actually separated to that which could theoretically be formed by the reaction.

Table 4-1 Experimental results

Experiments Rates	Results
CO_2 Absorption Rate	67.85%
NaOH Regeneration Rate	85.37%
$CaCO_3$ Filtration Efficiency	82.17%

According to these results, the gas absorption rate is found to be nearly 68%. This is only the reaction rate with laboratory equipment. For an industrial application, a much higher mixing rate of gas and solution can be obtained by using a packing or a tray column design. These design structures could increase the contact area between phases so that the absorption rate will be higher than that in laboratory. However, another factor to be considered in the industrial processes is the purity (concentration) of the CO_2 gas. Due to the impurities in the gases, purification treatment will be required to guarantee the gas purity. The $CaCO_3$ filtration efficiency is also expected to be much higher in a practical application because industrial filtration methods, such as centrifugal separation or pressure disc filters, can be applied to improve the efficiency. This table also indicates that the NaOH regeneration rate and $CaCO_3$ filtration efficiency are close to each other because they are based on the same reaction process (the precipitation reaction: Equation (2)). The difference is due to the losses from the processes, such as left in test tube and flask.

Five parameters were examined to find out their impacts on CO_2 absorption rates during the experiment: NaOH initial concentration, gas flow rate, change in absorption with change in cylinder diameter and fixed volume of solution, change in absorption with change in cylinder diameter and unchanged solution column height, and change in absorption with change in solution column height and the same diameter of the cylinder. The following sections will present the analysis and results derived from these experiments.

4.4.1. Impact of Initial NaOH Concentration on Absorption Rate

In this section a study of how initial NaOH concentrations impact on the absorption rate is presented through a series of experiments. Five different concentrations are selected for testing: 5%, 10%, 15%, 20% and 25%. The procedures for solution preparation are following:

1. Calculate the molar concentrations (mole/L) of solutions for different mass concentrations
2. Then calculate and weigh for the quantity (mass) of NaOH need to prepare solution with certain molar concentration
3. Add some water and then the measured NaOH into water. Stir for rapid dissolution
4. Add water to 1L after the temperature of solution goes down to room temperature

For each selected concentration, three runs of the experiment are carried out and the average results are used in the analysis. The results are presented in Table 4-2 and Figure 4-5.

Table 4-2 Change of absorption rates with initial NaOH concentrations

Mass fractions	*5%*	*10%*	*15%*	*20%*	*25%*
Average absorption rates	22%	36%	47%	41%	30%

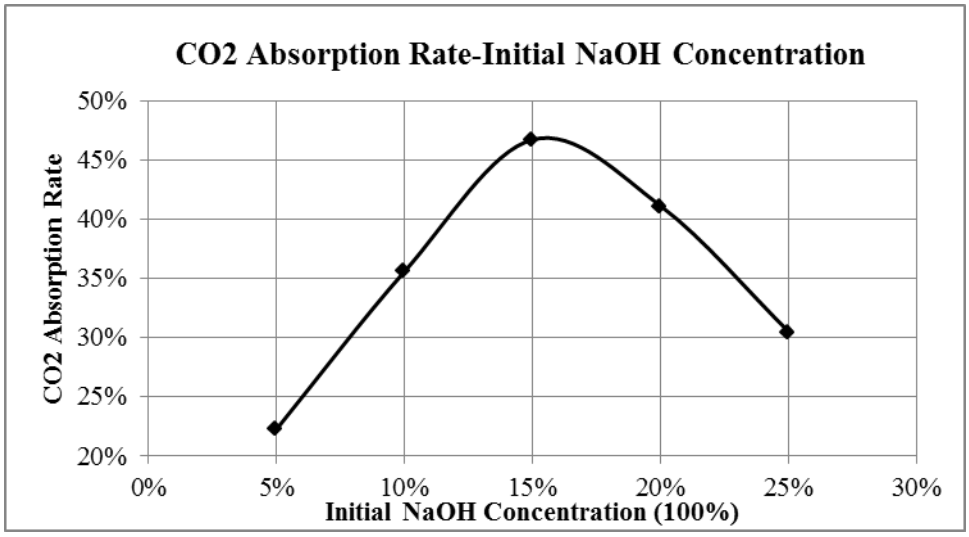

Figure 4-5 CO_2 absorption rate vs. initial NaOH concentration

It is apparent that the gas absorption rate has an optimal value when the concentration of the solution is 15%. There are two factors dominating the reaction rate between the gas and solution: the NaOH solution concentration and the contact area between the two phases. When the concentration is lower than 15%, the gas absorption rate grows with the increased concentration of the solution. However, the rate drops when the concentration is greater than 15%. It is because the density of the solution grows with the concentration of the solution increases. It results larger pressure and lead to small bubble sizes in the solution. Smaller bubbles will have a smaller contact area between gas and solution. At about 15% NaOH concentration, the gas bubble size is decreased to a critical value. Therefore when the initial NaOH concentration is 15%, the absorption process has an optimal absorption rate.

4.4.2. Impact of Gas Flow Rate on Absorption Rate

To find out the effect of the gas flow rate on the CO_2 absorption rate, three runs of the experiment with different gas flow rates are conducted. The selected gas flow rates are 1, 2 and 3 L/min. The selection of gas flow rate is restricted by the experimental equipment because a gas flow rate which is too high will lead to an unstable pipe connection and even

disconnection. To guarantee accuracy of readings on the flow meter, only integer scales (gas flow rates) are selected for comparison. For the three selected runs, the quantity of the solution is controlled. The 1 L measuring cylinder is selected which has a diameter of 6 cm. The solution column height is fixed at 30 cm so that the quantity of solution is also fixed. The concentration of NaOH solution is also constant. As the optimal absorption rate is our target, the optimal concentration of NaOH solution of 15% is selected. The results are presented in Table 4-3 and Figure 4-6.

Table 4-3 Change of absorption rate with gas input flow rate

Solution volume (ml)	Solution column height (cm)	Cylinder diameter (cm)	CO_2 Flow Rate (L/min)	CO_2 Absorption Rate
~900	30	6	1	78%
			2	76%
			3	75%

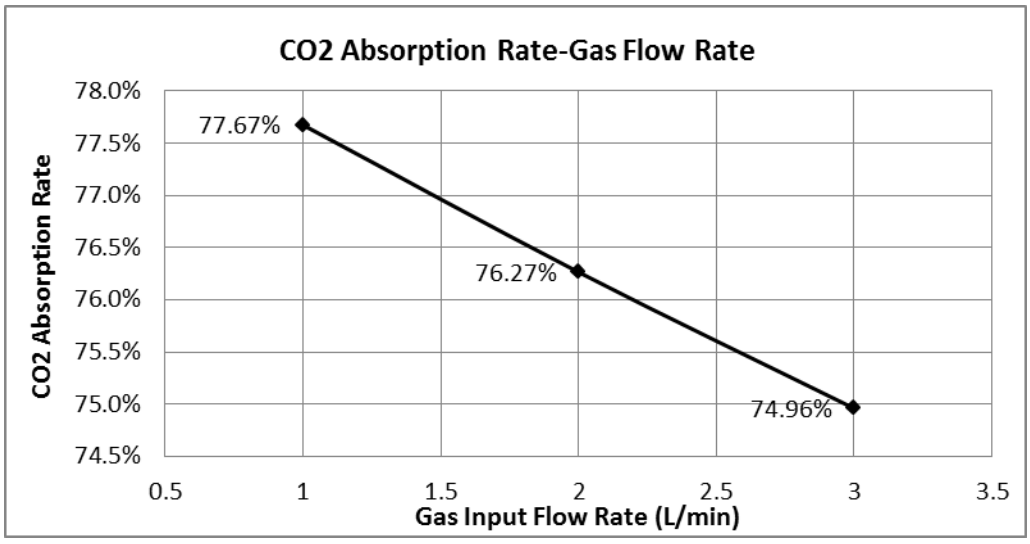

Figure 4-6 CO_2 absorption rate vs. gas flow rate

According to the experimental results, the CO_2 absorption rate increases as the input gas flow rate decreases. This is reasonable because a lower gas flow rate allows more time for contact between the gas and the solution. As the gas flow rate increases, the amount of CO_2

missed by the absorption process will be increased. However, the rate difference is only 2.7% when the gas flow rate is increased from 1 L/min to 3 L/min. Hence, it is obvious that the flow rate has a less significant effect on the absorption rate under the conditions used in the experiment. However, a prediction can be made that when the gas flow rate is too high, the mixing will be impacted. Gas may not be able to come into contact with the solution, which will decrease the absorption rate.

4.4.3. Impact of Cylinder Diameters on Absorption Rate with Fixed Volume of Solution

According to Table 4-4 and Figure 4-7, the absorption rate is lower when the container has a larger diameter. It is easy to see that a container with a large diameter leads to a lower column height. This is because column height is reduced as the cylinder diameter is increased when the volumes of the solution are fixed. From the observation, a lower solution column height means a shorter time between the CO_2 gases going in and releasing from the solution. When the diameter is increased from 6 to 8 cm, 3% more of the gas is released and wasted. The absorption rate grows from 65.44% to 72.08% when the diameter is increased from 8 to 10 cm. From the curve above, the decline of the curve is obviously faster along the X axis. Hence, the absorption rate will be increasingly reduced when enlarging the diameter. On the contrary, narrowing the diameter will greatly increase the absorption of gas, when changing the diameter of the cylinder with fixed volume of solution. It is a feasible and effective way of enhancing CO_2 absorption rate by simply increasing the contact rate between the gas and the solution.

Table 4-4 Changes in absorption rate with container diameter (solution quantity fixed)

Solution volume (ml)	Solution column height (cm)	Cylinder diameter (cm)	CO_2 Flow Rate (L/min)	CO_2 Absorption Rate
~900	30	6	3	75%
	18	8		72%
	10.5	10		65%

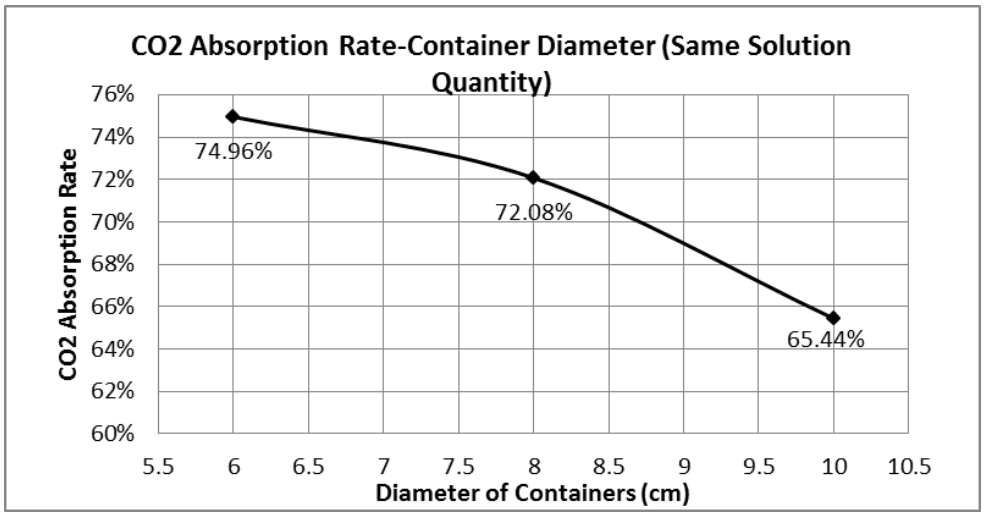

Figure 4-7 Effect of container diameter on gas absorption rate with unchanged solution quantity

4.4.4. Impact of Cylinder Diameters on Absorption Rate with Fixed Solution Column Height

According to the conclusion above, a better mixing and longer contact time between gas and solution will result in a higher absorption rate of the CO_2 gas. The results in Table 4-5 and Figure 4-8 show the effect of changing cylinder diameter (cross-sectional area) on absorption rate with fixed solution column height.

Table 4-5 Changes of absorption rate with container diameter (fixed solution height)

Solution volume (ml)	Solution column height (cm)	Cylinder diameter (cm)	CO_2 Flow Rate (L/min)	CO_2 Absorption Rate
296.88		6		54%
527.79	10.5	8	3	64%
824.67		10		65%

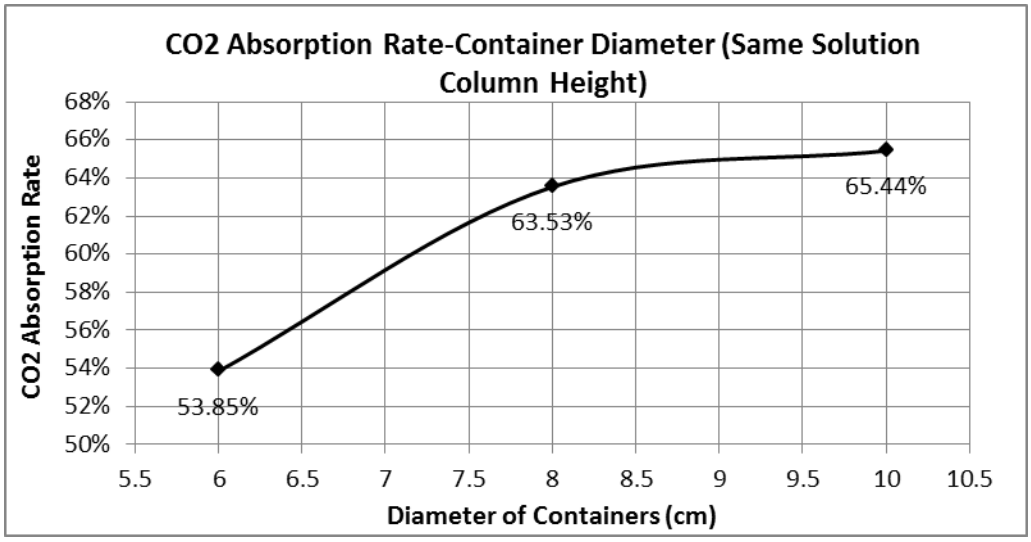

Figure 4-8 Effect of container diameter on gas absorption rate with fixed solution height

Results show that when the cylinder diameter grows from 6 to 10 cm with the same column height of 10.5 cm, the highest absorption rate takes place when the diameter is 10 cm. When the diameter is increased from 6 to 8cm, the absorption rate is increased by 9.7%. With a further increase in the diameter from 8 cm to 10cm, the rate is further increased by only 1.91%. The results indicate that the increase of container diameters will lead to increment in absorption rate. However the increment rate is getting slower which is because the size of diffuser is not changed with the diameter increasing. It is reasonable because when the cross-section is too large the gas bubbles could not reach the edges of the cylinder. Hence, this means that test rig optimisation can be achieved by the combined optimisation of solution column cross-sectional area, diffuser size and column height.

4.4.5. Impact of Column Height on Absorption Rate with a Fixed Diameter

According to Table 4-6 and Figure 4-9 above, the absorption rate is increased when the height of the solution column is increased. This is because as the solution height increases, the distance the gas has to travel is increased, resulting in an increase in the contact time between the gas and solution hence more gas will be absorbed. When the height is increased from 10.5 to 18cm, the absorption rate is raised by 16.09%. The rate grows only a further

5.02% when the solution column height is changed from 18 to 30cm. This is because the path for the gas is so short that the contact time with the solution is not enough with a small solution column height. When the solution height increases, the improvement in absorption rate increases significantly at the beginning and then it becomes minor. This indicates that there is an optimal match between the column height and the gas supply rate. The experiment results all these cases are shown in Appendix 2.

Table 4-6 Changes in absorption rate with solution column heights (fixed container diameter)

Solution volume (ml)	Solution column height (cm)	Cylinder diameter (cm)	CO_2 Flow Rate (L/min)	CO_2 Absorption Rate
848.23	10.5			54%
508.94	18	6	3	70%
296.88	30			75%

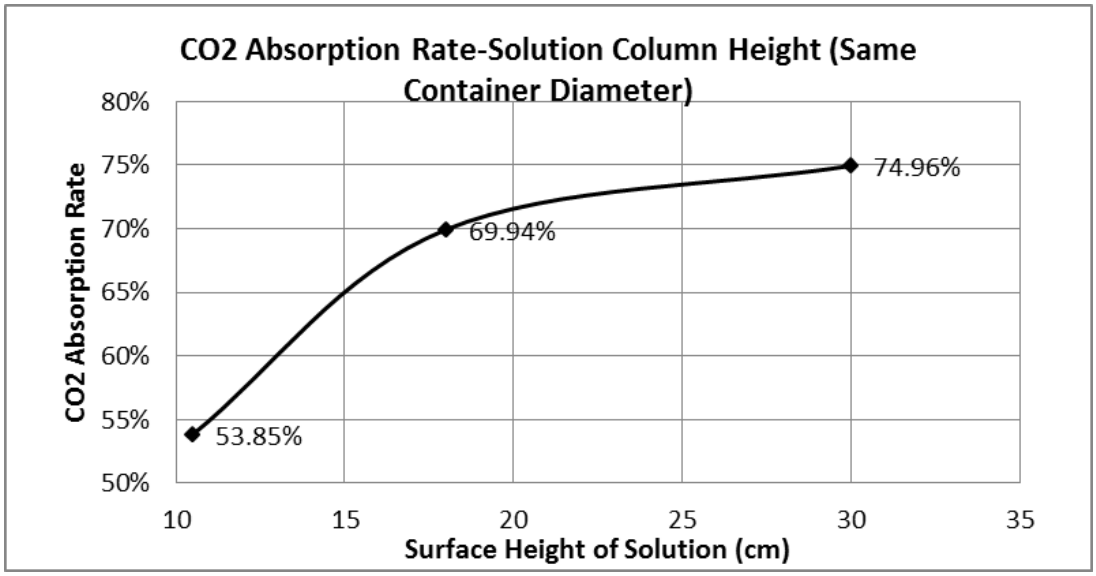

Figure 4-9 Effect of solution column height on gas absorption rate with same cylinder diameter

4.5. Experimental Errors and Accuracy

Two scales are applied to measure the weights of the CO_2 tank and the reaction tank. The weight of the full CO_2 tank is around 18 kg and the initial weight of the reaction tank (with designed quantity of solution) is about 1 kg. The minimum increment of the scale for the CO_2 bottle is 0.01 kg and that of the scale for the reaction tank is $1\ 10^{-7}$ kg. The accuracy of the scales is presented in Table 4-7. The accuracy of the scale for CO_2 bottle measuring is $\pm5\times10^{-3}$ kg and that of the scale for the reaction tank measurement is $\pm1\ 10^{-4}$ kg.

Another scale is applied to measure the weights of the chemical materials. The weights of these materials are around 0.1 kg. The minimum increment of the scale for the chemical raw material measurement is 1×10^{-4} kg. The accuracy of this scale is $\pm2\times10^{-7}$ kg.

Table 4-7 Details of scales used in experimental measurements

Item	*Type*	*Range (kg)*	*Accuracy (kg)*
Scale for CO_2 bottle measurement	EHI-B	0-50	$\pm5\ 10^{-3}$
Scale for reaction tank measurement	OHAUS GT-8000	0-8	$\pm1\ 10^{-4}$
Scale for chemical raw material measurement	AND HR-200	0-0.21	$\pm2\ 10^{-7}$

During the absorption process, a regulator is applied to control the pressure of the gas inlet and a flow meter is used to control the volume flow rate. The minimum increment for the regulator is 0.01bar and the gas inlet pressure is set to 1.00 bar so that the reading is also acceptable. The flow meter has a minimum increment of 1 L/min so three different flow rates are eventually selected: 1, 2 and 3 L/min. The selected flow rates are no larger than 3 L/min because the fitting between the diffuser and the pipe could be damaged. The reading is limited by the flow metre so a reasonable selection of flow rates is applied. Only integer values are selected since there are only integer graduations. If non-integer values are selected, the reading accuracy is unacceptable.

In order to reduce the impact of errors during the measurements, three runs were carried out for each set of experiment. Then the average results were derived for different experiment sets and therefore these average values would be used for calculation and compared with simulation results. For example, when evaluating the impacts of solution

concentrations on the absorption rate, three sets of experiments were carried out for different concentrations: 5%, 10%, 15%, 20% and 25%. For experiments with 15% NaOH, the absorption rates are 47.6%, 46.7% and 46.0% and the average result is 46.7%. Hence, this value will be used for following calculations in precipitation reaction and also for validation of simulation models.

4.6. Conclusions

The laboratory experiments examined the impacts of five key factors in the proposed carbon capture and storage system. The results show that the CO_2 absorption rate varies with various parameters, such as NaOH solution volume, height, cross-sectional area and CO_2 gas flow rate. The results provide an insight into the carbon absorption effectiveness and offer a useful reference for on-board system design.

Based on the principles of the carbon capture solidification processes introduced, three steps to the experiment were designed: chemical absorption, precipitation, and physical filtration. The experimental rigs and apparatus involved were presented and explained in this chapter. The results from the experiments indicate the impacts of several significant factors on absorption rate. The optimal NaOH initial concentration is 15% and gas flow rate has only a very slight impact on absorption rate under experimental conditions. However, the geometry of the reaction tanks has a significant influence on absorption. When the volume of solution is fixed, reducing the tank diameter can improve the absorption rate. If keeping the column height constant, increased absorption rate can be achieved by increasing the diameter. With the same diameter, a higher solution column height results in a better absorption rate. In the last section, the accuracy of the experiments was analysed. Through this it can be concluded that the proposed chemical processes for carbon dioxide solidification are effective as they can effectively absorb 67% of CO_2 gas and store it in the form of a solid compound. Moreover, the experimental data can be applied in further research such as a case study on a ship and in system CFD simulations.

CHAPTER 5. SIMULATION OF THE ABSORPTION PROCESS

5.1. Introduction

This chapter presents numerical simulations of the lab-scale absorption process. No full scale simulations will be carried out at this stage. The numerical simulations will provide fundamental details and understanding for the design of a proto-type demonstration system on-board a ship. Parameter variations in the simulations such as pressure drop, solution concentration change and gas phase velocity will be considered and presented. Comparisons between the experimental data and simulation results are presented and the optimised conditions for the factors mentioned are also analysed in this chapter.

5.2. Methodology for Simulation

The chemical process comprises of two main components: species transportation and multiphase flow. To simulate a chemical process with CFD tools, both components should be considered. Species transportation is considered in the numerical simulation by transferring masses, energy and momentum of the reactants into the products. Multiphase flow is simulated using bubble column effects due to the mixing of liquid and gas in the reactants. The involved gases are CO_2 and air while the NaOH and Na_2CO_3 solutions are in liquid form.

The commercial CFD software package ANSYS Fluent solves conservation equations for chemical species by predicting the local mass fraction of each species through the solution of a convection-diffusion equation. The convection-diffusion equation for the specified species (ANSYS Fluent theory guide 14.5, 2012) is shown as follows:

$$\frac{\partial}{\partial t}(\rho Y_i) + \nabla \cdot (\rho \vec{v} Y_i) = -\nabla \cdot \vec{J}_i + R_i + S_i \quad (5)$$

Where:

Y_i = the local mass fraction of each species;

R_i = the net rate of production of species i by the chemical reaction;

S_i = the rate of creation from the dispersed phase and sources;

J_i = the mass diffusion flux;

$\vec{v}$ = the overall velocity vector (m/s);

t = time;

ρ = the density of the species.

For an Eulerian multiphase model, the concept of phasic volume fractions is introduced and the volume of one phase can be defined as:

$$V = \int_V a dV \tag{6}$$

Where:

a = the volume fraction of the phase.

The continuity equation of phase q (for fluid-fluid mass exchange) is:

$$\frac{\partial}{\partial t}\left(a_q \rho_q\right) + \nabla \cdot \left(a_q \rho_q \vec{v}_q\right) = \sum_{p=1}^{n}(\dot{m}_{pq} - \dot{m}_{qp}) \tag{7}$$

Where:

$\vec{v}_q$ = the velocity of phase q;

$\dot{m}_{pq}$ = the mass transferred from phase p to q ;

$\dot{m}_{qp}$ = the mass transferred from phase q to phase p.

The energy conservation equation in the Eulerian model is:

$$\frac{\partial}{\partial t}\left(a_q \rho_q h_q\right) + \nabla \cdot \left(a_q \rho_q \vec{u}_q h_q\right) = a_q \frac{\partial p_q}{\partial t} + \bar{\tau}_q : \nabla \vec{u}_q - \nabla \cdot \vec{q}_q + S_q + \sum_{p=1}^{n} (Q_{pq} + \dot{m}_{pq} h_{pq} - \dot{m}_{qp} h_{qp}) \qquad (8)$$

Where:

h_q is the specific enthalpy of the q^{th} phase;

$\vec{q}_q$ is the heat flux,

S_q is a source term that includes sources of enthalpy, such as from the chemical reaction;

Q_{pq} is the intensity of the heat exchange between the p^{th} and q^{th} phases, and

h_{pq} is the interphase enthalpy (for example, the enthalpy of the vapour at the temperature of the droplets, in the case of evaporation). The heat exchange between phases must comply with the local balance conditions $Q_{pq} = -Q_{qp}$.

The conservation of momentum for a fluid phase is:

$$\frac{\partial}{\partial t}\left(a_q \rho_q \vec{v}_q\right) + \nabla \cdot \left(a_q \rho_q \vec{v}_q \vec{v}_q\right) = -a_q \nabla p + \nabla \cdot \bar{\bar{\tau}}_q + a_q \rho_q \vec{g} + \sum_{p=1}^{N} (K_{pq}\left(\vec{v}_p - \vec{v}_q\right) + \dot{m}_{pq} \vec{v}_{pq} - \dot{m}_{qp} \vec{v}_{qp})$$
$$+ (\vec{F}_q + \vec{F}_{lift,q} + \vec{F}_{wl,q} + \vec{F}_{vm,q} + \vec{F}_{td,q}) \qquad (9)$$

Where:

ρ = the density;

p = the pressure for all phases;

g = the gravitational acceleration;

K = the momentum exchange coefficient between fluid phases;

$\vec{F}_q$ = external body force;

$\vec{F}_{lift,q}$ = lift force;

$\vec{F}_{wl,q}$ = wall friction force;

$\vec{F}_{vm,q}$ = virtual mass force;

$\vec{F}_{td,q}$ = turbulent dispersion force (for turbulent flow only).

$\bar{\bar{\tau}}$ is the stress-strain tensor of q^{th} phase:

$$\bar{\bar{\tau}}_q = a_q \mu_q \left(\nabla \vec{v}_q + \nabla \vec{v}_q^{\,T} \right) + a_q \left(\lambda_q - \frac{2}{3} \mu_q \right) \nabla \cdot \vec{v}_q \bar{\bar{I}} \tag{10}$$

Where:

μ_q = shear of phase q

λ_q = bulk viscosities of phase q

$\bar{\bar{I}}$ = unit tensor.

$\vec{v}_{pq}$ = the interphase velocity, defined as follows: If $\dot{m}_{pq} > 0$ (that is, phase *p* mass is being transferred to phase *q*), $\vec{v}_{pq} = \vec{v}_p$; If $\dot{m}_{pq} < 0$ (that is, phase q mass is being transferred to phase p), $\vec{v}_{pq} = \vec{v}_q$. If $\dot{m}_{pq} > 0$, then $\vec{v}_{qp} = \vec{v}_q$; If $\dot{m}_{pq} < 0$, $\vec{v}_{qp} = \vec{v}_p$.

The reaction rate, *r*, between phases can be derived by the following equation:

$$r = k(T)[A]^m[B]^n \tag{11}$$

Where:

k(T) = the reaction rate constant that depends on temperature,

[A] = the concentrations of substances *A* in moles per volume of solution (assuming the reaction is taking place throughout the volume of the solution) and the exponents, *m* and *n*, are partial orders of the reaction which depend on the reaction mechanism.

The reaction rate constant, *k*, is estimated by using the Arrhenius expression:

$$k = AT^{\beta}e^{-E/RT} \tag{12}$$

Where:

A = the pre-exponential factor;

T = the temperature of the reactants (K);

β = the temperature exponent;

E = the activation energy for the reaction;

and R = the universal gas constant.

The surface tension is required in the modelling of the bubbling effect:

$$\Delta p = 2\sigma/R \tag{13}$$

Where:

Δp = the pressure difference between two sides of the surface (Pa);

σ = the surface tension coefficient;

and R = the radius of the bubbles.

Wall adhesion is also considered for the bubbling effect and the surface normal at the live cell next to the wall is:

$$\hat{n} = \hat{n}_w cos\theta_w + \hat{t}_w sin\theta_w \tag{14}$$

Where:

$\hat{n}_w$ = the unit vectors normal to the wall

$\hat{t}_w$ = the unit vectors tangential to the wall;

θ_w = the tangent angle of the gas bubbles or liquid droplets to the wall as indicated in Figure 5-1.

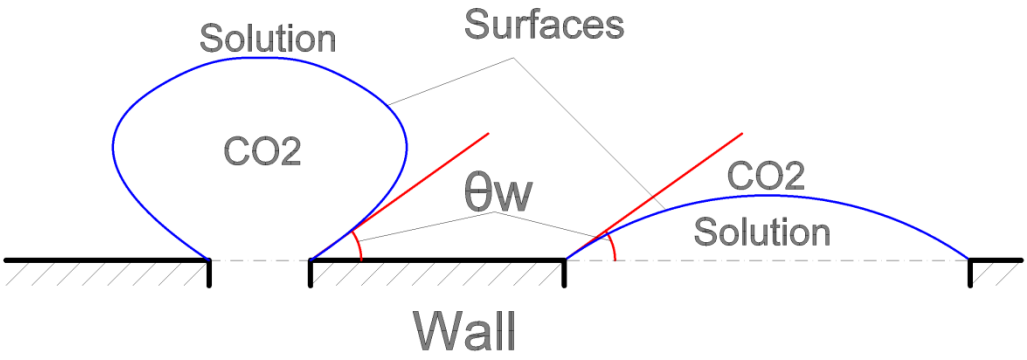

Figure 5-1 Demonstration of the contact angle between gas-solution surface and wall.

5.3. CFD Simulations

5.3.1. Assumptions, Modelling and Simulations using CFD

Before the modelling and simulation, it is essential to apply a range of assumptions during these procedures in order to simplify the problem and model the geometry. These assumptions are highlighted below:

- The conditions of the surrounding environment are set as follows: temperature of 298 K, pressure of 101325 Pa and gravity of 9.81 m/s^2.

- As the simulation focuses on the reaction in the measuring cylinder, the whole rig is simplified to a 2-dimensional model which is shown in Figure 5-2.

- For the bubble column simulation, the diffuser is simplified as ten separated inlets at the bottom to avoid the need for an unstructured grid. For simulating the combination of the chemical reaction with the bubble column, further simplification of the inlet is applied to reduce computational intensity.

- The gas fed in is an ideal gas. Fluids and gases are both incompressible.

- The gas bubbles have a minimum diameter of $1x10^{-5}$ metres.

- An artificial extension of the measuring cylinder is applied to avoid the impacts of backflow on the absorption reaction.

- All the solutions are modelled as hydrated compounds to consider them as individuals.

The model is a 2D column which comprises of solid walls with ten inlets on the bottom and one outlet at the top. The geometry of the model uses actual scale parameters from the experiments. The column height is 0.6 metres and the width of the column is 0.06 metres.

The height of the solution in the column is 0.3 metres. The structured grid is applied with a minimum length of 5 10^{-4} m and there are 108,000 mesh units in this model. Structured meshing is selected as the shape of the reaction tank is also rectangular (Jiyuan et al., 2013). The flow rate in the experiment is 3 L/min so the gas input flow rate in the simulation is 1.90 10^{-3} kg/s.

The simulation of the absorption reaction is based on the use of the Fluent software and it includes both the chemical reaction and the bubble column simulations. Since the simulation involves a chemical reaction and a two-phase flow at the same time, the Eulerian model is selected. This is simply because the Eulerian model is compatible with multiphase reaction simulations and can also simulate the process very closely compared to the practical hydrodynamic phenomena (Asendrych et al., 2013). One simulation case of the absorption reaction will be presented, and it takes 405 s to finish the reaction. However, when numerically simulating the reaction, the total number of time steps will be 81000 with a time step size of 5 10^{-3}s. With the support of the High Performance Computer facility from ARCHIE-WeST, the real-time cost of each time step is about 2 s when using 4 cores. Hence, for each case, the CPU-hours required are about 45 CPU-hours.

The mesh is selected through a mesh analysis comparing the accuracy and time consumed for different mesh sizes: 0.005m, 0.01m and 0.02m. With same simulation model, geometry model with different mesh sizes were simulated and the results were compared with experiment in Figure 5-3. This figure indicates that with finer mesh, the computing time cost is much higher and so is the accuracy. However, the calculation time cost with mesh size 0.005m is 8 times longer than 0.01m and the accuracy is only increased by about 10%. Therefore, considering both the acceptable accuracy and computing time, the mesh size is selected to be 0.01m.

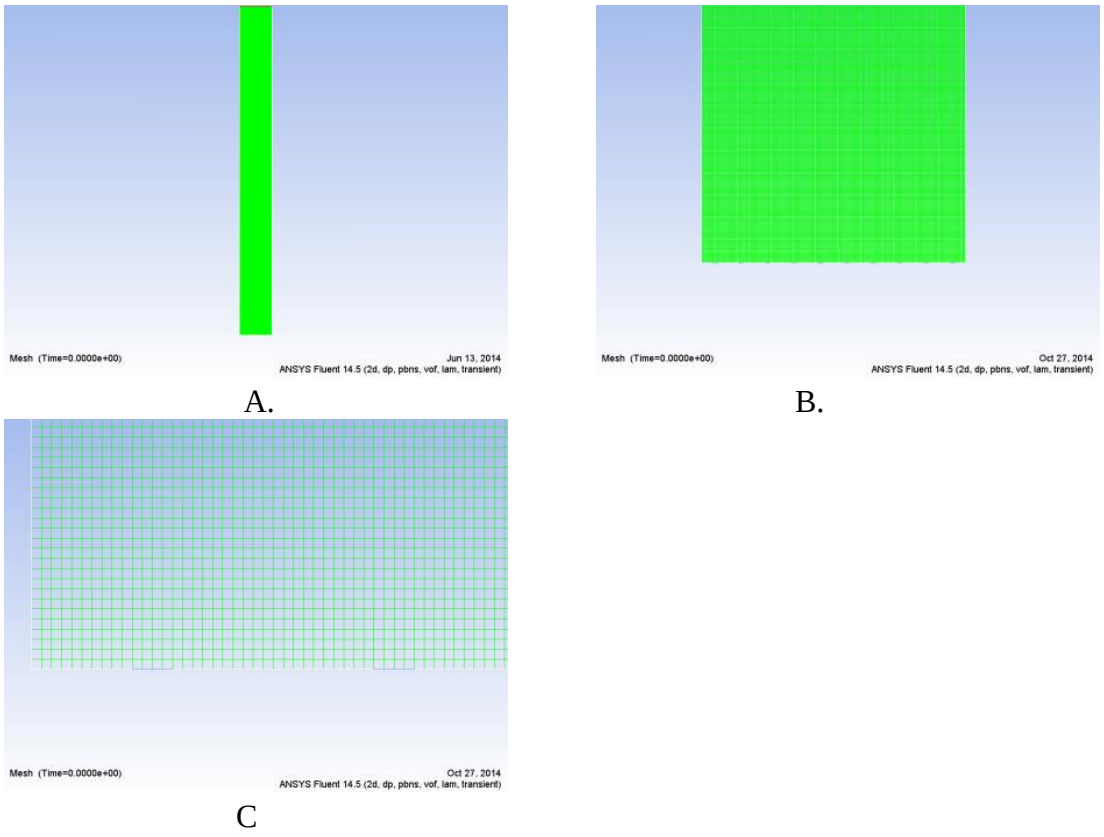

Figure 5-2 Modelling and meshing of the experimental rigs (A: graph of the whole model and mesh; B: the distribution of inlets at the bottom of model; C: the size of meshing)

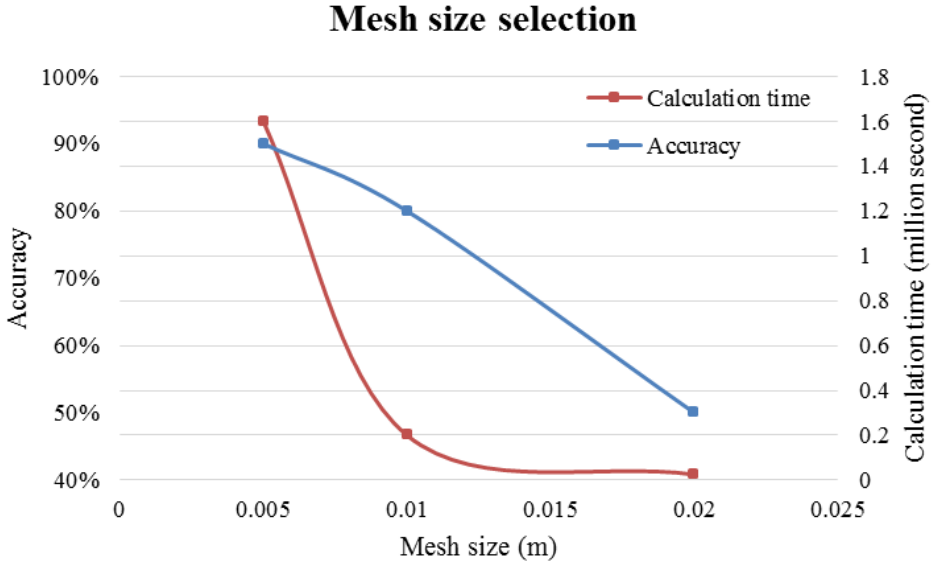

Figure 5-3 Mesh size analysis: simulation accuracies and time under different mesh sizes.

5.3.2. Parameters and Settings

After selection of the phase interaction model and reaction model in the last section, the selection of other models will be presented in this section. There are also many significant parameters in these models therefore this section will demonstrate how to derive and set these parameters. This section will also illustrate how the results are monitored and analysed.

5.3.2.1. Model Selections

In the model setting panel of Fluent, there are several models which can be added and considered in a CFD model. The absorption process is a two-phase interaction and reaction so the multiphase, energy, viscous and species models should be included in the simulation. It is discussed in the literature reviews presented in Chapter 2 that the Eulerian model is the preferred option for our case. The energy model in Fluent is enabled to capture the energy exchange.

Hjertager and his colleagues note that most of the industrial chemical processes contain turbulent flows (Hjertager et al., 2002). Mohammad I. and Mohammad A. K. used the standard k-ε model for turbulence modelling and the results of the gas hold-up in the simulation showed good consistency with experimental data. Laminar simulations were also tested during their work and were found not to be capable of presenting the behaviour of the interaction adequately (Mohammad and Mohammad, 2011). Therefore, for all CFD work presented in this thesis, a standard k-ε model is selected as the turbulence model.

For the species model, the species transport model is enabled in order to enable phase interaction as the reaction processing.

5.3.2.2. Material and Phases Settings

The settings of materials refer to the materials database in Fluent and are also based on their actual properties in the experiments. In the materials database, air and CO_2 have already been created and can be imported into the model. Some properties of the materials in the database require slight adjustment because these data may have been achieved at different conditions. For example, the properties of CO_2 from the database are derived at 298.15K which is different from the laboratory temperature used in this work. Therefore, the temperature-related properties, such as density, are set based on standard values (Properties of carbon dioxide, Union engineering).

As there are no NaOH and Na_2CO_3 solution in the material database, these materials should be created and their properties input accordingly. The properties of NaOH are derived by applying software, the Lauterbach Verfahrenstechnlk GmbH evaluation version. One example of the results from the software is presented in

Figure 5-4. The enthalpies of the NaOH solution at different temperatures and concentrations have been researched by Haward and Warren (1942).

Other modifications to the properties are for the molecular masses. The standard molecular masses of NaOH and Na_2CO_3 solute are 40 and 106 g/mole but they will be in the solutions during the simulations. Therefore, the molecular mass of the NaOH and Na_2CO_3 solutions should be calculated to include the water content in the solutions. The integrated molecular mass is derived based on the total mass of the solution for every mole of NaOH. For example, 1 mole of NaOH has a mass of 40 g. When the concentration is 5%, 1 mole of NaOH solution (NaOH and water) will have a mass of 800 g. For the Na_2CO_3 solutions, the integrated masses are based on the molecular mass of Na_2CO_3 and also the quantity of water in the solutions. Since the reaction is consuming NaOH and turning it into Na_2CO_3 and water, the amount of water in the Na_2CO_3 solutions can be calculated. For 1 mole of NaOH consumed, 0.5 moles of Na_2CO_3 and 0.5 moles of water can be generated according

to Equation 1. The mass of 1 mole of 5% NaOH solution is 800 g so water is 760 g. Therefore there is 1 mole of NaOH and 42.22 mole of water in 1 mole of 5% NaOH solution. After the reaction, there are 0.5 moles of Na_2CO_3 solution which contains 0.5 moles of Na_2CO_3 solute and 42.72 moles of water (include 0.5 moles of water from the reaction). Hence, 1 mole of the Na_2CO_3 solution comprises 1 mole of Na_2CO_3 and 85.44 moles of water so the integrated molecular mass of the Na_2CO_3 solution is 1644 g/mole. The integrated molecular masses of the Na_2CO_3 solutions under different concentrations can be derived using the same procedures. Therefore, the properties of the NaOH and Na_2CO_3 solutions can be derived and are listed in Table 5-1 and Table 5-2.

Properties of sodium hydroxide NaOH

	State 1			State 2		
	ϑ_1 =	25	°	ϑ_2 =	25	°
	c_1 =	5	Weight%	c_2 =	10	Weight%
	c_1 =	52.5	g/l	c_2 =	110.4	g/l
	c_1 =	1.313	mol/l	c_2 =	2.76	mol/l
Saturation pressure	$p_{S,1}$ =	3020	Pa	$p_{S,2}$ =	2850	Pa
Properties:						
Density	ρ_1 =	1048	kg/m3	ρ_2 =	1102	kg/m3
Specific heat capacity	cp_1 =	3984	J/(kg·K	cp_2 =	3785	J/(kg·K
Thermal conductivity	λ_1 =	.6265	W/(m·K	λ_2 =	.6375	W/(m·K
Dynamic viscosity	η_1 =	1.191	mPa·	η_2 =	1.587	mPa·
Kinematic viscosity	ν_1 =	0.000001	m2/s	ν_2 =	0.000001	m2/s
Prandtl number	Pr_1 =	7.573	-	Pr_2 =	9.425	-
Coeff.o.thermal expansion	β_1 =	.0003816	1/K	β_2 =	.0003629	1/K
Thermal diffusivity	a_1 =	1.501E-7	m2/s	a_2 =	1.528E-7	m2/s

M = 39.997 g/mol

Validity range: 20 < ϑ < 100 0 wt-% < c < 50 wt-%

Figure 5-4 Properties of 5% and 10% NaOH solution at 298 K (see Appendix 3 for other concentrations)

As a two-phase flow model is being used, there are both liquid and gas phases considered in the materials settings. The NaOH and Na_2CO_3 solutions are included in the liquid phase and the CO_2 and air are included in the gas phase. The properties of the mixture materials are derived using different mixing laws. The volume weighted mixing law is applied to calculate the density of the mixture material which calculate the new density based on

volume ratio, and its thermal conductivity and viscosity are obtained using the mass weighted mixing law.

Table 5-1 Properties of the NaOH solutions under different concentrations

Property					
Mass fraction	5%	10%	15%	20%	25%
Density (g/mL)	1.048	1.102	1.156	1.211	1.265
Heat value (J/kgK)	3984	3785	3707	3629	3582
Thermal conductivity	0.6265	0.6375	0.644	0.6505	0.6535
D Viscosity (kg/m·s)	$1.19\ 10^{-3}$	$1.59\ 10^{-3}$	$2.50\ 10^{-3}$	$3.94\ 10^{-3}$	$6.38\ 10^{-3}$
Molecular mass	40	40	40	40	40
Integrated mass	800	400	266.67	200	160
Standard state enthalpy (J/kg)	$1.39\ 10^{5}$	$1.28\ 10^{5}$	$1.22\ 10^{5}$	$1.21\ 10^{5}$	$1.28\ 10^{5}$

Table 5-2 Properties of the Na_2CO_3 solutions after reactions

Property						
Mass fraction	6.45%	12.56%	18.36%	22.60%	23.87%	29.12%
Density (g/mL)	1.064	1.128	1.198	1.25	1.268	1.33
Heat value (J/kgK)	3924.55	3807.40	3690.25	3600.75	3573.10	3455.95
D Viscosity (kg/m·s)	0.00128	0.00192	0.00294	0.00475	0.00575	0.00675
Integrated mass	1644	844	577.33	469.08	444	364

In the setting of the phases, the solutions mixture is selected to be the primary phase and the gases are the secondary phase. The reaction model in the phase interaction is enabled to consider the chemical reaction between the phases. The Arrhenius reaction rate function is applied to simulate the chemical reaction. There are three significant input parameters required for simulation: the reaction order, the pre-exponential factor and the activation energy. The value of these parameters are derived based on the experimental data.

a. Reaction Orders

Reaction orders determine the relationship between the reaction rate and the rate constant. In the reaction rate equation, the reaction orders are the exponents of the reactant

concentrations. To determine the reaction orders, an integrated rate equation is applied. The equation transfers solution concentrations for different orders of the reaction. The transferred values are then checked and if they are in a straight line or rather show a linear trend, it means the reaction is in this order. One example is given in the following paragraph.

For zero order, the equation is:

$$O_0 = C \tag{15}$$

Where:

O_0 = the transferred value from the zero order equation;

and C = the concentration of the solution.

For first order, the equation is:

$$O_1 = \ln(C) \tag{16}$$

Where:

O_1 = the transferred value from the first order equation.

For second order, the equation is:

$$O_2 = 1/C \tag{17}$$

Where

O_1 = the transferred value from the second order equation.

Table 5-3 Results transferred from order equations

Time (min)	*Concentration (mole/L)*	*Zero order (C)*	*1st order [ln(C)]*	*2nd order (1/C)*
0	4.4	4.4	1.5	0.2
2.5	3.7	3.7	1.3	0.3
4.5	3.4	3.4	1.2	0.3
6.5	3.0	3.0	1.1	0.3
8.5	2.6	2.6	1.0	0.4
12	0.03	0.03	-3.6	38.2

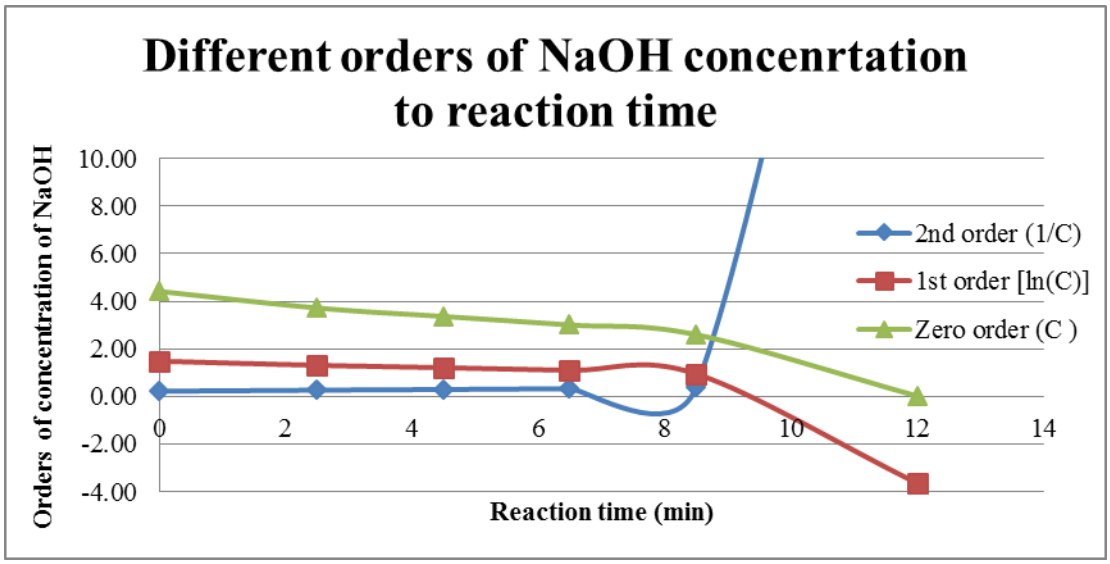

Figure 5-5 Plots of results transferred from order equations

For one example experiment, the experimental data provided the reaction time and the concentrations at the corresponding time. Table 5-3 presents the results of different order values derived from the order equations presented above. The plots of these results are presented in Figure 5-5. From the figure, it is apparent that the results from first and second order are not linear but that from zero order are relatively linear so the reaction is determined to be a zero order reaction based on the experimental data.

b. Pre-Exponential Factor and Activation Energy

The pre-exponential factor indicates the frequency of the molecular and ion collisions and their orientation, which is slightly influenced by temperature. In a small temperature range, (the temperature of the laboratory is around 297 K), the impact is often negligible. The activation energy is the minimum energy required to start a reaction. It is constant for a reaction with similar reactant concentrations. Therefore, according to the Arrhenius equation, the rate constant and temperature data are required to find the pre-exponential factor and activation energy.

To derive the activation energy, two sets of experimental data are selected first and their reaction rate can be derived with this equation:

$$r = \Delta C/t \tag{18}$$

Where

r = the reaction rate;

ΔC = the difference of concentrations between the initial and final solution;

and t = the reaction time.

As a zero order reaction, the rate constant is equal to the reaction rate so the k value in the Arrhenius equation is derived. One Arrhenius equation is then divided by the other one, and the following equation for the activation energy can be obtained:

$$\frac{k_1}{k_2} = \frac{Ae^{\left(-\frac{E_a}{RT_1}\right)}}{Ae^{\left(-\frac{E_a}{RT_2}\right)}} = e^{\left(\frac{1}{T_2}-\frac{1}{T_1}\right)\frac{E_a}{R}}$$

$$\Rightarrow \quad \mathrm{Ln}\frac{k_1}{k_2} = \left(\frac{1}{T_2} - \frac{1}{T_1}\right)\frac{E_a}{R}$$

$$\Rightarrow \quad E_a = R\frac{T_1 T_2}{T_1 - T_2}\ln\frac{k_1}{k_2} \qquad (19)$$

Therefore the activation energy is a function of temperatures and rate constant which are all available from the experimental data. As long as the activation energy is found, the pre-exponential factor can be calculated based on the Arrhenius equation. After the pre-exponential factor and the activation energy for all cases are derived, the average values are calculated and applied in the reaction model of the simulation. This calculation is shown in Appendix 2.

5.3.3. Solution Methods, Monitors and Run Calculation

The phase coupled SIMPLE method is used for the Eulerian multiphase model in the simulation. It has been applied in many different types of multiphase flow simulations according to the user guide for Fluent. The Geo-Reconstruct spatial discretisation method for volume fraction is selected. Despite the computational intensity of the method, the Geo-Reconstruct method is the best for capturing the interface between gas and fluid phases so that the bubbling effect can be taken into account.

Since the entire reaction process is important, a fixed time stepping method is applied. The time step size is modified and selected to be 0.005 s considering the simulation convergence and computational intensity. The number of time steps is 80000 due to both the reaction time in the experiment and the selected time step size. In order to reduce the time cost of simulation, the data files are saved every 1000 time steps (0.5 s). Since the concentration of the product Na_2CO_3 is an indicator for the reaction, a volume monitor of Na_2CO_3 concentration is utilised. When the concentration reaches 100%, it means the reaction is completed.

5.4. Results, Comparisons and Discussions

This section will demonstrate the numerical simulations that were carried out for the reaction process and critical parameters will be highlighted and analysed and will then be used for further investigation and research on designing a proto-type demonstration system on-board a ship. The second part of this section will present the comparisons between, and the discussions on, the experimental data and numerical simulation results.

Figure 5-6 presents the CO_2 bubble flow in the fluid domain, indicating the volume fraction contours of the solution at t = 0 s and t = 3 s. It is limited to a 3 second simulation of the bubbling effect because the project is mainly focusing on the reaction part, with high computing intensity being another reason to limit the time. The bubbling effect observed is reasonable as there is a range of different diameters for the bubbles. Since the chemical reaction is not taken into account, the height of the solution is increased only because the gas and liquid phases are immiscible. Both the gas phase and liquid phase occupy volumes in the reaction tank.

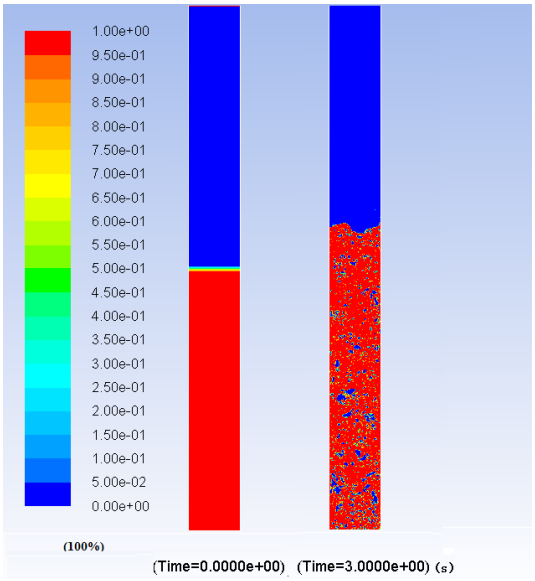

Figure 5-6 Bubble flow phenomenon under contours of solutions volume fraction (Left: contours graph at t = 0 s; Right: contours graph at t = 3 s.)

Since the simulation is of the combined chemical reaction with the bubbling effect, further simplification of the inlet is applied to reduce computational intensity and make the simulation less time consuming. Ten separated inlet boundaries are merged into one integrated gas inlet. With the integrated inlet, the minimum size of the mesh is increased resulting in a reduction of the number of cells in the reaction tank model mesh.

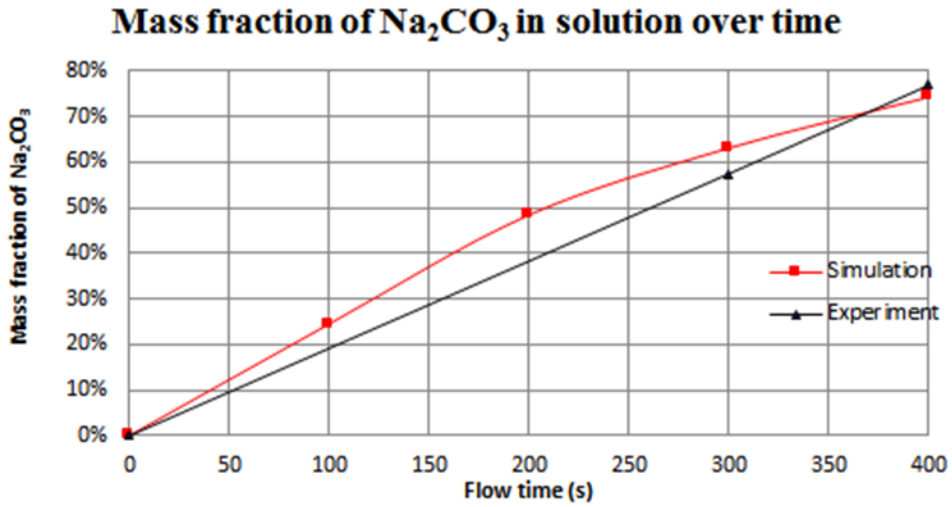

A

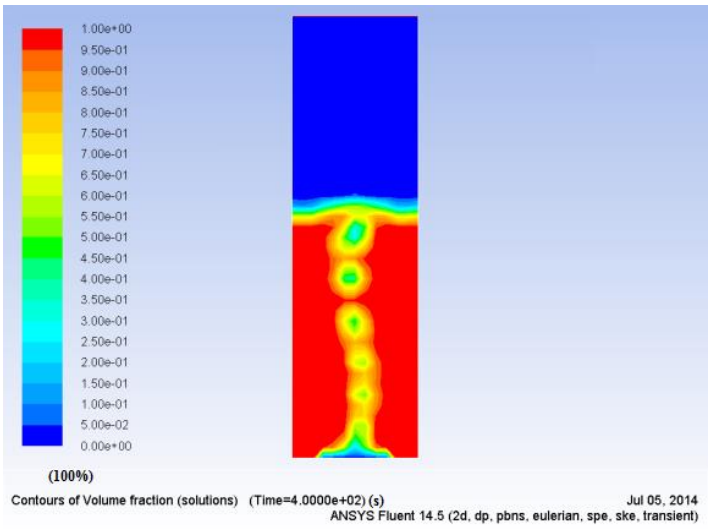

B

Figure 5-7 A: Comparison of Na_2CO_3 mass fractions over time between experiment and simulation results; B: Volume fraction of solutions at t = 400 s.

The mass fraction of Na_2CO_3 in the solution phase is monitored during the simulation. In the experiments, the final mass fraction of Na_2CO_3 was 76.8%, so the simulation will be terminated when the mass fraction reaches the same value. According to the Arrhenius expression shown in Equation 18, the reaction rate constant (k) is determined from three factors, i.e. the pre-exponent factor, the activation energy and the temperature, and thus, the reaction in the CFD simulation is dominated by these factors as well. The simulation can be optimised by controlling these factors. Figure 5-7A presents the mass fraction of Na_2CO_3 changing over time for both the simulation and the experiments. It indicates that the maximum difference between the simulation and the experiments is 5.6%. Since these two curves are well matched, the fundamental factors in this simulation are verified and will be applied in further simulations. Figure 5-7B presents the volume fraction of solutions at t = 400 s. It illustrates the distribution of gas and solution and the gas moving path while the reaction is processing.

5.4.1. Pressure Distribution

Figure 5-8 shows the pressure contour diagrams of the simulation which are derived from the ANSYS Fluent software. The contour diagrams present how the pressure is distributed and changed during the absorption process. A minor pressure fluctuation is found during the feeding and absorption stages. The pressure of CO_2 gas at the inlet is the highest. In order to estimate the gas pressure at the inlet, a surface monitor is applied at the inlet to monitor the real time pressure. Figure 5-9 gives a visual display of the variation of pressure at the gas inlet of the system. The pressure rises at the gas inlet over time. The maximum pressure at the gas inlet is about 102,570 Pa during the absorption process. The rise in pressure over time is due to the progress of the absorption reaction as explained by the following equation:

$$P = \rho g h \qquad (20)$$

where, ρ is the density of the solution; g is the gravitational acceleration and h is the solution height.

Referring to Equation 26, the pressure ratio at two different times can be expressed as follows:

$$P_1/P_2 = (\rho_1 h_1) / (\rho_2 h_2) \quad (21\text{-}1)$$

Density can be expressed as the ratio of mass and volume. Volume is proportional to the solution height when the cross sectional area is constant. The equation can be further expressed as:

$$P_1/P_2 = [(m_1/v_1)\, h_1] / [(m_2/v_2)\, h_2] = [(m_1/h_1)\, h_1] / [(m_2/h_2)\, h_2] = m_1/m_2 \quad (21\text{-}2)$$

Where:

m = the mass of the solution;

v = the volume of the solution;

and h = the height of solution in the column (the subscripts 1 and 2 present for different times during the process).

Therefore, the pressure at the gas inlet is proportional to the mass of the solution in the column. Because the mass of the solution is increasing as the absorption progresses, the pressure at the inlet is increased accordingly.

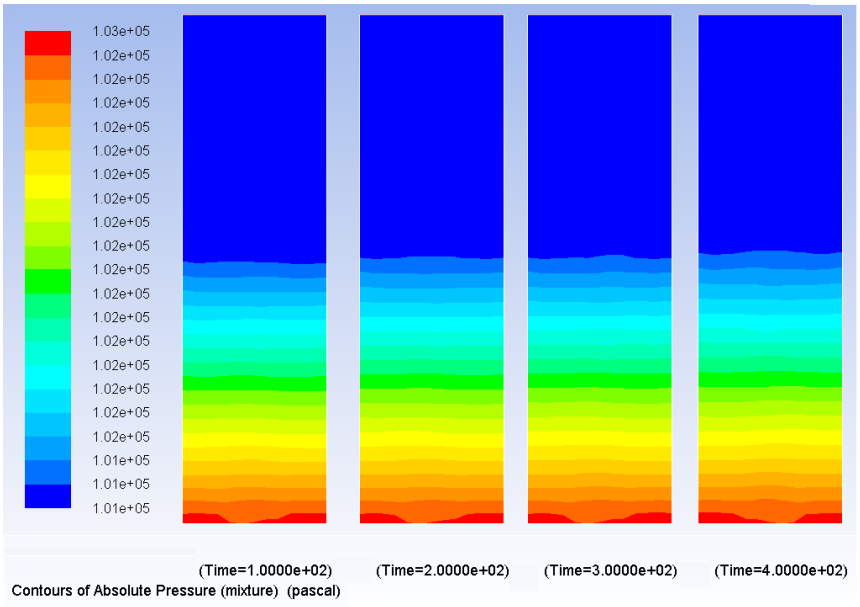

Figure 5-8 Pressure contours over flow time (at 100, 200, 300 and 400s).

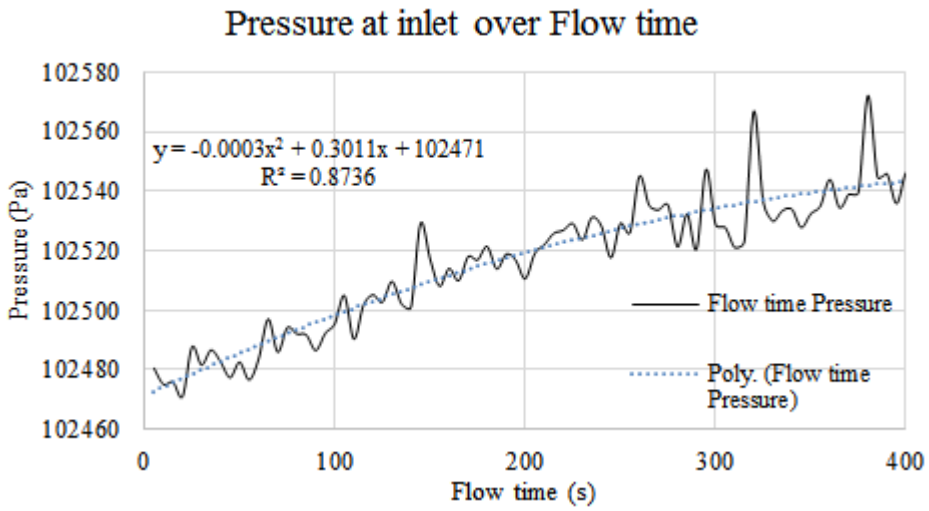

Figure 5-9 CFD results: static pressure variations at the gas inlet over flow time

5.4.2. Temperature variation

The temperature of solution during the absorption reaction is monitored in CFD simulations as well. As the absorption reaction is an exothermic reaction, the heat released is 109.4 kJ/mole CO_2 absorbed (Mahmoudkhani and Keith, 2009). For 1 mole of CO_2

absorption, the required quantity of 15% Na_2CO_3 solution is 706.67 g. The specific heat value is 3690 J/kg·K so the theoretical temperature risen due to heat released is derived (51.56 K). However, due to heat losses and incomplete absorption reaction, the actual temperature difference between before and after reaction is lower than the calculated value.

The temperature variation is derived with the CFD simulation and presented in Figure 5-10 and Figure 5-11. It indicates that with the progressing of the reaction, the temperature of solution is increased. The increasing rate of temperature is faster from the beginning of the reaction processes to 25 s and then it slows down and fluctuates until the end of the simulation. It is because at the beginning the temperature of solution is low (298K) and the temperature difference between solution and atmosphere is insignificant. Hence, the heat exchange between solution and atmosphere is slow. However as the temperature of solution increased with the reaction processing, the difference between temperature of solution and atmosphere is increased, resulting high heat exchange between them.

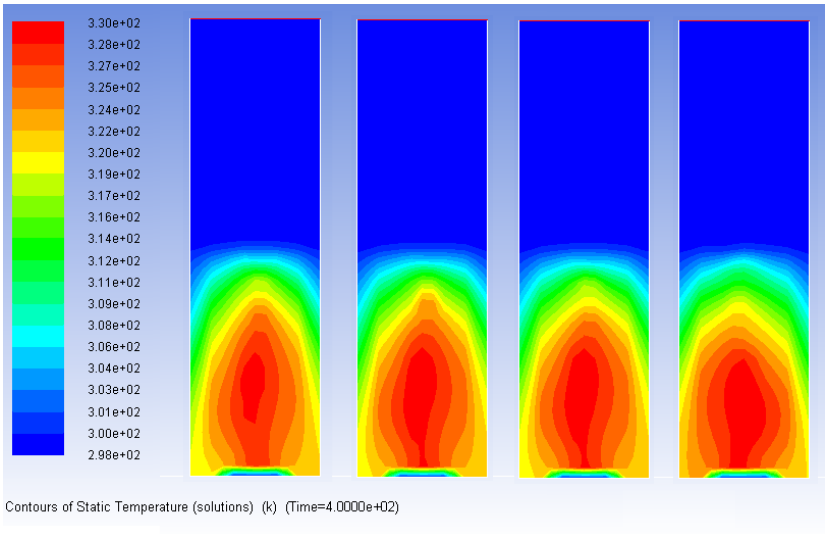

Figure 5-10 Temperature contours over flow time (at 100, 200, 300 and 400 s)

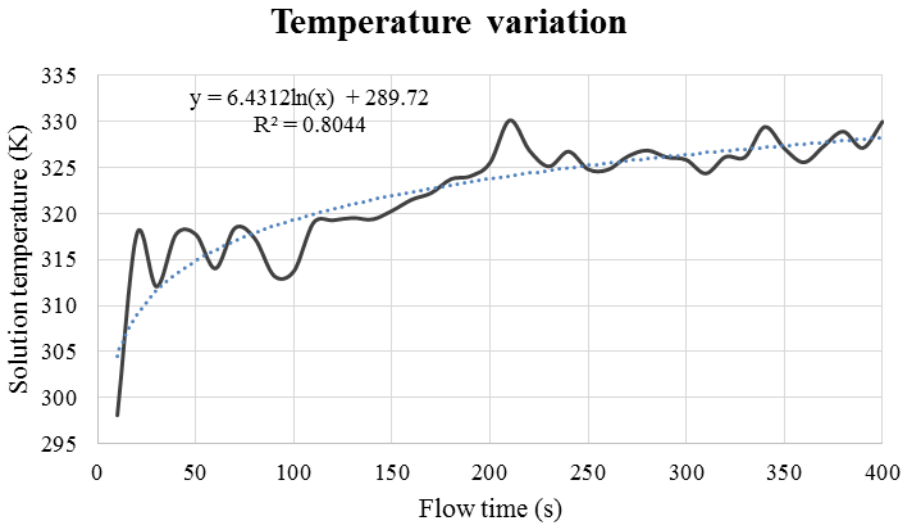

Figure 5-11 CFD results: static temperature variations over flow time

In order to recycle the heat from absorption reaction, a heat exchanger can be applied in practical system. The heat released will be reused for heating purpose. Furthermore, with heat exchanger as a temperature control, it maintains the absorption process temperature in a safe level. The benefits of steady and controlled temperature are extending the life of reaction tanks and recovering heat to increase energy efficiency.

5.4.3. Concentration of Solution

As the absorption progresses, the solution of NaOH reacts with the CO_2 and generates Na_2CO_3. The CO_2 absorbed at different times can be indicated by the mass of the solution. The increments of the increase in the mass of the solution represent the quantity of CO_2 being absorbed. Since all the CO_2 trapped in the solution will be in the form of the ion CO_3^{2-}, the mass fraction of the Na_2CO_3 solution can also indicate the amount of CO_2 gas absorbed. The mass concentration of Na_2CO_3 changing over time is presented in Figure 5-12. In this figure, the colour code represents the mass fraction of Na_2CO_3 in the solution. The change in the colour of the solution from blue to red means that the mass fraction of

Na_2CO_3 increases from 0 to 100%. These changing illustrates the increase of the Na_2CO_3 mass fraction during the process of CO_2 absorption.

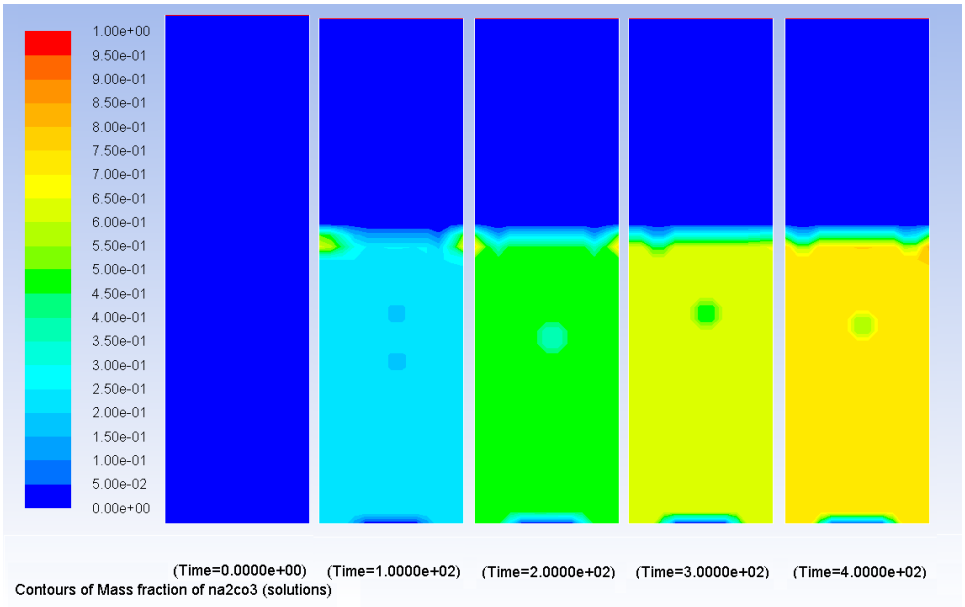

Figure 5-12 Concentration contours of Na_2CO_3 in solution over flow time (at 0, 100, 200, 300 and 400 s).

5.4.4. Velocity of Gas and Solution

Once the CO_2 is released from the diffuser into the solution, the gas will travel upward to the free surface of the solution. The path and the velocity of the gas at different flow times are presented in Figure 5-13. This illustrates that the gas velocity in the central area is the highest. This is because the viscous forces between the two phases drag the gas and slow the upward speed. According to Figure 5-14, the reaction force also drives the solution to circulate in the fluid region. The velocity of the solution in the centre is the highest because part of the solution in the centre is mixed and is moving with the gas.

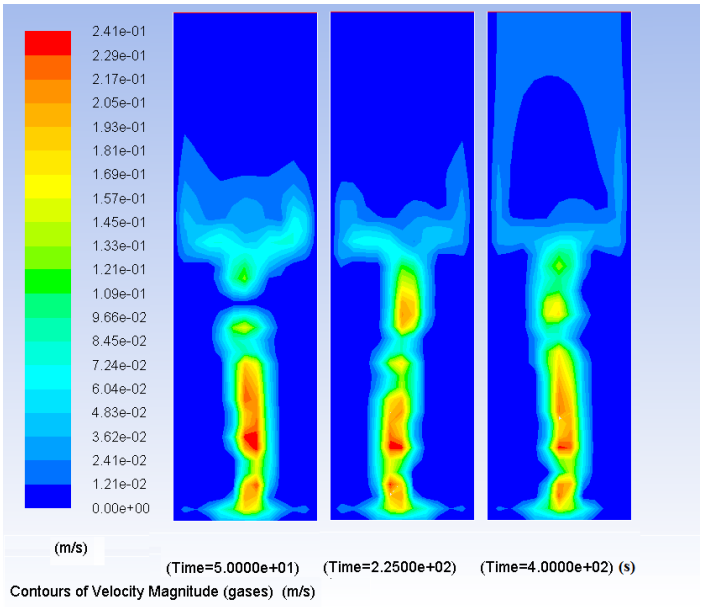

Figure 5-13 Gas velocity contours over flow time (at 50, 225 and 400 s).

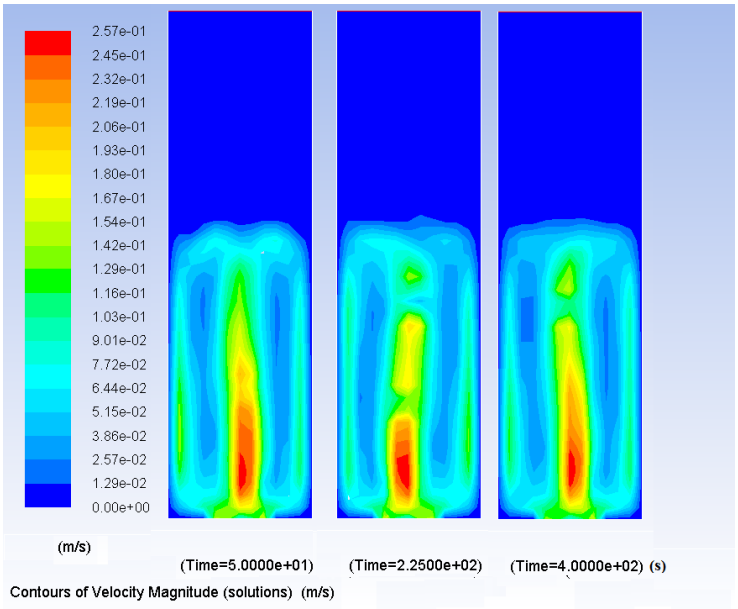

Figure 5-14 Solution velocity contours over flow time (at 50, 225 and 400 s).

5.5. Comparisons of Results from Numerical Simulations and Experiments

5.5.1. Impact of Initial NaOH Concentration on Gas Absorption Rate

The effect of the initial concentration of the NaOH solution on the gas absorption rate is examined for the experiments. Gas from the CO_2 bottle is fed into NaOH solutions of several different concentrations. The results of the experiment are shown in Figure 5-15, and are compared with the simulation results. The comparison of the results indicates that the simulations and experiments have a good agreement, including a similar trend in gas absorption rate change for different initial concentrations of NaOH solution. The absorption rate of gas varies with the NaOH concentration. It reaches a maximum value when the initial NaOH concentration is 15%.

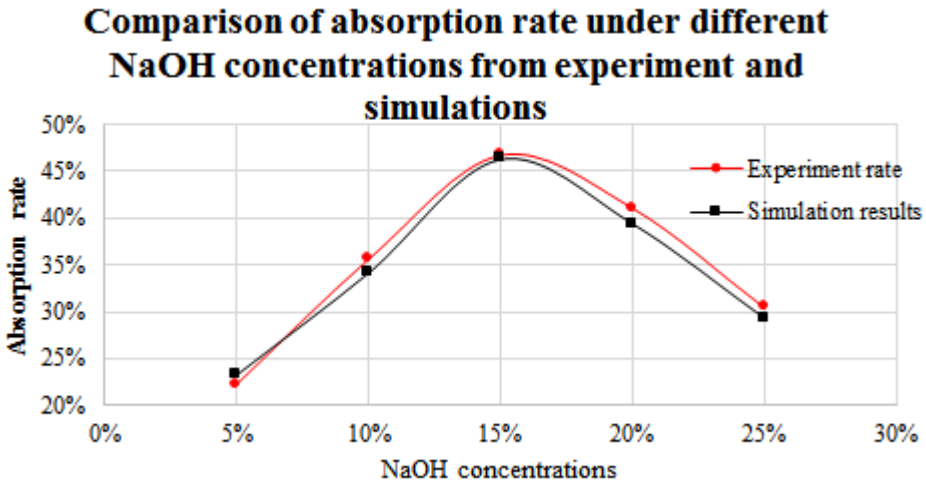

Figure 5-15 Comparison of experimental and simulated gas absorption rate with different concentrations of NaOH solution

With the same reaction tank geometry, there are two factors dominating the reaction rate between the gas and the solution, i.e. the NaOH solution concentration and the contact area between the two phases. At a low concentration of NaOH, the gas absorption rate is increased as the concentration of the solution is increased. While the concentration of the

solution increases, the density of the solution is also increased. As indicated by Equation 26, a high density of solution will lead to a high pressure on the gas bubbles. According to Equation 19, the bubble size will be decreased while the solution pressure grows. At about 15% NaOH concentration, the gas bubble size is decreased to a critical value at which a further increase in the concentration of solution will lead to a decrease in the gas absorption rate.

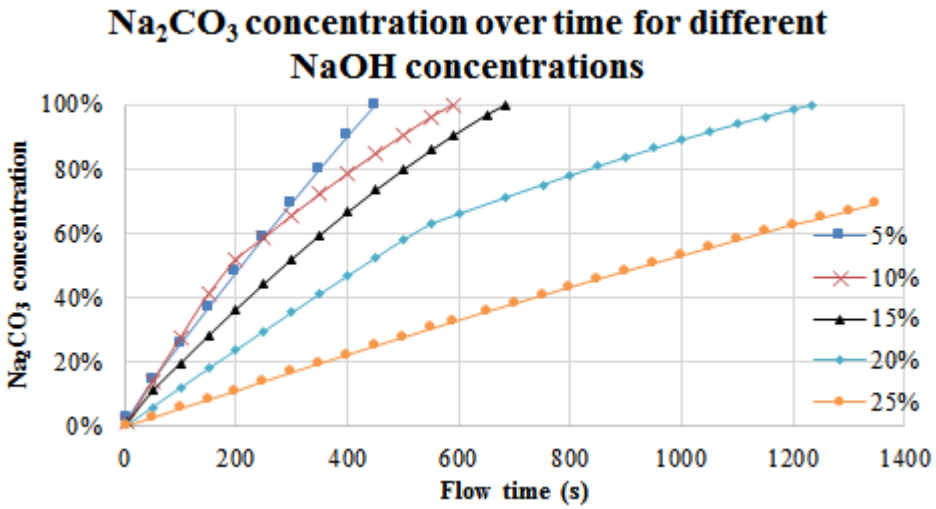

Figure 5-16 Na_2CO_3 concentrations over time for different concentration of NaOH solutions.

Figure 5-16 presents the CFD simulation results for the changes in mass fraction of Na_2CO_3 over the flow time for different solution concentrations. When the initial concentration of the NaOH solution is 5%, it only takes about 450 s to achieve a 100% reaction (full reaction of NaOH solute). With the increase of NaOH concentration, more NaOH solute is available in the solution so the time taken to reach full reaction becomes longer. Although the time spent for full reaction is lowest when the concentration of NaOH solution is 5%, the actual gas absorbed here is also the lowest compared with the other cases. To select the optimised initial concentration of NaOH solution, the NaOH solute reacted per second is considered.

This presents the reaction rate with various concentrations of NaOH solution. It can be derived using the following equations:

$$A = C/t \tag{22}$$

Where:

A = the mass of NaOH solute reacted per second in unit volume;

C = the mass of NaOH solute in unit volume of solution;

and t is the total time for a full reaction.

$$C = 1\rho c \tag{23}$$

Where:

ρ = the density of the NaOH solution

and c = the mass fraction of NaOH in the solution (Quantity 1 presents a unit volume of NaOH solution. Unit volume is used to simplify the calculation as the volumes of all these cases are constant).

The quantities of NaOH solute reacted per second for all concentrations of NaOH solutions are derived and shown in Table 5-4. From the table, when the concentration of NaOH solution is 15%, the NaOH solute reacted per second is the highest. Together with the gas absorption rates shown in Figure 5-15, and considering both gas absorption rate and solute reaction rate, an initial NaOH concentration of 15% is found to be an optimal value.

Table 5-4 Solute reaction rate via initial NaOH concentrations

Mass fraction	*5%*	*10%*	*15%*	*20%*	*25%*
Mass of NaOH solute in unit volume of solution (g/cm^3)	0.05	0.11	0.17	0.24	0.32
Total time for fully reaction (s)	450	590	685	1235	1960
Mass of NaOH solute reacted per second in unit volume (10^{-4} $g/cm^3 \cdot s$)	1.16	1.87	2.53	1.96	1.61

5.5.2. Effect of Gas Flow Rate on Absorption Rate

Three different gas flow rates (6.32 10^{-4}, 9.49 10^{-4}, 1.90 10^{-3} kg/s) are selected in the experiment to estimate the effect of the gas flow rate on the CO_2 absorption rate. Accordingly, three sets of simulations are conducted with the same flow rates to verify the applicability of the CFD simulations. To predict the trend at a higher gas flow rate, two more sets of gas flow rates (2.09 10^{-3}, 2.85 10^{-3} kg/s) are applied and tested in the CFD simulations. The results from the simulations and experiments are presented in

Figure 5-17. Compared with the experimental results, the simulation results match well when flow rates are 9.49 10^{-4} and 1.90 10^{-3} kg/s. The simulation results with a flow rate of 2.09 10^{-3} kg/s are also well matched with the values predicted by the experiments. However, for the flow rates of 6.32 10^{-4} and 2.85 10^{-3} kg/s, the differences between the experimental and simulation results cannot be neglected. It indicates that either the CFD model is compatible with certain range of velocity or the experiment exhibits inaccuracy.

From the simulation results shown in

Figure 5-17, the percentage of gas absorbed is as high as 85% when the gas flow rate is 6.32 10^{-4} kg/s. This is because the gas is fed into the solution slowly and can be absorbed more thoroughly. It means there is more time for the contact between the gas and the solution than in the other cases. With the flow rate of 2.85 10^{-3} kg/s, the gas input rate is

the largest of all the cases tested. It results in the lowest absorption rate. This is because the contact time between the gas and the solution is too short at a high gas flow rate, leading to a low absorption rate. However, in the experiments, there are friction losses along from the flow metre to the diffuser impacting on the actual gas flow rate. Due to the friction, the actual gas input flow rate into the reaction tank is smaller than the reading on the flow meter would suggest. The theoretical analyses are still using the value of 6.32 10^{-4} kg/s from the reading on the flow meter, thus, the value of the gas flow rate used in the analyses is larger than the actual one. Therefore this results in the calculated gas absorption rate for the experiments being smaller than the actual rate. According to the effect of flow rate on absorption rate, it is obvious that the difference between experiment and simulation results when the flow rate is 1.90 10^{-3} kg/s. Therefore, this flow rate would be used for CFD model simulation to eliminate the reading error of flow rate.

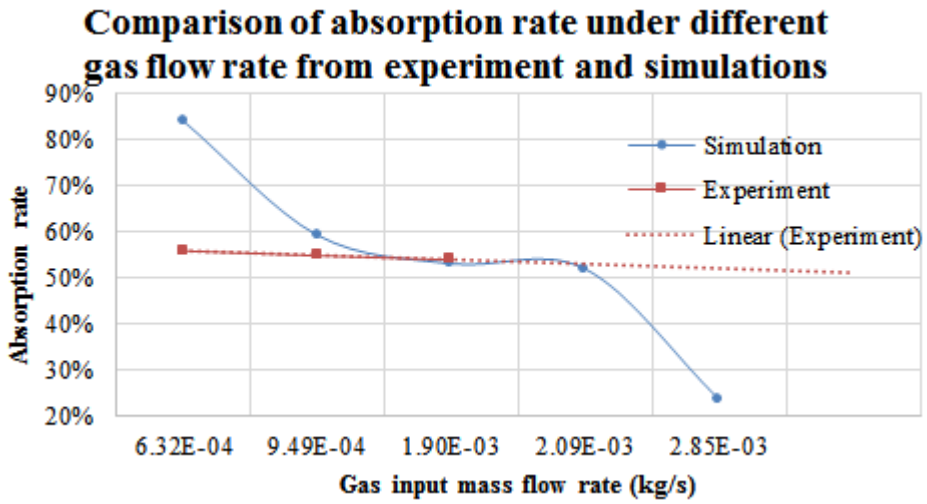

Figure 5-17 Comparison of experimental and simulated gas absorption rate under different gas flow rate

Figure 5-18 presents the CFD simulation results for the change of Na_2CO_3 mass fraction in the solution over time at different CO_2 gas feeding rates. It illustrates the time taken for the absorption process to reach a full reaction under different gas flow rates. The quantity of reacted NaOH solute per second under the set gas flow rates is considered in order to estimate the optimised gas flow rate for the maximum reaction rate. As the volume and concentration of NaOH solution are constant, the amount of NaOH solute per unit volume

(Equation 28) is constant. Table 5-5 indicates a comparison of the solute reaction rates at different flow rates. It is found that the reaction rate is increased as the gas flow rate increases. Combining

Figure 5-17 and Figure 5-18 it can be seen that a slow gas flow rate improves the absorption rate but it takes a longer time to reach a full reaction. Experimental and simulation results have shown good agreement when the CO_2 gas flow rate is in the region of 9.49 10^{-4} to 2.09 10^{-3} kg/s. However, a flow rate at the higher end of the region is preferred as it offers a higher reaction rate.

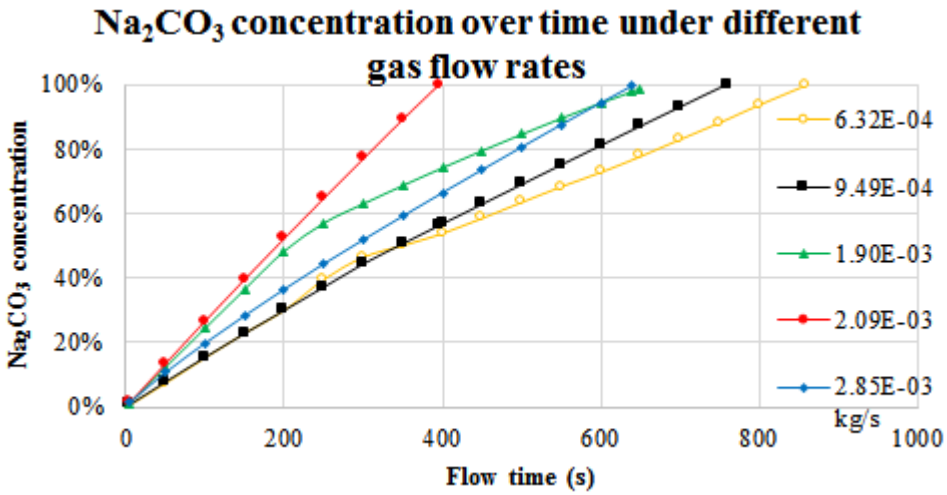

Figure 5-18 Na_2CO_3 concentration over time for different gas input flow rates

Table 5-5 Solute reaction rate under different gas input mass flow rates

Mass flow rate (10^{-3} kg/s)	*0.95*	*1.90*	*2.09*
Mass of NaOH solute in unit volume of solution (g/cm^3)	0.17	0.17	0.17
Total time for fully reaction (s)	760	650	395
Mass of NaOH solute reacted per second in unit volume (10^{-4} g/cm^3·s)	2.3	2.7	4.4

5.5.3. Impact of Reaction Tank Geometry on Gas Absorption Rate

The geometry parameters of the reaction tank are factors that could impact the gas absorption rate significantly. This section discusses the results from the simulations and experiments on how the geometry parameters affect the absorption reaction process. Three conditions are considered: change of solution column height for the same tank diameter, change of tank diameter with constant solution column height and change of tank diameter with the same solution volume.

5.5.3.1. Impact of Solution Column Height

To find out how the solution column height affects the absorption, a group of experiments was conducted with a controlled diameter and variable column height. Figure 5-19 shows a comparison of experimental and simulation results and it indicates a good agreement between them. The maximum difference between the experimental and simulation results is 5.27%. The figure illustrates that with the same reaction tank diameter, an increase in the solution column height will bring a better gas absorption rate. The reason for this phenomenon is simply because the path of the gas in the solution is longer with the higher solution column, resulting in a longer contact time and good absorption.

Figure 5-20 presents the simulation results for the mentioned three cases. It indicates that a low column height will have a fast reaction speed. At 30 cm column height, it takes almost 1100 s to complete the reaction whereas it only takes 570 s for the case with a 10.5 cm column height. This can be explained by stating that with the same tank diameter, the quantity of solution with a 30 cm column height is almost three times that with a 10.5 cm column height. According to the mass balance and reaction formula in Equations 1 and 4, an increase in solution quantity directly leads to an increase in CO_2 required for a complete reaction and therefore it increases the total time of the reaction.

The quantity of NaOH solute reacted per second is considered here to find out the reaction rate under different solution column heights. Since the solution concentration is constant, the mass of NaOH solute per unit volume of solution in Equation 28 is constant. Then, considering the reaction time in Figure 5-20, the mass of NaOH solute reacted per second in a unit volume can be derived and presented in Table 5-6. However, the solution quantity (volume) is not constant at different solution column heights so a correction coefficient, in the form of a ratio of solution column heights, is introduced. The mass of NaOH solute reacted per second (A') in Table 5-6 represents the corrected NaOH solute reaction rate. It indicates that the reaction rate is higher with a higher column height when the tank diameter is constant. Therefore, Figure 5-19 and Table 5-6 indicate that a high solution column height brings better gas absorption and a faster solute reaction. During system design, a longer contact period between gas and solution should be preferred.

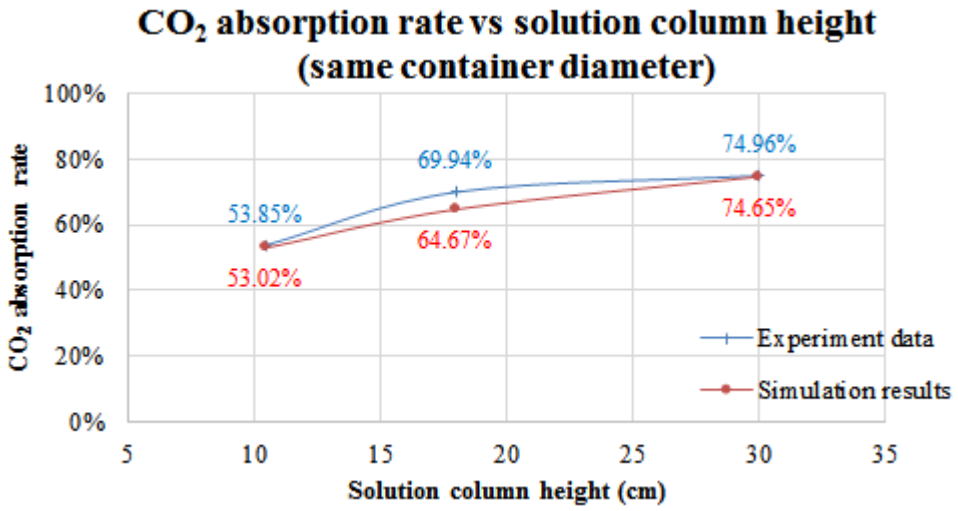

Figure 5-19 CO_2 absorption rate for different solution column heights with constant tank diameter

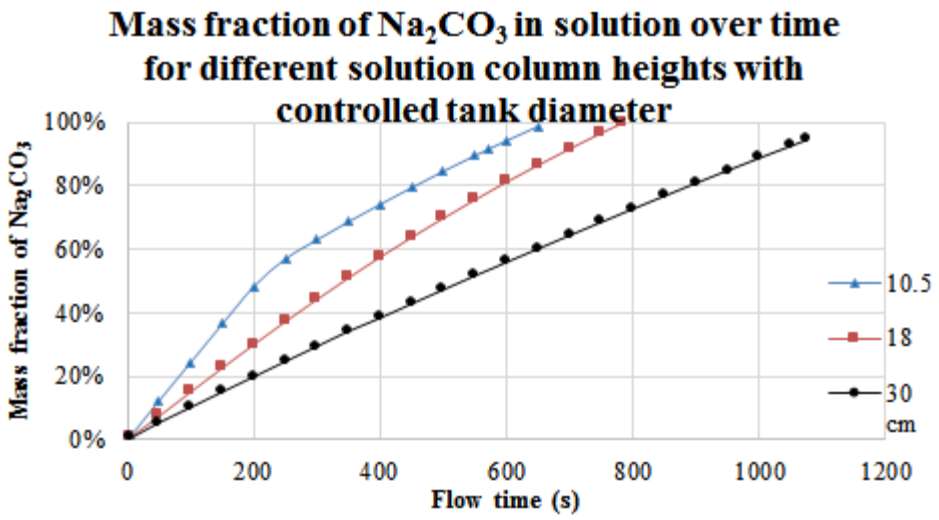

Figure 5-20 Mass fraction of Na_2CO_3 over time for different solution column heights with controlled tank diameter

Table 5-6 Solute reaction rate under different solution column heights with fixed tank diameter

Column height (cm)	*10*	*18*	*30*
Mass of NaOH solute in unit volume of solution (g/cm^3)	0.17	0.17	0.17
Total time for fully reaction (s)	650	780	1150
Mass of NaOH solute reacted per second in unit volume (10^{-4} $g/cm^3 \cdot s$)	2.7	2.2	1.5
Mass of NaOH solute reacted per second (10^{-4} g/s)	2.7	4.8	8.0

5.5.3.2. Impact of Tank Diameter with the Same Solution Column Height

This group of experiments has a condition of using the same solution column height but varying tank diameter. Figure 5-21 illustrates a comparison of simulation and experimental results. Again, a good agreement has been found between the experimental and simulation results. The difference between the simulations and experiments is minor and no greater than 1.5%. In the figure, the gas absorption rate is to be increased when increasing the reaction tank diameter due to an increased contact area between the gas and solution. The gas fed into the reaction tank will not only move upwards but will also be diffused

horizontally. The profile of gas distribution is the same under all experimental conditions and the simulations due to the usage of the same diffuser. When the height of the solution column is constant, the larger the diameter is, the wider the solution area is. Therefore, a large diameter of reaction tank leads to a good absorption rate of gas when the solution column height is constant.

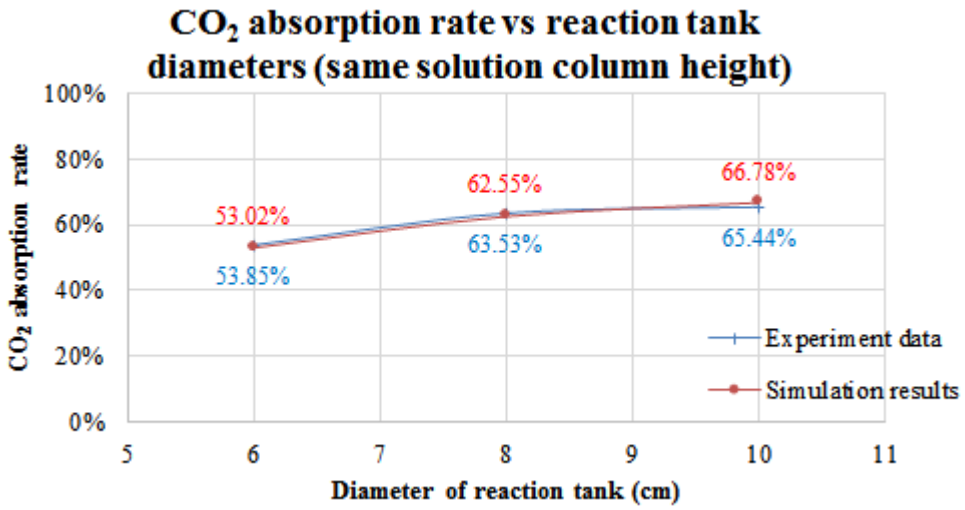

Figure 5-21 CO_2 absorption rates for different reaction tank diameters with controlled solution column height

According to Figure 5-22, the fastest reaction occurs with the tank of the smallest diameter due to a lower quantity of solution being contained in a small diameter tank. The difference in reaction time among the three cases varies from about 30s to 100s. Compared with the effect of the other geometric parameters, the impact of diameter on reaction rate is lower when the solution column height is fixed. The mass of solute reacted is analysed in order to find out how the reaction rate varies with the diameter of the reaction tank. Similar to Section 5.5.3.1, the concentration of the NaOH solution is constant but the solution quantity is not constant. The mass of NaOH solute per unit volume is constant but the corrected mass of NaOH solute reacted per second, A', is used for analysis. Table 5-7 indicates that with the same column height, a larger tank diameter will provide a faster reaction rate.

Therefore, together with Figure 5-21, a large tank diameter results in both good gas absorption rate and fast reaction rate.

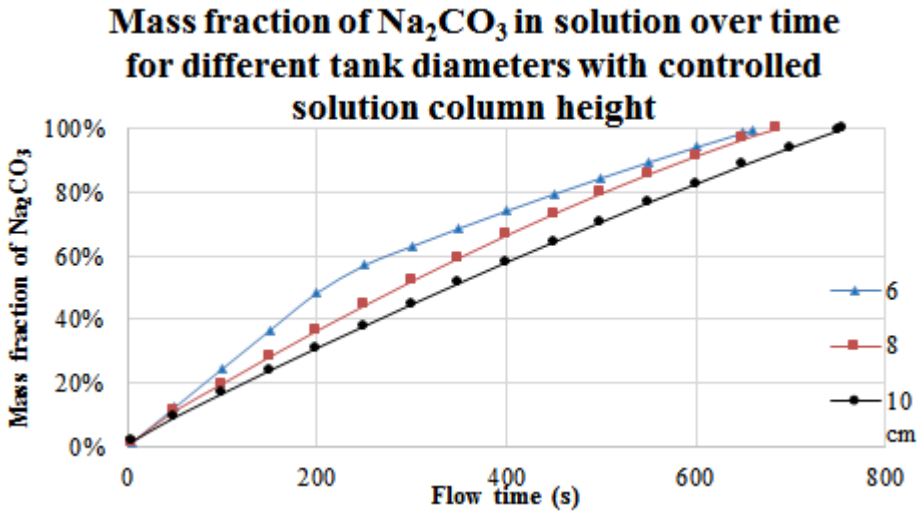

Figure 5-22 Mass fraction of Na_2CO_3 over time for different tank diameters with controlled solution column height

Table 5-7 Solute reaction rate under different tank diameters with fixed solution column height

Tank diameter (cm)	*6*	*8*	*10*
Mass of NaOH solute in unit volume of solution (g/cm^3)	0.17	0.17	0.17
Total time for fully reaction (s)	650	780	1150
Mass of NaOH solute reacted per second in unit volume (10^{-4} $g/cm^3 \cdot s$)	2.7	2.2	1.5
Mass of NaOH solute reacted per second (10^{-4} g/s)	2.7	3.6	4.5

5.5.3.3. Impact of Tank Diameter with the Same Volume

Three sets of experiments were conducted for different tank diameters with a controlled solution volume. Figure 5-23 presents a comparison between the experimental and simulation results. The difference in values between the simulation and experimental

results is a maximum of around 2.88%. The figure indicates that the gas absorption rate decreases as the tank diameter increases. There are two factors that dominate this phenomenon: gas diffusion profile and gas path. Referring to Section 5.5.3.2, the diffusion of gas will lead to a better gas absorption rate. However, with the same solution volume, a small tank diameter results in a high column height. Based on Section 5.5.3.1, a higher solution column leads to a longer gas path and longer contact time between the gas and the solution. In this set of experiments and simulations, the effect of column height is dominant, so a smaller diameter of reaction tank leads to a better gas rate.

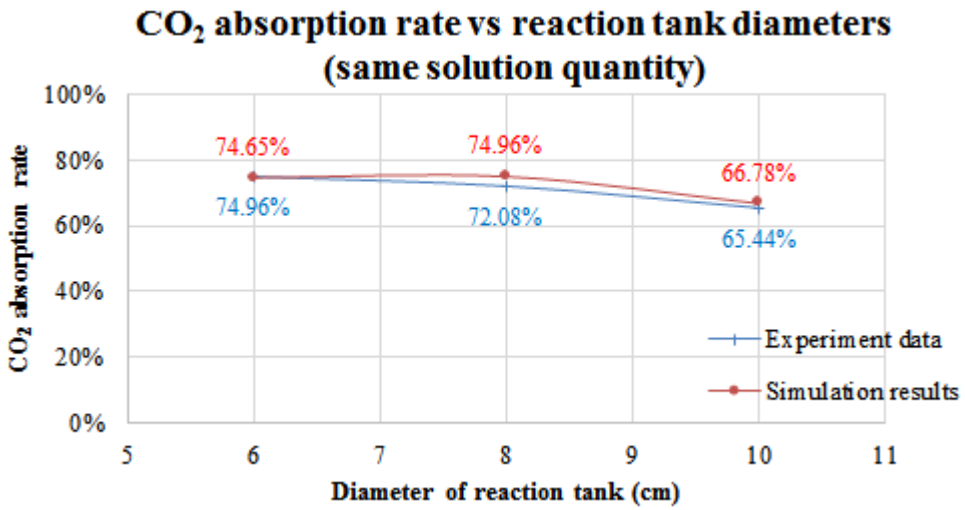

Figure 5-23 CO_2 absorption rates for different reaction tank diameters with controlled solution volume.

Figure 5-24 illustrates the time cost obtained by the simulation for a complete reaction with different tank diameters. It indicates that small diameters lead to a faster reaction. The largest difference between the reaction times at different simulation conditions is about 100 s. Since the concentration and quantity of solution is constant, the mass of NaOH solute per unit volume is also constant so that the reaction rate is inversely proportional to the reaction time. Therefore, when the solution quantity is fixed, a smaller diameter of reaction tank leads to both a better gas absorption rate and a faster reaction rate.

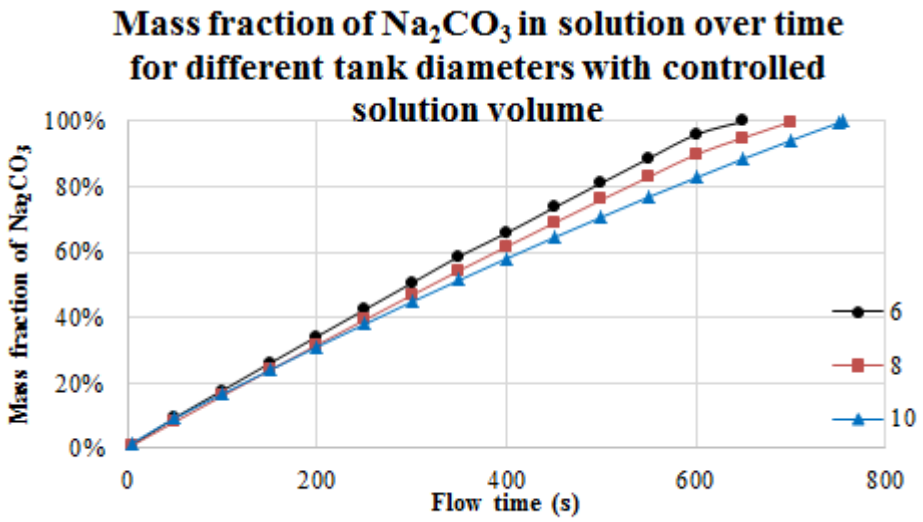

Figure 5-24 Mass fraction of Na_2CO_3 over time for different tank diameters with controlled solution volume

5.5.4. Impact of Operational Temperature

Having evaluated the effect of gas input flow rate and geometry of the tank on the CO_2 absorption rate in Sections 5.5.2 and 5.5.3, the effect of environmental conditions during the experiments on the absorption rate is examined. According to Equation 18, the environmental temperature is one of the key factors affecting the reaction rate. In this section, the simulation results of the absorption process under different environmental temperatures will be presented. As the atmosphere condition will be changed from the assumptions listed in Section 5.3.1, a new assumption is made that the gas initial temperature is 298 K.

Figure 5-25 presents the simulation results under different initial solution temperature conditions (which has the same temperature with boundaries). The range of temperatures varies from 278 to 318 K. Referring to Figure 5-25, the chemical reaction rate of the process increases as the temperature rises. According to Equation 18, the chemical reaction rate is affected by initial solution temperature. Due to heat exchange taking place between the

atmosphere and the mixture of gas and solution, a high initial solution temperature leads to a high temperature of the mixture of gas and solution, resulting in a high reaction rate.

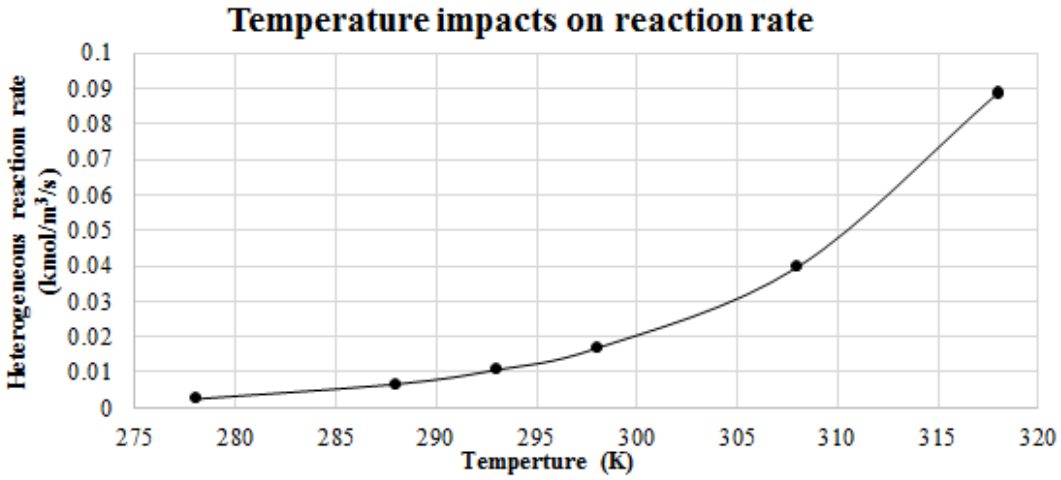

Figure 5-25 Simulated absorption rates under different boundary temperatures

Figure 5-26 shows the time elapsed to reach full reaction at various environmental temperatures. It is apparent that the fastest reaction happens when the environmental temperature is 318K and the slowest one happens at 278 K. The fastest reaction rate is 35 times that of the slowest one. Hence, the environmental temperature has a significant effect on the reaction speed and absorption rate. The results show that for the selected range of environmental temperatures, when the temperature is below 298 K, the time spent for a full reaction is significantly higher. Therefore the environmental temperature on-board ship for the system's operation should be maintained above 298 K.

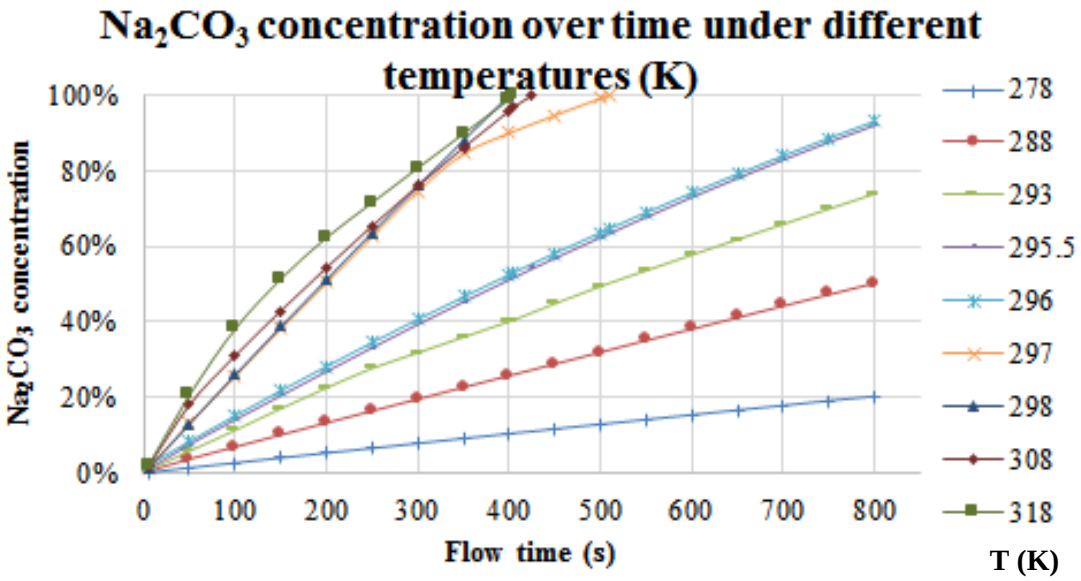

Figure 5-26 Na_2CO_3 concentrations over time for different operation temperatures

5.6. Conclusions and Further Studies

This chapter has demonstrated the feasibility of using CFD software to model, design and analyse the proposed carbon solidification method for CO_2 emission reduction in lab scale. It illustrates that the laboratory-scale simulation results have an acceptable agreement with the data from the experiments. It also indicates that the developed simulation model can be utilised as a fundamental tool for design and scale-up of a real system on a ship. A series of investigations has been carried out on factors which have significant effect on the carbon absorption process. Conclusions have been reached that a 15% mass fraction of NaOH solution offers an optimal gas absorption rate, and a low CO_2 gas flow rate could lead to a high absorption rate in a specific region of flow rates from $9.49\ 10^{-4}$ to $2.09\ 10^{-3}$ kg/s. Results from both experiments and simulations also prove that the contact between gas and solution will impact absorption rate and the absorption reaction also benefits greatly from a high temperature of solution. A good contact between gas and solution can be achieved by optimising the three geometry factors, i.e. tank diameter, solution volume and solution height. The CO_2 gas flow rate is also an important parameter affecting the contact between gas and solution.

In the next stage of this study, a proto-type of the absorption system will be designed by utilising the models developed in this chapter, since the model has been shown to be accurate enough for simulation of the lab-scale experiments. A case study will be carried out for a ship on modelling, designing and analysing a full scale practical ship model and presented in the next chapter.

CHAPTER 6. CASE SHIP STUDY

6.1. Comparison of the Chemical and Liquefaction Methods

6.1.1. Introduction

Nowadays, there are two technologies used for the storage and transportation of the different forms of CO_2 captured in onshore applications, i.e. compressed CO_2 and liquefied CO_2. For pipeline transportation, compressed CO_2 is the preferred option (Ciferno et al., 2010; Witkowski and Majkut, 2012). If captured CO_2 is transported by ship, both compressed CO_2 and liquefied CO_2 technologies can be used, where the latter is achieved by a combination of increased pressure and reduced temperature (IPCC, 2005). Currently, only the liquefied CO_2 method has been used for ship transportation (Aspelund et al., 2006) due to the density of the liquid form CO_2 being 580 times that of the gas form CO_2. Although there are many other technologies which can be applied for post-combustion capture (polymeric membranes, zeolites and activated carbon), eventually the transportation of gas will be in compressed or liquefied state. Therefore, in this section of the case study on a ship, the proposed chemical method will be analysed and compared with a liquefaction method regarding their economic feasibility.

There are some technical challenges in storing and transporting CO_2 in liquid form on ships. As a requirement of low temperature and high pressure, liquefied CO_2 has a low critical point (304K) and the point indicates the highest temperature for carbon dioxide liquefaction. If the temperature exceed this point, it is impossible to liquefy the gas with pressure increasing. Therefore, storage of CO_2 liquid places special requirements on the materials used for the storage tanks in order to cope with the conditions of high pressure and low temperature. It is also essential to make sure that there is no water or moisture contained within the liquefied CO_2 in order to prevent corrosion of the tank materials. Compared with the method of CPCS, the volume occupied by the liquefied CO_2 is 3% more than that of $CaCO_3$ (EIGA, 2010). In addition, ship stability should be well

considered as sloshing may occur with carrying liquefied CO_2 (Wischnewski; ITTC, 2011). In summary, in comparison with CO_2 liquid, storing solid CO_2 in the form of $CaCO_3$ on ships has the following advantages:

- $CaCO_3$ is a steady and corrosion free substances and no particular requirements on storage tank;
- Less volume is required;
- The storage has less impact on ship stability;
- $CaCO_3$ can be reused or placed in land disposal.

Other than the above ship operational and CO_2 storage advantages, a case study on a selected ship indicates the profit returned by selling the by-products from the chemical process. The following section presents a feasibility study of applying CPCS on the case study ship and a comparison with the liquefaction method.

6.1.2. Case Study Ship Selection

International shipping relies on different means of transportation and the majority of emissions from shipping are contributed by three main types of ships: container ships, bulk carriers and oil tankers. A case study ship should be selected from these ship types so that the study on emissions control and economics can then be generally applied to these vessel types. For tanker, there is inert gas system existing and the demand of carbon emission is lower so that the following case study will focusing on container ships and bulk carriers.

The specifications of the selected case study ship are listed in Table 6-1, along with the details of the voyage of the vessel. The ship is a bulk carrier transporting coal from China to the USA. The range, the service speed and the duration of one return voyage is estimated and presented in the table. The table also illustrates the vessel dimensions and engine specifications. Since the power output of the auxiliary alternators is only about 8.4% of the main engine power, fuel consumption and CO_2 emissions from the auxiliary engines are not considered for the case study.

Table 6-1 Specifications of the case study ship

Route details			Vessel dimensions			Engine specifications		
Origin	Qinhuangdao		Type	Bulk Carrier [a]		Engine	MAN B&W: 6S70MC-C7	
Destination	San Francisco		LOA	292	m	Number	1	
Range	5,547	Nm	LBP	283.5	m	Speed	91	rpm
Service Speed	15.2	Knot	Breadth	45	m	MCR	18,660	kW
Duration	16	Days	Depth	24.8	m	SFOC	174	g/kWh
			Draught	16.5	m	Generators	HHI/Himsen: 7H17/28	
			Gross	94,360	ton	Generators	3 (1 stand-by)	
			DWT	157,500	ton	Speed	900	rpm
			Water ballast	78,000	m^3	Power	780	kW
			Fuel	HSFO		SFOC	189	g/kWh

a: Sources of data: Significant Ships of 2011: Hyundai Trust.

6.1.3. Cost Estimation for CPCS

6.1.3.1. Total CO_2 Generated During a Voyage

According to the project guide of the selected engine and fuel type used, the gas flow rate of CO_2 emissions can be estimated as shown in Equation (5):

$$\dot{m}_{CO_2} = C_{HSFO}\, P\, SFOC \tag{24}$$

Where:

$\dot{m}_{CO_2}$ = mass flow rate of CO_2 in exhaust gas (kg/s);

SFOC = specific fuel oil consumption (g/kWh);

P = power output of main engine (kW);

C_{HSFO} = carbon conversion factor of HSFO.

With this flow rate of CO_2, the total CO_2 generated during a voyage (16 days) is 3,766.54 tonnes.

6.1.3.2. Exhaust Gas By-Pass into CPCS System

Based on the IMO target of 20% CO_2 emissions reduction by 2020, the CPCS system will be designed to absorb and store 20% of the CO_2 emitted by the engine of the case study ship, i.e. 753.31 tonnes of CO_2 for this voyage. According to the experimental results, the average CO_2 absorption rate is 67.9%. To achieve a 20% reduction in CO_2 emissions, the amount of exhaust gases by-passed to the CPCS system can be derived using Equation (6):

$$R_{by\text{-}pass} = R_{target} / R_1 \tag{25}$$

Where:

$R_{by\text{-}pass}$ = percentage of exhaust gas by-passed into the CPCS system;

R_{target} = targeted CO_2 reduction required by IMO regulations;

R_1 = absorption rate of CO_2.

According to the above estimation, about 30% of the exhaust gas should be fed into the CPCS system in order to achieve the target of 20% CO_2 reduction from the main engine exhaust gas. The mass flow rate of CO_2 fed into the CPCS can be derived: 0.80 kg/s. The quantity of CO_2 by-passed per voyage is 1,110 tonnes.

6.1.3.3. Initial Quantities of Chemical Substances Required

The quantities of all chemical substances involved in the reaction can be derived by applying Equation (4) in conjunction with Equation (1), (2) and (3). Thus, the quantities of caustic soda (NaOH) and quicklime (CaO) required per voyage are 86 tonnes and 959 tonnes, respectively. The limestone $CaCO_3$ finally produced per voyage is 1,712 tonnes.

6.1.3.4. Consumption of NaOH by CPCS System

In the CPCS system, the NaOH solution will be regenerated after the precipitation (causticisation) reaction. For the case study ship, the NaOH is assumed to be replenished on a daily basis. Since its regeneration rate is 85.37% according to the experimental results, the daily consumption of NaOH can be calculated using the following equation:

$$m_{refilled} = m_{system} (1 - R_2) \quad (26)$$

Where:

$m_{refilled}$ = daily consumption of NaOH (tonnes);

m_{system} = the theoretical quantity of NaOH needed by system (tonnes);

R_2 = regeneration rate of NaOH.

The total NaOH consumed during a voyage can be derived as follows:

$$m_{total} = m_{refilled}\, t \tag{27}$$

Where:

m_{total} = total NaOH required during a voyage (tonnes);

t = duration of a voyage (days);

6.1.3.5. Operational Costs of CPCS System

The operational costs of the CPCS consist of 3 components, i.e. the cost of the chemicals consumed, the cost of fuel operating the CPCS and the cost of the cargo loss penalty due to space taken by the chemical reactant and CPCS product.

6.1.3.5.1. Cost Estimation of Chemical Substances

There are 2 chemicals consumed during the chemical processes. CaO is consumed to precipitate the CO_3^{2-} ions into solution and turn them into $CaCO_3$ which is stored on-board. The consumption of NaOH is based on its regeneration rate. Since not all of the NaOH can be recycled, the replenishment of NaOH solute is necessary to maintain the required concentration of the NaOH solution. Table 6-2 presents the quantities of chemicals consumed per case study voyage and their unit prices.

Table 6-2 Quantities of substances consumption and costs

Chemicals	Quantities (tonne)	Unit price ($/tonne)	Cost ($)
Caustic soda (NaOH) consumed	200	83.33a	16,695
Quicklime (CaO) consumed	959	11.11	10,652
Sum			27,347

a: Sources of data: Prices achieved from Alibaba.com.

6.1.3.5.2. Energy Consumption and Fuel Costs

The energy consumed by the CPCS process includes the energy required for CO_2 separation from the engine exhaust gases, energy for the transfer of CO_2 gas and chemical solutions through the CPCS system, and energy used for handling and storing the solid chemicals and the end product of the CPCS process ($CaCO_3$) on the ship. Since the energy consumed in handling the solid materials is much lower compared with that for CO_2 gas separation and transportation, the energy consumed for solid materials handling is neglected in estimating the system energy consumption.

The power required for gas separation is due to the application of a membrane device which is about 500 kJ/kg CO_2 separated (Barbieri et al., 2011). Thus, the energy consumption by the membrane system can be obtained as shown below:

$$P_M = \dot{P}_M \, m_{CO_2}/t \tag{28}$$

Where:

P_M = power required by membrane device (kW);

$\dot{P}_M$ = energy required for CO_2 separation (kJ/kg CO_2);

$\dot{m}_{CO_2}$ = mass of CO_2 separated (kg);

t = operation time of membrane device (s).

CO_2 gas blowers are used to feed the CO_2 gas from the separation unit through the CPCS system. To estimate the power required for gas input, some assumptions are made on fittings and pressure head loss in reaction tank:

1. The solution height in the reaction tank is 6.44 metres;
2. The diameter and the length of the duct from the outlet of the membrane device to the reaction tank are 1 m and 10 m respectively;
3. There is one baffle and two 90° bends along the system
4. The pressure drops due to friction and fittings are estimated at about 0.99 Pa (Massey and Ward-Smith, 2012).

Therefore, the power required for gas input can be obtained with this equation:

$$P_B = \dot{m}_{CO_2} \Delta P_B / \rho_{CO_2} \tag{29}$$

Where:

P_B = power required by gas blower (kW);

$\dot{m}_{CO_2}$ = mass flow rate of CO_2 (kg/s);

ΔP_B = pump pressure required to transfer fluid or gas (Pascal);

ρ_{CO_2} = density of CO_2 (kg/m^3).

Thus, the total power demand for CO_2 separation and the CPCS is 402 kW. The fuel oil consumed due to the gas blower and membrane is 29 tonnes per voyage and the fuel cost is estimated to be $18,073.

6.1.3.5.3. Cargo Penalty Due to CPCS System Application

Table 6-3 lists the densities and volumes of the chemicals involved in the CPCS. The total volume taken by the chemicals is 1,112 m^3. The density of coal is 929 kg/m^3 so the mass of coal cargo in an equivalent volume is 1,034 tonnes (Anval Valves Ltd.). According to the current coal shipping price of 15 $/ton (CCM, 2013), the total cost of the cargo freight penalty due to the CPCS system application is$ 15,502.

Table 6-3 Volumes of coal lost due to storage of chemicals

Chemical substances	Density (kg/m^3)	Volume (m^3)
NaOH	2,130	94
CaO	3,355	286
$CaCO_3$	2,711	632
Sum		1,112

6.1.4. Profits Made from Selling the Product of the CPCS System

There are two kinds of profit resulting from applying the CPCS system:

a. Profit made from selling the final product of CPCS

b. Saving from carbon credits.

The final product from CPCS is $CaCO_3$ (limestone) which is an industrial raw material widely used in many different industries, such as the papermaking, construction and plastic industries. The commercial price of limestone is 50 $/tonne. Carbon credit is 15 $/tonne based on the report of '2012 Carbon Dioxide Price Forecast' (Wilson et al., 2012). Thus, the profits made from selling $CaCO_3$ and saving of CO_2 credits are $85,603.23 and $11,299.63 respectively per case study voyage.

6.1.5. Cost Comparison between CPCS and Liquefaction Method

Having conducted the above cost analysis, Table 6-4 presents the costs and profits of CPCS in comparison with the conventional liquefied CO_2 storage method.

It can be seen that if the $CaCO_3$ were sold at the destination of a voyage, applying CPCS could make $ 35,981 profit while also capturing 20% of the CO_2 emissions from the engine exhaust gases.

The operation costs and profit made from the liquefaction method are listed in the table above. There are no chemical substances involved in the liquefaction method so there is no cost due to the purchase of chemical substances. However, energy costs due to the CO_2 liquefaction processes are considerable as shown in the table. The freight reduction is a result of the storage of liquefied CO_2. The saving carbon credits and selling the captured CO_2 for enhanced oil recovery (EOR) are included in the profits.

Table 6-4 Cost and profit comparison

Costs per voyage ($)	Operation costs				Profits			Total costs
	Capture cost	Chemicals cost	Liquefaction cost	Freight reduction	Carbon credits	$CaCO_3$	CO_2	
CPCS	18,073	27,347	-	15,502	-11,300[a]	-85,603	-	-35,981
Liquefaction	18,073	-	21,021[b]	9,932	-11,300	-	-18,833[c]	6,758

a: Negative sign means earning profits; b: Wischnewski; The physics hyper textbook, 1998; c: Melzer, 2012.

6.1.6. Operational profile

In this case ship study, an assumption of using MCR during operation is considered which results a much higher quantities of CO_2 are captured comparing with practical situation. In a practical situation, the operation of an engine is dynamic and changing along with the voyage. Here is an example of operational profile for a bulk carrier in Figure 6-1 (Charlotte,

2015): 41% loaded, 32% in ballast and 27% in port. This example indicates that the vessel is operated only 73% of a year. Furthermore, the operation power is varied under each conditions. Even under loaded condition, the engine power output will be lower than MCR to reduce the vessel speed as well as the fuel consumption and emissions.

Considering operational profile of voyage, the realistic engine power (NCR: nominal continuous rating) can be derived. Therefore the carbon emission at NCR can be obtained with the same processes above. The consideration of operational profile will reduce the carbon emission quantity for capture and solidification. However, although the comparison results will be changed, it doesn't have impact on the advantage of chemical absorption method.

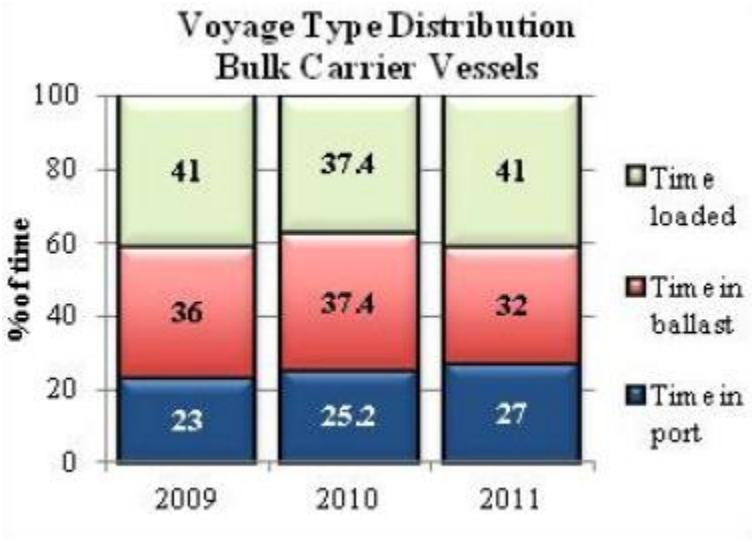

Figure 6-1 Voyage type distribution for bulk carriers

6.1.7. Conclusions

The comparative study between the chemical processes and liquefaction for CCS on-board ships has shown that one merit of the liquefaction method is relatively low operational costs. However, the CPCS method yields a higher profit from selling the product of the processes. The profit is sufficient to outweigh the running costs and freight penalties. The study proves that CPCS for marine CO_2 capture and storage offers advantages in terms of fewer requirements for the captured CO_2 storage and transportation. CPCS is a cost-effective method and can yield profits from every voyage as its product ($CaCO_3$) can be traded. It can be concluded that the proposed chemical absorption process for carbon dioxide solidification is a cost-effective method for ship CO_2 emissions reduction.

The next stage of the work covers the development of a Computational Fluid Dynamics (CFD) model based on the experimental data so that a full scale practical system for the ship can be designed and analysed.

6.2. Case study for practical installation on-board a ship

6.2.1. Introduction

Since the simulations of the lab-scale experiments were achieved in the previous chapter, the developed and optimised CFD model can now be applied for practical system simulations in full scale. It is essential to carry out an actual ship system simulation because the theory in the laboratory should be verified regarding its feasibilities for a real ship. In this chapter, a case study ship will be selected and a practical carbon absorption system will be designed and simulated for the selected ship. The specifications of the selected ship will be presented and utilised for modelling. The processes of the simulations cover the modifications of the simulation model, the design of the physical model, the application of the orthogonal design method, the introduction of the equipment and software, and the analysis of the results. After obtaining simulation results for the absorption process, the following processes can be designed: precipitation process, separation process and storage process. The weights and volumes occupied by these processes will be estimated according to the case study ship specifications and the requirements of the absorption system. After all the details of the processes and systems are derived, the next steps will be tank geometry design, tank positioning and creating a CAD drawing of the system positioning on-board. This chapter presents the general processes for carbon solidification system design for a case study ship which also provides a design guide for further applications on new ships.

6.2.2. Case Study Ship Selection

Nowadays the density of international shipping is advantageous for transportation. Many different types of ships are available for cargo transportation. Container ships, bulk carriers and tanker ships are vessels which are typically used for international transportation and they also contribute the majority of the carbon emissions according to the Third IMO GHG study from 2012. Figure 6-2 indicates the emissions of carbon dioxide from all types of vessels for international shipping. Among them, container ships contribute the most CO_2 emissions at around 205 million tonnes. Due to the large quantity of carbon emissions from container ships, this case study will focus on this vessel type and a container ship is therefore selected as the research target.

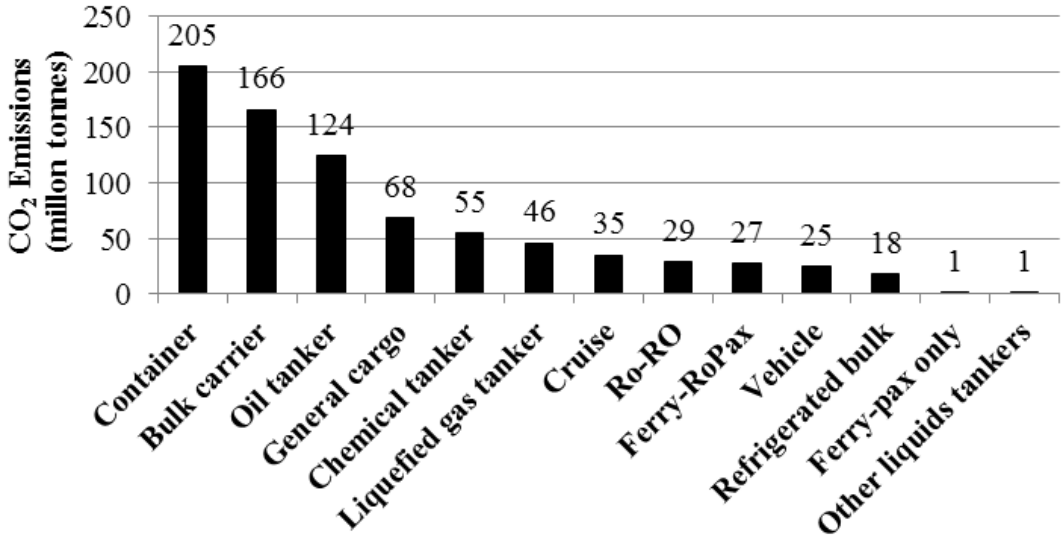

Figure 6-2 CO_2 emissions from international shipping by ship type 2012

6.2.3. Simulation Processes

To design a practical system, the simulation of the full scale system was firstly designed so that the feasibility analysis can also be carried out. The practical system can use the CFD simulation models and results which have been developed, optimised and analysed against the lab-scale experiments in the previous chapter. Since the results from the simulations match well with the experimental data, it indicates that the model represents the reaction processes accurately.

The design of the carbon solidification system should consider both engine specifications and practical feasibility on-board ships so that a reasonable physical model can be achieved. At this stage of simulation, the orthogonal design method is applied to reduce the otherwise considerable simulation numbers. The computing equipment and software are the same as previously used and detailed in Chapter 6. The results from the simulations will provide an optimal design for the practical system. After analysing the significant factors, an analysis optimal design will be compared with the optimal case which arises from the simulations. According to the comparison results, the better design from these two will be utilised for the case study ship.

6.2.3.1. Simulation Model Modifications

The simulation model for the lab-scale experiments is applied for this new practical system simulation. Since it has been shown that the results obtained agree well with the experiments, the reaction model can also present the practical reaction between the gas and solution phases so that it can be directly used for practical system simulation. Other internal models, such as the multiphase model and species model, will remain unchanged because the chemical materials used in the practical design are not changed. The only differences are the scale of the physical simulation parameters, such as container sizes, structures, additional gas and solution inlet and outlet and so on, which will now be simulated in full scale rather than lab-scale. Therefore, no reaction-related models are changed. With only the physical model changed, the previous simulation model can be applied for further system design and simulation.

The physical model will be enlarged from a lab-scale system because the capacity of the carbon absorption system should meet the requirement of the case study ship exhaust gas flow. Hence, the dimensions of the system should be carefully considered. Moreover, industrial processes usually apply a packed column or tray column system for the absorption process to increase the contact between the two phases, for example in the oil refinery industry. There are also many research works on CFD simulation of flow in packing and tray columns. Gao et al. modelled and analysed flow in random packing columns for seawater desulfurisation (Gao et al., 2011). Chen et al. from Tianjin University modelled and investigated the flow behaviour of two phase flows in a structured packing distillation column (Chen et al., 2009). The hydrodynamic characteristics of sieve trays in distillation columns were studied by Teleken and his colleagues (Teleken et al., 2009). A suitable physical design of the system should be selected and designed to satisfy the requirements of absorption efficiency and ship performance.

Other changes in this physical model are the flow rates of the two phases. It is apparent that the inlet flow rate of the gas and solution should be adjusted since the gas input is now

from the engine exhaust. The solution inlet flow rate should be controlled to prevent flooding and keep a high contact area between the two phases. The physical model design will be presented in the next section.

6.2.3.2. Physical Model Design

The physical model is designed based on a cylindrical container. Gas outlets and solution inlets are added on the top while gas inlets and solution outlets are added at the bottom of the container. In the laboratory, a measuring cylinder was used as the absorption reaction container. The simulation of the lab-scale experiments is in 2-dimensions and the results from the simulation matched well with those from the experiments. While simulating the practical absorption system, a 2-dimensional model will be built, simulated and analysed. Hence, this new model will present the practical cylindrical container for the case study ship.

6.2.3.2.1. Absorption System Selection

Currently, there are two popular absorption system structures used for chemical absorption: packing columns and tray columns. Compared with tray columns, packing columns have many advantages according to Perry's handbook of chemical engineering (Perry's handbook of chemical engineering, 8th edition):

- Low initial cost;
- Corrosion resistant (plastics and ceramics materials are available);
- Low pressure drop (which can be an advantage when a fan or compressor is applied for the tower);
- Easy and economic adaptability to small-diameter (less than 0.6 m or 2 ft.) columns;
- Excellent handling of foams.

According to Klemas and Bonilla's research, comparisons between column types are listed in Table 6-5. The research agrees with the statements above that packing columns can be

anti-corrosion, and have a low pressure drop. Furthermore, a packing column is able to work with a high capacity. At low liquid flow rates (less than 136 m^3/h), a packing column also has a better performance than a tray column. However, the disadvantages of a packing column are also presented in this table:

- Low performance at high pressure;
- Bad performance with high liquid flow rates (above 408 m^3/h);
- Anti-fouling system requires improvements;
- High inspection and maintenance costs.

Table 6-5 Packing and tray column rating comparison

Application in distillation	*Random packing*	*Structured packing*	*Traditional trays*	*High-capacity trays*
Pressure drop	2	1	3	3
Efficiency at high pressure	2	4	2	1
Efficiency at low pressure	2	1	2	3
Efficiency at low liquid rate[a]	2	1	3	4
Efficiency at high liquid rate[b]	3	4	2	1
Foaming systems	2	2	3	3
Non-metallic services	1	2	4	4
Fouling systems	4	2	1	1
Inspection and maintenance	3	4	1	1
Low cost	2	4	1	3

Application rating: 1, best; 2, good; 3, fair; 4, poor.
a. System flow rate is less than 136 m^3/h; b. Systems flow rate is over 408 m^3/h (Klemas and Bonilla, 2000.)

Since both packing columns and tray columns have advantages according to industrial experience, further consideration regarding applying them on ships will be made. Considering ship stability, a tray column is not preferred because there are large quantities of liquid accumulating on each tray until the liquid height reaches the height of the weir. The large quantities of liquid could slosh with the movement of the vessel which is definitely a potential risk against safe transportation. For a packing column, the liquid will be separated and obstructed by the packing material from accumulating, so that the sloshing effect is small compared to a tray column. Therefore, considering both industrial

experience and a practical situation on a ship, a packing column is a better option and will be selected for the practical system.

6.2.3.2.2. Absorption System Design

A typical packing column can increase the contact area between the liquid and the gas so that a high absorption rate is guaranteed. For most packing column applications, a counter flow design is preferred. It has a relatively high contact between gas and solution. Another reason is that gravity can be utilised to separate the gas and liquid phases as liquid is driven to move downwards by gravity. If using parallel flow, there is a requirement for more power output to maintain either the liquid moving upwards with the gas, or the gas moving downwards with the liquid.

Taking into account the counter flow design, the position of the inlets and outlets are set and designed as introduced in the previous section. However, even though the gravity effect is utilised, it is hard to ensure that both the liquid and the gas leave through their designated outlets. To prevent liquid from leaving through the gas outlets, mist eliminators are applied. The mist eliminators are nets fitted inside the reaction tank just before the gas outlets. When liquid mist touches the net, the liquid mist will attach, accumulate and drop from the net. This is also another reason why counter flow is preferred. To prevent gas from leaving through the liquid outlets, a pump is fitted at the outlets which can control the liquid outflow rate. A liquid seal on the liquid outlet will also ensure that gas only leaves from the gas outlets.

In the simulation, the gas outlets are covered by a region of porous medium to represent the mist eliminator. The porous medium provides resistance to the liquid phase, which prevents liquid from moving upwards. A pressure outlet boundary condition is applied on these outlets. For the liquid outlet, the mass flow inlet boundary condition is utilised to simulate the pump which constantly pumps liquid out of the reaction tank.

As the packing column will be applied in the absorption system, the designed system will be filled with spherical packing to increase the contact area. The size of the packing material will be further studied to find out its impact on the absorption process. A support will be included in the design so that the spherical packing can be fixed in the middle of the reaction tank.

Seven main factors are considered while designing the absorption system. For each factor, three different values will be selected in order to determine their impact on the absorption processes and to find an optimal case for the practical design:

- Tower height:

1.5, 1.75 and 2 metre are selected. These heights are selected considering the height of a container on the vessel and that volume on-board is limited.

- Tower diameter:

Three different diameters are selected, 2, 2.25 and 2.5 metres, taking into consideration that volume on-board is limited and that a small diameter is preferred when the liquid quantity is the same.

- Solution sprayer number and position:

Three different sprayer numbers, and positions between sprayers are chosen: 9, 10 and 11; 0.1, 0.125 and 0.15 metres. These two factors are considered together. When designing the sprayer layout, the distance between the left-most and right-most sprayers should be smaller than the tower diameter and should also leave enough space for the gas outlets.

- Packing material size:

Generally, for sphere packing material, the radius available on the market ranges from 0.01 to 0.08 metres (AceChemPack Tower Packing Co. Ltd). Therefore, three general sizes are selected: 0.02, 0.03 and 0.04 metres.

- Solution flow rate:

These solution flow rates are designed to prevent flooding and keep a reasonable contact area. 40, 60 and 80 kg/s liquid flow rates are selected.

- Gas flow rate:

The system is design such that 20% of the CO_2 the from engine exhaust gas is removed, as discussed previously. The flow rate of CO_2 is about 1.6 kg/s so gas flow rates of 1.2, 1.6 and 2 kg/s are selected for analysis.

One example of the designed system is presented in Figure 6-3. It indicates the positions of the gas and liquid outlets and inlets, mist eliminators, packing material and supports in the reaction tank. The blue lines represent the tank walls and the grey sections are the flow regions. The practical 3-D system can be derived by revolving this 2-D model, and the liquid distributor and gas outlets are presented in Figure 6-4. After designing the system, the next step will be testing this system with the developed CFD model. However, there are too many possible combinations of these factors to be tested within a limited time. The orthogonal design method will be introduced in the next section, and used to reduce the numbers of combinations which need to be tested hence saving computing time.

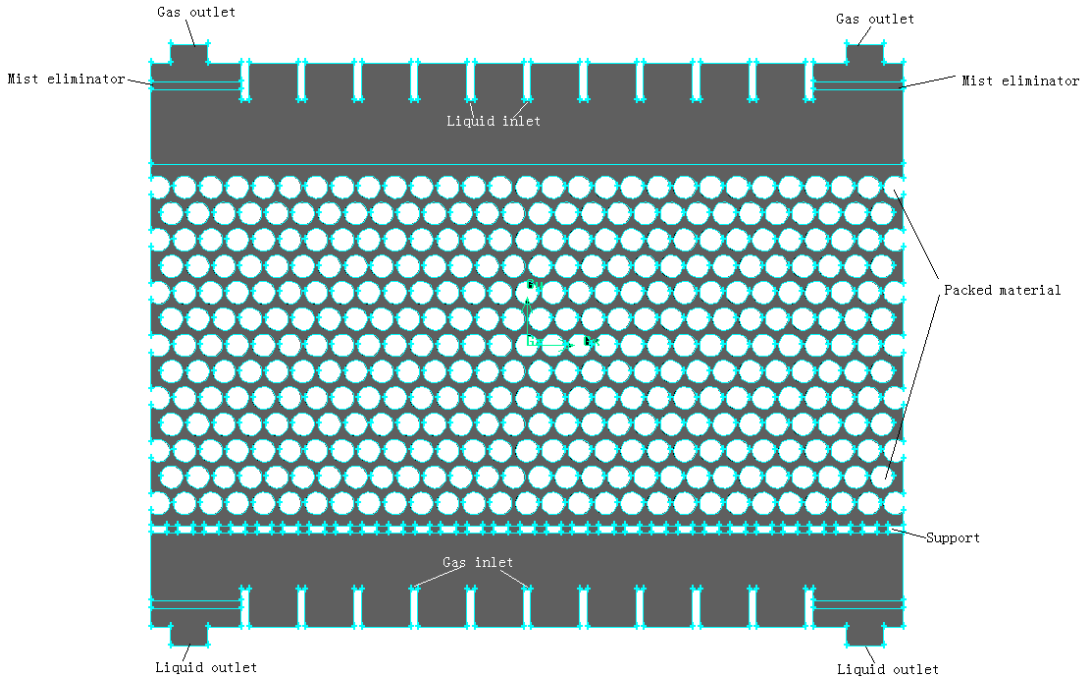

Figure 6-3 Example physical model of absorption system design.

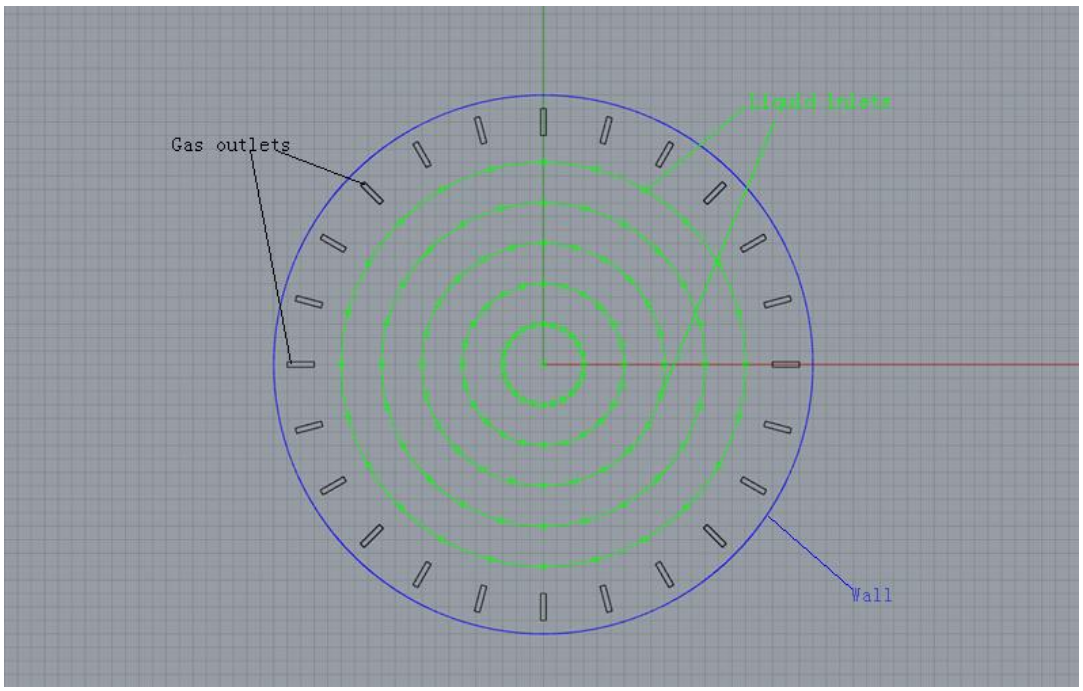

Figure 6-4 Schematic of liquid distributors and gas outlets.

6.2.3.3. Orthogonal Design Method Introduction and Application

The orthogonal design method is an experimental process which can be applied to test and compare the effectiveness of multiple different factors on a target system or process. It is an efficient way to discover new phenomenon, materials or regular patterns during scientific researchand with these findings, research results can be developed to discover more meaningful results. Design of experiment (DOE) was established by Ronald Aylmer Fisher in the 1920s (Ronald, 1935). DOE was futher developed and improved by Genichi Taguchi's research team during 1940~1950 and the Taguchi methods were established. The orthogonal design method has been widely used in many different fields. Qiu et al. applied this method on their slewing bearing models to test the performance of connecting bolts while analysing siginificant factors (Qiu et al., 2011). The orthogonal design method is also applied to improve optimisation algorithms and find an optimal solution in Gong and his colleagues' research (Gong et al., 2008). Kim and his colleagues utilised the orthogonal design method to develop and test a dual phase steel. Three levels of three controllable factors were considered: intercritical annealing, aging and galvanizing temperatures during the heat treatment process (Kim et al., 2009).

The orthogonal design method will be appliedto find out how the selected factors will impact on the absorption rate during the absorption process. The application of the orthogonal design method utilises a normalized table to the design experimens. It is an efficient, accurate and reliable way to discover optimal conclusions with a relatively small amount of trials. The selected factors are considered because they are important ones and are also controllable. A seven factors by three level orthogonal design method table (L_{18} 3^7) is designed as shown in Table 6-6 (Hong et al., 2012). According to the previous section, the factors and their levels are set up and presented in Table 6-7. Using a normalised orthogonal design method table, it is found that 18 different cases need to be tested which are presented in

Table 6-8.

Table 6-6 Seven factors with three level orthogonal design method table ($L_{18}\,3^7$)

	A	***B***	***C***	***D***	***E***	***F***	***G***
1	1	1	1	1	1	1	1
2	1	2	2	2	2	2	2
3	1	3	3	3	3	3	3
4	2	1	1	2	2	3	3
5	2	2	2	3	3	1	1
6	2	3	3	1	1	2	2
7	3	1	2	1	3	2	3
8	3	2	3	2	1	3	1
9	3	3	1	3	2	1	2
10	1	1	3	3	2	2	1
11	1	2	1	1	3	3	2
12	1	3	2	2	1	1	3
13	2	1	2	3	1	3	2
14	2	2	3	1	2	1	3
15	2	3	1	2	3	2	1
16	3	1	3	2	3	1	2
17	3	2	1	3	1	2	3
18	3	3	2	1	2	3	1

Table 6-7 Orthogonal design factors and levels

Factor code	***Factors***	***Levels***		
		1	2	3
A	Tower height (m)	1.5	1.75	2
B	Diameter (m)	2	2.25	2.5
C	Sprayer number	9	10	11
D	Sprayer position (m)	0.1	0.125	0.15
E	Packed material size R (m)	0.02	0.03	0.04

F	Solution flow rate (kg/s)	40	60	80
G	Gas flow rate (kg/s)	1.2	1.6	2

Table 6-8 18 cases derived using orthogonal design method table ($L_{18}3^7$)

Case No.	*A*	*B*	*C*	*D*	*E*	*F*	*G*
1	1.5	2	9	0.1	0.02	40	1.2
2	1.5	2.25	10	0.125	0.03	60	1.6
3	1.5	2.5	11	0.15	0.04	80	2
4	1.75	2	9	0.125	0.03	80	2
5	1.75	2.25	10	0.15	0.04	40	1.2
6	1.75	2.5	11	0.1	0.02	60	1.6
7	2	2	10	0.1	0.04	60	2
8	2	2.25	11	0.125	0.02	80	1.2
9	2	2.5	9	0.15	0.03	40	1.6
10	1.5	2	11	0.15	0.03	60	1.2
11	1.5	2.25	9	0.1	0.04	80	1.6
12	1.5	2.5	10	0.125	0.02	40	2
13	1.75	2	10	0.15	0.02	80	1.6
14	1.75	2.25	11	0.1	0.03	40	2
15	1.75	2.5	9	0.125	0.04	60	1.2
16	2	2	11	0.125	0.04	40	1.6
17	2	2.25	9	0.15	0.02	60	2
18	2	2.5	10	0.1	0.03	80	1.2

6.2.3.4. Software and Equipment

The simulation of the practical system is conducted according to the simulations of the lab-scale experiments. Since an example model was set up in the previous section, all the other models can be set up in the same way. Based on the simulation of the lab-scale experiments, the Fluent software is applied and 10 second simulations of 18 difference cases are carried out due to the limited computing resources. Since 18 different cases of the simulation are

required for system optimisation, the high performance computers from ARCHIE-WeST are applied. CAD software, Rhinoceros, will be used for modelling the case study ship and also the practical system installations. The absorption rate calculated for these cases will be presented and analysed in the following section.

6.2.3.5. Results and Analysis

The absorption rate in the practical system simulations is derived based on the same method as the lab-scale experiments, which is to monitor the concentration of Na_2CO_3. The absorption rate at 10 seconds for every case is derived and presented in Table 6-9. It is obvious that case 12 has the highest absorption rate so this case is found to be the optimal case.

Table 6-9 Results of absorption rates under different cases.

Test number	*1*	*2*	*3*	*4*	*5*	*6*	*7*	*8*	*9*	*10*	*11*	*12*	*13*	*14*	*15*	*16*	*17*	*18*
Absorption rate	12.97%	16.95%	13.42%	15.77%	16.22%	15.18%	20.65%	9.35%	19.63%	16.30%	13.61%	23.05%	18.27%	20.15%	11.45%	21.52%	18.26%	9.78%

6.2.3.5.1. Significance of Factors (R value):

After obtaining the absorption rates for all cases, analyses are carried out to find the impacts of the different factors on the absorption rates. For each level of every factor, a sum of the absorption rate value (K) is introduced which is presented as K1, K2 and K3. Also, average values of K and the ranges of average values (R) are derived and presented in

Table 6-10. The R value is applied to present the significance of these factors with regard to the absorption rate. As shown in the table, changing factor G, which is the gas flow rate, has the most significant impact on the resultant absorption rate. Therefore, the relative significance of these factors on the absorption rate can be derived as follows: Gas flow rate > Solution flow rate > Sprayer number > Width > Sprayer position > Tower height > Packed material size (or G>F>C>B>D>A>E). For the different factors, their impacts on the absorption rate are presented in Figure 6-5.

6.2.3.5.2. Comparisons between Analysis and Optimal Case

After obtaining the significance of the different factors, the optimal levels for different factors are also obtained from the results in the last section. Therefore another optimal case

based on the analysis only can be derived and presented in Table 6-11. This analysis optimal case is compared with the simulation optimal case, case 12, derived in the last section.

From Table 6-11, the levels of some factors are the same in both cases. Considering the significance of these factors, the gas and solution flow rate and sprayer numbers are three of the most effective factors for impact on absorption rate. In this table, these three factors are the same. Since these three factors would have the most impact on the absorption rate, it is reasonable to ignore the effect of the other factors, which have been found to be different in the two optimal cases. Therefore, these two optimal cases derived from the simulation and analysis show good agreement. The design of the practical system for the case study ship will use the parameters of optimal case. After the absorption system is designed, the remaining parts of the system can be designed. The next section will list some of the detailed information about the design of the whole system for a selected case study ship.

Table 6-10 Results of analysis from orthogonal design

Target	***Factor code***	***A***	***B***	***C***	***D***	***E***	***F***	***G***
Absorption rate	K_1	96.30%	105.48%	91.68%	92.35%	97.08%	113.55%	76.07%
	K_2	97.04%	94.54%	104.92%	98.09%	98.59%	98.79%	105.16%
	K_3	99.20%	92.51%	95.93%	102.09%	96.86%	80.19%	111.30%
	$K_1/6$	16.05%	17.58%	15.28%	15.39%	16.18%	18.92%	12.68%
	$K_2/6$	16.17%	15.76%	17.49%	16.35%	16.43%	16.47%	17.53%
	$K_3/6$	16.53%	15.42%	15.99%	17.01%	16.14%	13.37%	18.55%
	Range (R)	0.48%	2.16%	2.21%	1.62%	0.29%	5.56%	5.87%

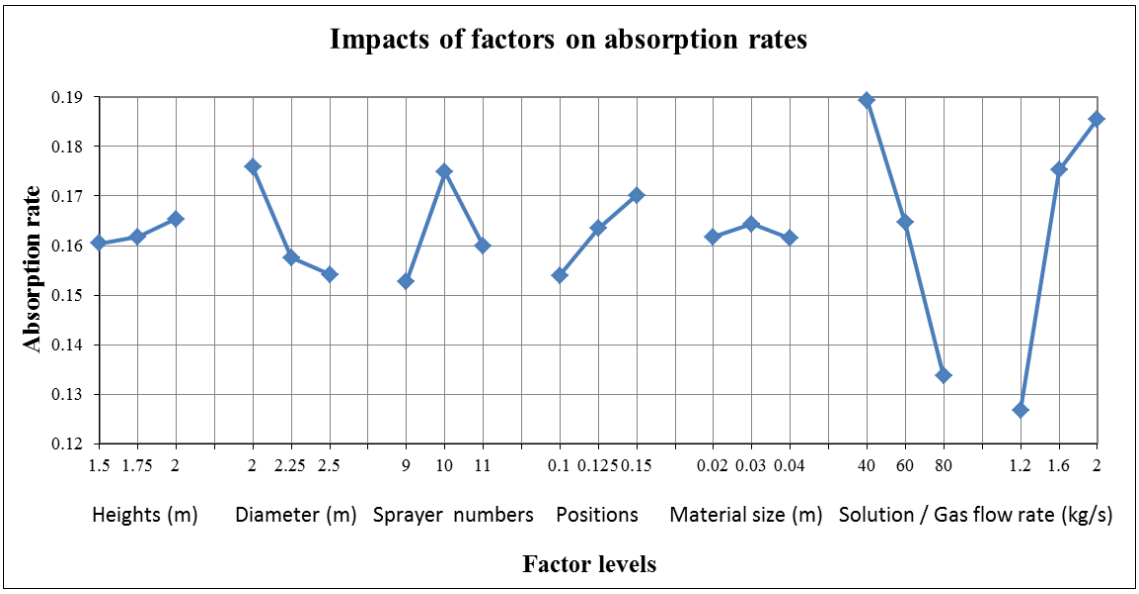

Figure 6-5 Impacts of factor levels on absorption rates

Table 6-11 Comparisons of simulated and analysis optimal cases

G>F>C>B >D>A>E	*Tower height(m)*	*Diameter (m)*	*Sprayer number*	*Sprayer position(m)*	*Packed material size R (m)*	*Solution flow rate(kg/s)*	*Gas flow rate (kg/s)*
From analysis	2	2	**10**	0.15	0.03	**40**	**2**
Optimal case	1.5	2.5	**10**	0.125	0.02	**40**	**2**

6.2.4. Case Ship Study

After designing and analysing a practical system for the case study ship, this section will design the remaining parts and processes of the system, and the specifications of the case study ship will be introduced as well. Figure 6-6 presents a schematic of the processes within the whole system. The exhaust gases from the funnels are bypassed through a separation system to remove other gases and to purify the CO_2. Then the high concentration CO_2 gas will be fed into the absorption reaction tank where the alkaline solution will be injected and reacted with the gases. The product solution will be transported to one precipitation tank until it is full. When this precipitation tank is full, the solution will be transported to another precipitation tank. The first tank will have CaO added to generate

$CaCO_3$ sediment and the products will be transported into a centrifuge separation system to remove the sediment from the solution. Finally, the pure alkaline solution from the centrifuge separation system will be recirculated back into the absorption reaction tank. The sediment will be stored in $CaCO_3$ storage tanks.

The positions of all parts and processes of the system will be considered and a drawing based on the use of the Rhinoceros 3-D modelling software will be presented for the case study ship in a CAD model. The calculations in this section are based on the results of the absorption tank from the simulations. The specifications of a standard 20 foot container are listed in Table 6-12 and equivalent container spaces required by the different tanks will be derived in the next section.

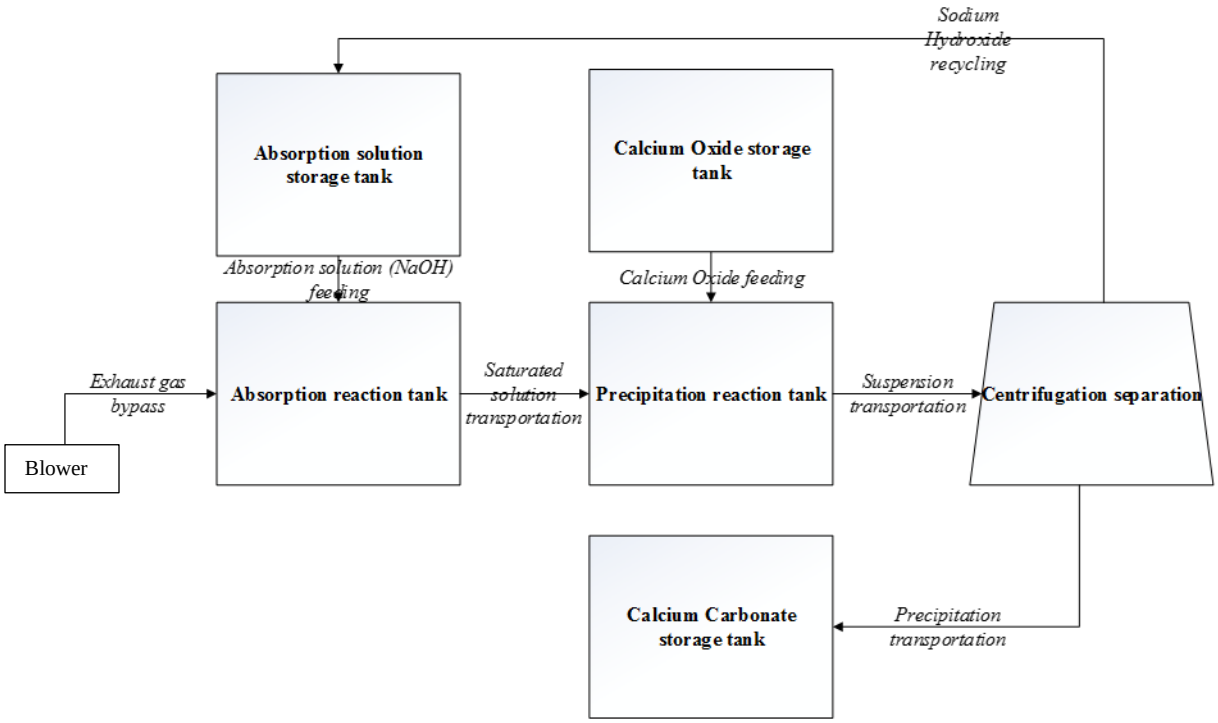

Figure 6-6 Schematic of on-board installation

Table 6-12 Specifications of a standard 20 foot container

Length (m)	***Width (m)***	***Height (m)***	***Inside Capacity (m^3)***	***Gross Weight (tonne)***	***Tare Weight (tonne)***	***Net Weight (tonne)***
5.87	2.33	2.35	32.85	24	2.44	21.56

6.2.4.1. Tank Volumes

The calculations will follow the absorption processes and calculate the volumes of the following: absorption tanks, precipitation tanks, NaOH supply tanks, CaO storage tanks, centrifuge separation systems and $CaCO_3$ storage tanks. All the volumes are based on the reaction equations with some additional margins for practical applications.

6.2.4.1.1. Absorption Tank

After analysing the simulation results, an analytical optimal model and an optimal case were obtained in Table 6-11. Both cases have similar solution and gas flow rates, and sprayer numbers. The factors which differ are the tank height, diameter, sprayer position and packing material size. Among these factors, the tank height and diameter have a direct impact on the tank volume. For the analysis optimal case, both the height and diameter are 2 metres, which means the volume can be derived using a basic cylinder volume equation which gives a result of approximately 6.28 m^2:

$$V = \frac{\pi d^2 h}{4} \tag{28}$$

Where:

V = the volume of the cylinder;

d = diameter;

and h = height.

For the optimal case derived from the simulation, the tank height is 1.5 metre and the diameter of the tank is 2.5 metres. Based on the volume equation above, the volume of this tank is about 7.36 m^2. It is apparent that the smaller tank would be preferred under the same working capacity since volume on a ship is very valuable. Moreover, the volume of the absorption tank is smaller than that of a standard container so one container position is assigned for the absorption tank installation.

6.2.4.1.2. Precipitation Tanks

The next process after absorption is precipitation and the solution resulting from the absorption process and the CaO will be fed into the precipitation tank. To maintain the output from the absorption reaction, two precipitation tanks are designed to work separately and hourly. In the first hour, precipitation tank A will be filled with product solution from the absorption process and CaO will be added in simultaneously. The stirring device will start working to accelerate the precipitation reaction process. In the second hour, the filling and precipitation of the solution into tank A will be paused and instead, the transportation of products into the centrifuge separation system will start, for separation of the sediments and solution. At the same time (during the second hour), the product solution from the absorption process will be filled into precipitation tank B (in the same way as it was into tank A in the first hour) so that a continuous absorption and precipitation reaction can be maintained. Therefore the volume of the precipitation tank should be enough to be able to store the feed of the solution from the absorption reaction for one hour. As the solution flow rate in the absorption process is 40 kg/s and also considering the molecular formula, molar mass and density, the quantity of product solution in each tank is about 151.02 tonnes per hour and the volume should be therefore be 126.06 m^3. An assumption is made here that a full precipitation reaction and final product transportation can be completed in one hour. The assumption is based on the experiments carried out in the laboratory where the precipitation process usually takes 3 hours for a full reaction. With more advanced

industrial mixing systems like the stirring devices, the reaction could be faster so an approximate reaction time is assumed. Further work can be targeted on finding out more accurately the timings of the full process and the required volumes of the precipitation tanks, and these could then be changed accordingly if required.

The maximum allowable gross weight of a standard 20 foot container is 24 tonnes and the tare weight of a container is 2.4 tonnes. The inside capacity of a standard 20 foot container is 32.85 m^3. Hence, considering weight, each precipitation tank requires the equivalent of 8 containers spaces. When considering volume, each precipitation tank also requires 8 containers spaces. Further consideration on the dimensions of the precipitation tanks will be discussed in Section 7.4.3.

6.2.4.1.3. NaOH Storage Tank

The supplement of NaOH for the absorption solution is based on the results from the experiments, taking into account that the efficiency of the NaOH regeneration rate is 85.37% so that the loss of NaOH in the solution can be calculated. This comes to around 1213.47 tonnes required for supplementing the NaOH lost, which occupies 569.48 m^3 on board. Considering the weight limitation of the containers, the NaOH supply tank requires 57 container spaces and while the volume of the container requires only 18 containers spaces. In Section 7.4.3, the dimensions of the NaOH storage tank will be further considered.

6.2.4.1.4. CaO Storage Tanks

According to the last section, the CaO should be prepared before the precipitation reaction, as it is a reactant in the process. The quantity of CaO required can be derived from the target carbon emissions reduction. Since this case study aims to reduce 20% of the total carbon emissions over the case study voyage, the quantity of CaO can be calculated based on the relationship between CaO and CO_2 in the final product, $CaCO_3$. Hence, 2881.16 tonnes of CaO are required for an entire voyage in Table 7-8 which is about

858.77 m^3 per voyage and 53.67 m^3 per day. Again considering the weight limitation of typical containers, the CaO storage tank requires 134 containers spaces and considering the volume of a container, only 27 containers spaces are required to accommodate the volume of the CaO tank. In Section 7.4.3, the dimensions of the CaO storage tank will be further considered.

6.2.4.1.5. Centrifuge Separation

For a centrifuge separation system, two factors are considered during selection: the type and capacity of the separator. For separation type, liquid and solid separation is required because the feed from the precipitation process is a mixture of liquid and solid. Since the mixture feed also has a constant flow rate, the selected separation system should be able to deal with this amount of mixture. Since the flow rate in the precipitation tank is 252.12 m^3/h, the capacity of the separation system should be at least this value. Finally two centrifuge separation systems with the same capacity are selected, each with a separation capacity of 160 m^3. The selected systems are Flottweg decanter centrifuge C7E from Flottweg Separation Technology and their dimensions are derived as shown: length 4.8 m × width 1.72 m × height 1.4 m. Hence, the volume occupied by the two separation systems is 23.12 m^3 in total.

6.2.4.1.6. $CaCO_3$ Storage Tanks

The last process of the system is the storage of the final product, $CaCO_3$. Like the quantity of CaO, the quantity of $CaCO_3$ can be obtained from the target for carbon emissions reduction. Hence, referring to the reaction formula and the chemical molecular masses, the quantity of $CaCO_3$ is found to be 5145 tonnes per voyage (shown in Table 7-8) or 322 tonnes per day. Considering the density of $CaCO_3$, the volume taken by the final product is 1898 m^3 per voyage and 119 m^3 per day. Again considering the weight limitation of a container, the $CaCO_3$ storage tank requires the equivalent of 239 containers spaces and while considering the volume of the container, only 58 containers spaces are required to

accommodate the volume of the $CaCO_3$ storage tank. The dimensions of the $CaCO_3$ storage tank will be further considered in Section 7.4.3.

6.2.4.2. Case Study Ship Specification and Modelling

Before designing the dimensions of the different tanks, the modelling of the selected container ship is first conducted. The selected ship is a 6300 TEU (twenty-foot equivalent unit) class container carrier, called Sealand Michigan, from Hyundai. The details of this vessel and the engine specifications are listed in Table 6-13 and Table 6-14 respectively.

The CAD model of this containership is established and presented in Figure 6-7 and Figure 6-8. The red and light blue parts represent the ship's hull below and above the water line. The pink part is the superstructure and the dark blue part is the funnel. The grey sections in Figure 6-8 are the containers carried on the ship. In the next section, all the required tanks will be designed and positioned within this CAD model.

Table 6-13 Container ship details

LOA	303.96	m
LBP	292.00	m
Breadth	40	m
Depth	24.2	m
Draught	12	m
Voyage duration	16	days
Shipping capacity	6300	TEU

Table 6-14 Main engine specifications

Engine type	*B&M 10K98MC-C*	
MCR	57059	kW
SFOC	171	g/kWh
Fuel carbon factor	3.021	

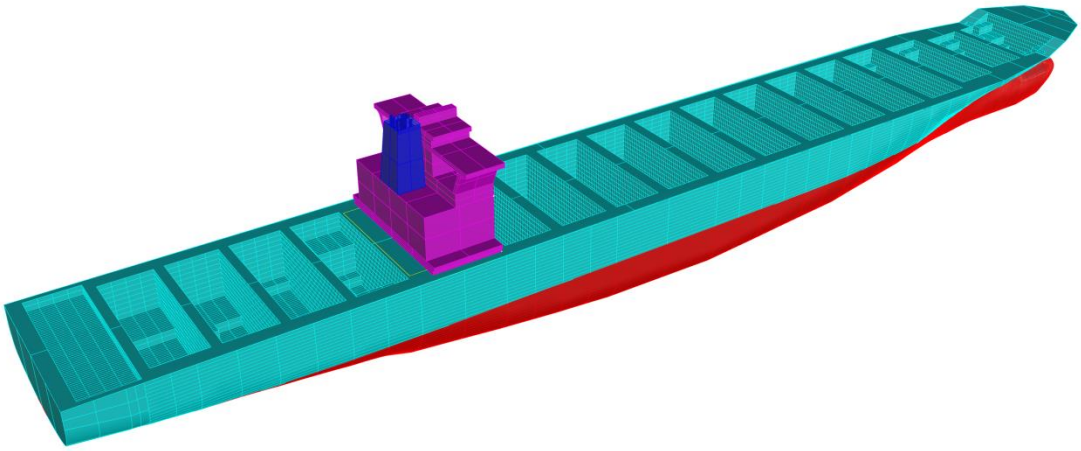

Figure 6-7 CAD model of the selected containership: empty load case

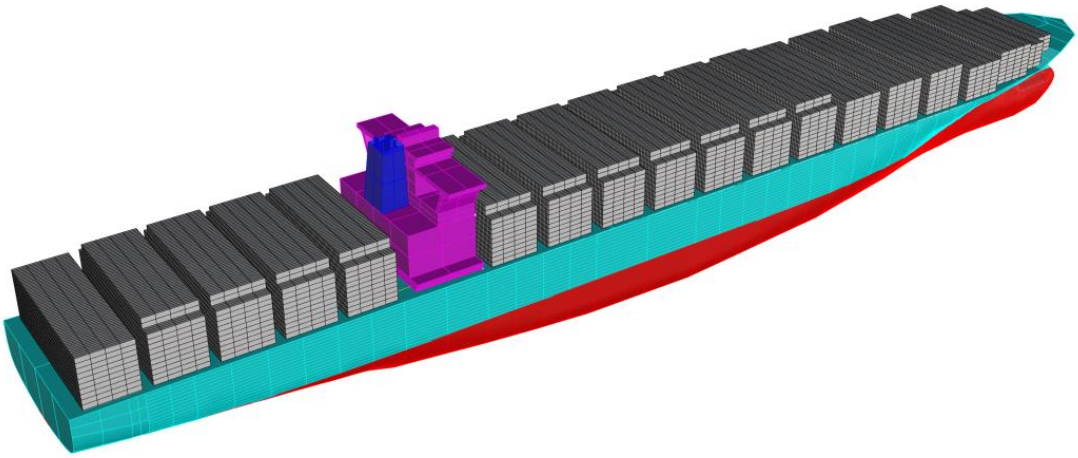

Figure 6-8 CAD model of the selected containership: full load case

6.2.4.3. System Design, Positioning and Drawing

6.2.4.3.1. Absorption Tanks:

The dimensions of the absorption tanks are fixed based on the simulation and analysis results. The volume taken by the absorption tanks is only about 0.2 container volumes. To

make sure that there is enough space for associated pipelines, blowers and pumps, 1 container volume is assigned to the absorption tanks. The position of these tanks should be near the main engine and the funnel so that the exhaust gas could be by-passed from them and the power required for transportation is low.

6.2.4.3.2. Precipitation Tanks:

The precipitation tanks are aiming to deal with the product from the absorption process hourly so that the volume taken by each precipitation tank is larger than that from the absorption process within one hour. To ensure the volume is sufficient for the precipitation process, a 20% margin is added and the final volume of one tank is therefore 302.54 m^3. Hence, 10 times the volume of a container is assigned to each precipitation tank. The total container volume required by the precipitation tanks is 20 container volumes. The location of these tanks should be next to the absorption tank because the precipitation process deals directly with the product from the absorption process.

6.2.4.3.3. Centrifuge Separation:

Centrifuge separation systems have a fixed dimension and the data is provided by the manufacturer. About 0.7 times a container volume is required for two sets of systems. Hence, 1 container volume will be designated for each, considering the fittings needed between systems, precipitation tank and $CaCO_3$ storage tanks. Since the centrifuge separation systems are fitted to these tanks, it is cost-effective to locate them near each other.

6.2.4.3.4. NaOH, CaO and $CaCO_3$ Storage Tanks:

If the NaOH, CaO and $CaCO_3$ are designed to be stored in containers, the limitations of the containers should be considered. Since the net weight of a container is limited, the numbers of containers required for NaOH, CaO and $CaCO_3$ storage tanks can be derived. This is found to be about equivalent to 57 containers for NaOH, 134 for CaO and 239 for $CaCO_3$.

This is about 7.02% of the total cargo in this container ship. To reduce the container spaces occupied by these storage tanks, a modified tank is designed. The weight limit of containers is set at 24 tonnes because the working load of the cranes used for container loading and unloading is limited. Therefore, considering the working load of the cranes, a new container can be designed with an acceptable weight and volume penalty.

The weight limit of a full load standard container is 24 tonnes. The maximum weight of a newly designed container with full load should be 24 tonnes. The tare weight of a standard 20 foot container is 2.44 tonnes so the cargo in the container can weigh up to 21.56 tonne. 21.56 tonne of NaOH has a volume of 10.12m^3. The same weight of CaO has a volume of 6.43 m^3 and that of $CaCO_3$ take 7.95 m^3. They are all less than one third of a container inside volume. To keep the original arrangement of containers on the ship, several new containers should share one slot of a standard container. Hence the new container will be designed to have 1/3 the volume of a standard container. This is selected while also considering the thickness of the container walls. In this way, not only is the volume on the ship saved with no change to the container arrangement but also the weight of the new container still meets the requirements of the crane working loads.

Since the total weight of CaO and $CaCO_3$ is related to operation time, the total weight reaches a maximum at the voyage destination. Therefore, although the total weight of NaOH, CaO and $CaCO_3$ is 9239.56 tonnes, the instantaneous weight is increasing from 4096.63 tonnes to 6358.40 tonnes. This is because the consumed NaOH and CaO are finally contained as $CaCO_3$. The locations of these storage tanks are above the absorption reaction tank. The locations of the containers filled with CaO and $CaCO_3$ are in the No. 7 hold of the container ship. With this arrangement of storage tanks, their weights are balanced with the help of the ballast water management system so that the risk of overload on one side of the ship is eliminated. Considering the dimensions of all tanks and assigned containers, a CAD drawing is derived. In Figure 6-9, 385 containers designated for CaO and $CaCO_3$ are assigned to No. 7 hold.

The layout of No. 7 hold is designed for the installation of the carbon solidification system and is shown in Figure 6-9. There are three areas in this container hold: container area, transportation area and system operation area. In this figure, the blue area is the container area and the grey area is for transportation. The system operation area is the green and yellow areas. With this arrangement, the storage tank can be transferred to the yellow area for collecting the product. In the green area, the absorption tank, precipitation tanks and centrifuge systems are located. A CAD drawing of the bottom section of No. 7 hold is displayed in Figure 6-10.

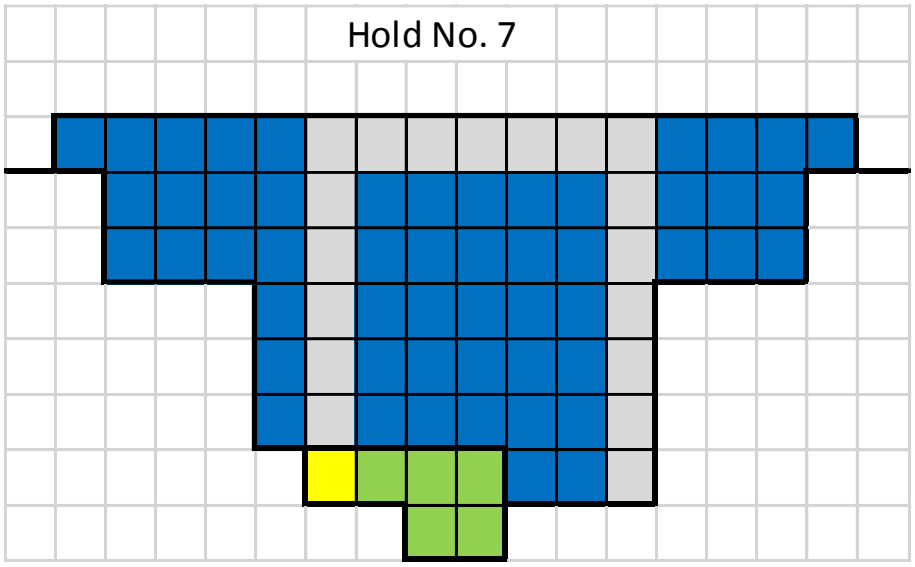

Figure 6-9 Mid-section view for arrangement of absorption, solidification processes and storage tanks on the container ship (Blue: storage tanks; Yellow: storage tank working place; Green: absorption, solidification and separation processes working place; Grey: transportation routes.).

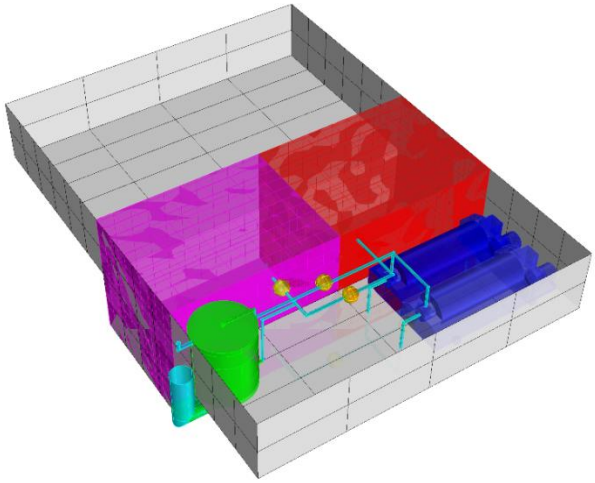

Figure 6-10 CAD drawing of carbon absorption and solidification system in working places of No. 7 hold (Green: absorption system; Pink: precipitation tank; Blue: Centrifugation separation systems; Light blue: fitting pipes; Yellow: dimensions of elements.).

6.2.5. Conclusions

This chapter introduces and presents a case study of a carbon solidification system design and application on a selected ship, based on previous work using CFD simulations and lab-scale experiments. The simulation processes apply a full scale CFD model based on previous simulation processes in lab-scale. A physical model of the absorption reaction tank is designed according to the limitations on-board the ship and also analysed using the orthogonal design method. After simulation and analysis, a simulation optimal case and an analysis optimal case are obtained. The analysis optimal case is eventually selected. This model occupies a lower volume of cargo space than the simulation optimal model while the levels of the most significant factors impacting on absorption rate are kept the same. Based on the output from the physical absorption tank model, the tanks and systems in the remaining processes can be derived. Then the case study ship is selected and modelled with CAD software and the positions of all the tanks and systems are designed and presented on a CAD drawing. This chapter also presents a good guide for the process of practical design, analysis and installation of a carbon solidification system on any vessel. However, further work is still required. For example, the time required for the precipitation process may need further consideration. Future work can also focus on designing the fittings between all of the tanks and the systems before the absorption reaction processes, such as the gas blower and CO_2 separator.

CHAPTER 7. SUMMARY, CONCLUSIONS AND FUTURE WORK

This chapter will summarize the contents and conclude on the results presented in this thesis. Recommendations will be made based on the research so that applications of the proposed method for new vessels can follow the design, analysis and installation processes presented.

7.1. Summary

7.1.1. Regulations Reviews

As a driving force behind this project, the emissions control regulations are also the main reason why ship owners are considering reducing carbon emissions from exhaust gases. In this thesis, current regulations were reviewed and discussed. Currently, IMO regulations have come into force which require ships to reach the EEDI standard by applying different technologies to increase energy efficiency. A 20% reduction of carbon emissions from ships is also set by the United Nations as a global target to be achieved by 2020. According to the Third GHG study from the IMO these regulations have already managed to reduce the emissions from ships. The CO_2 emissions from international shipping were 796 tonnes in 2012 and 870 tonnes in 2007. It is a great encouragement for further application of the emissions reduction regulations and also an excellent way to help mitigate global warming for a better future.

7.1.2. CCS Method Reviews

Three commonly applied CCS methods were introduced in this thesis: namely the pre-combustion method, the oxy-fuel combustion method and the post-combustion method. The principles of these methods were explained and available technologies were also listed in the literature review chapter. As the application of CCS on marine activities is of interest

in this work, especially on-board ships, all these three methods were considered based on the requirements, situations and conditions on ships. For the pre-combustion method, the most serious constraint was the required change in engine type, which is not currently acceptable for most ship owners. The limitation of applying the oxy-fuel combustion method is the combustion in the engine. Due to a high concentration of oxygen, the combustion is quite violent and the engine may become overloaded and damaged. For the post-combustion method, the changes are minor as they only require a separate system to be attached to the exhaust gas system with no major effects on the initial ship design. Therefore, after a review of CCS methods for onshore applications, the post-combustion method was seen as the most suitable one and a proposal for applying chemical absorption and solidification was introduced in the following chapters.

7.1.3. Proposed CCS Method

The proposed chemical absorption and solidification process aims to store the carbon element within a solid and stable compound in standard tanks or containers. If the carbon is contained in liquid or gas form, not only are highly specialised tank materials but also considerable tank volumes required. It is extremely expensive due to the high value of space on-board ships.

The principles of this absorption and solidification process are applying sodium hydroxide to absorb CO_2 from the exhaust gases and then treating the CO_2-rich solution with calcium oxide so that sediment calcium carbonate can be generated. In the processes, the nature of sodium hydroxide as an alkali is utilized. As a stable compound, calcium carbonate decomposes only at high temperature and that's why it can be used as a building material.

7.1.4. Laboratory Experiments

Experiments were carried out in a biochemistry laboratory which also provided most of the commonly used chemical experiment apparatus using within the tests, such as different types of glass containers, support stands and measuring equipment. A range of experiments

was carried out to examine the impacts of different factors on the absorption rate which could be achieved. There were several significant factors which were examined, such as the geometry of the absorption tank, gas input flow rates and solution concentrations. The data achieved from the experiments was applied for both an economic feasibility assessment and also for CFD model validation.

7.1.5. Economy Feasibility

The feasibility assessment from an economic point of view was carried out to find the cost of the solidification system application. Operational costs, benefits earned and cargo penalty were all considered. A cost comparison between the standard liquefaction method and the proposed solidification method were presented as well which indicated that the proposed solidification method could generate a profit at the end of the voyage by selling the final product, $CaCO_3$, to other industries.

7.1.6. CFD Simulations

The objective of applying CFD simulations was to design a practical system for installation on-board ships. The model was designed and optimised in lab-scale using the ANSYS Fluent software and the simulation results were compared with the experimental data. After optimisation, a CFD model which was consistent with the experiments was developed. This CFD model also illustrated some factors which couldn't be measured in the experiments, such as the pressure and movement of the gas and solution. As a validated and verified model was derived, the design and simulation of a practical system in full scale became possible.

7.1.7. Practical System Design and Installation

To design a practical system, a case study ship was first selected and all subsequent design work was based on the parameters of this ship and its main engine. There are two commonly used absorption systems in the chemical absorption industry, packed columns

and tray columns. As the system will be applied on a ship, the packed column was found to be better due to low sloshing effects. Based on the exhaust gas flow rate, the modelling of the absorption system was derived. After optimisation with the orthogonal design method, an optimal design was finally applied on a case study ship. The remaining tanks were then designed and the locations and operation of all tanks was considered. A CAD drawing indicating the design and installation was also presented.

7.2. Conclusions

Since climate change has become a popular topic, researchers have been looking for ways to mitigate it. Many projects aim to achieve a reduction in carbon emissions from many different sources. One good example is the carbon reduction from power plants which is one of the most significant emission sources. It is interesting to research the methods applied for carbon emissions reduction. Usually, a carbon capture and storage process is attached to these plants, which can separate the carbon from the initial fuel or exhaust gases and store it underground or under the ocean. There is also an inspiring way to deal with captured CO_2, as it can be utilised for oil production in oil fields in an approach called enhanced oil recovery.

Due to the pressure on the environment as a result of global warming, the IMO has also published regulations for ships with regard to their carbon emissions. The IMO aims to reduce the emission of CO_2 from marine activities by 14% by the year 2020. Currently, there are many methods targeting increasing the energy efficiency of ships, such as engine combustion chamber optimisation, hull coating and route optimisation. These methods have successfully reduced the carbon emissions of shipping from 1046 tonnes to 938 tonnes. The work presented in this thesis gained inspiration from CCS systems and tried to apply CCS on ships so that the reduction of carbon emissions could be enhanced.

After reviews on currently available CCS methods, there were three general methods found: the pre-combustion method, the oxy-fuel combustion method and the post-combustion

method. Unfortunately, there are few on-board CCS projects current under research. Therefore, reviews on the three different methods were carried out to find a suitable one for ship applications. The conclusion was that the post-combustion method required fewer changes at the ship design stage, such as engine type change and engine material enhancement. Considering the critical nature of the sloshing liquids on ships, a solidification method of CCS was proposed and examined through laboratory experiments. The experiments indicated the feasibility of the proposed processes and also provided data for economic feasibility assessment and CFD model validation. The economic feasibility assessment showed that the proposed method could generate profit after selling the final product, which is not possible in the liquefaction method. The CFD model was validated and applied for practical system design. A case study was carried out on a ship, looking at how to design and install the proposed system. This could also be a good guide for other ships when considering the design and installation of this system on-board.

The main findings of the research are following:

a. This research investigate the research gaps of using CCS as maritime carbon emission reduction methods.
b. Experimental testing and analysing a chemical absorption method for ship carbon emission reduction were conducted in this research works.
c. Compared with experimental data, a CFD model of lab-scale absorption system is developed and validated.
d. Financial analysis of chemical absorption method and its comparison with liquefaction method was carried out based on data provided from experiment section.
e. This research eventually design, optimisation and installation of the system a case ship practically.

7.3. Future Work

As this thesis proposed, designed, optimised and analysed a full CCS method for ship applications, there are still further aspects which should be considered in future work. One is the safety issue which mainly relates to the handling of chemical materials on-board the ship. A detailed handbook about these corrosive materials would be necessary. Also, it would be essential to train crews about how to operate this system. A risk analysis would also be very helpful in order to indicate the possible hazards and emergency solutions.

Another shortcoming is that the target in this thesis for the full practical system was just one case study ship (a container ship). In addition, the economic analysis was only carried out for one vessel (a bulk carrier) over one voyage. When applying the systems on another ship of a different type, size and specification, there might be some difference from the guideline case study. To ensure the feasibility of this method on all other scenarios, further effort should be made in carrying out case studies for these scenarios.

REFERENCES

Aspelund, A., Mølnvik, M.J., & Koeijer,G.D., 2006. Ship Transport of CO2 -Technical Solutions and Analysis of Costs, Energy Utilisation, Exergy Efficiency and CO2 Emissions.

ANSYS Fluent 14.5, Theory Guide, 2012, USA. http://www.ansys.com

Asendrych, D., Niegodajew, P., & Drobniak, S., 2013. CFD Modelling of CO2 Capture in a Packed Bed by Chemical Absorption. Chemical and Process Engineering, 34(2), pp. 269-282. Retrieved 17 Oct. 2014, from doi:10.2478/cpe-2013-0022. http://www.degruyter.com/view/j/cpe.2013.34.issue-2/cpe-2013-0022/cpe-2013-0022.xml

Barbieri, G., Brunetti, A., Scura, F., & Drioli, E., 2011. CO2 Separation by Membrane Technologies: Applications and Potentialities.

Banks C., 2015. Operational Practices to Improve Ship Energy Efficiency, PhD thesis, Department of Naval Architecture, Ocean and Marine Engineering, University Of Strathclyde, 2015

Barthelemy, H., Bourdeaud'huy, D., Jolivet, J.-L., Kohl, U., Krinninger, K., Teasdale, D., Webb, A., & Williams, S., 2010. IGC Doc 164/10/E: Safe Handling of Liquid Carbon Dioxide Containers that Have Lost Pressure, European Industrial Gases Association (EIGA) Aisbl.

Boden, T.A., G. Marland, and R.J. Andres. 2016. Global, Regional, and National Fossil-Fuel CO2 Emissions. Carbon Dioxide Information Analysis Center, Oak Ridge National Laboratory, U.S. Department of Energy, Oak Ridge, Tenn., U.S.A. doi 10.3334/CDIAC/00001_V2016.

Boundary Dam Integrated Carbon Capture and Storage Demonstration Project, SASKPOWER CCS, Canada, 2014. http://www.saskpower.com/wp-content/uploads/clean_coal_information_sheet.pdf

Bunker Price of Hong Kong, Marine Engineers Review, Institute of Marine Engineering, Science and Technology, November, 2013, page 38.

Bulk Density Chart, Anval Valves Pvt Ltd.

Chambers, C., & Holliday, A.K., 1975. Modern inorganic chemistry-An intermediate text, Butterworth & Co (Publishers) Ltd 1975, 133pp. http://files.rushim.ru/books/neorganika/Chambers.pdf .

Chen, J.B., Liu, C.J., Yuan, X.G. & Yu, G.C., 2009. CFD Simulation of Flow and Mass Transfer in Structured Packing Distillation Columns, Separation Science and Engineering, Chinese Journal of Chemical Engineering, 17(3) 381-388 (2009).

Cheng-Hsiu Y., Chih-Hung H., Chung-Sung T., 2012. A Review of CO 2 Capture by Absorption and Adsorption, Aerosol and Air Quality Research, 12: 745–769, 2012, doi: 10.4209/aaqr.2012.05.0132.

Chia-Chang L. and Bor-Chi C., 2007. Carbon Dioxide Absorption into NaOH Solution in a Cross-flow Rotating Packed Bed, J. Ind. Eng. Chem., Vol. 13, No. 7, (2007) 1083-1090.

Ciferno, J., Litynski, J., Plasynski, S., Murphy, J., Vaux, G., Munson, R., & Marano, J., 2010. Carbon Dioxide Capture and Storage RD&D Roadmap, Department of Energy and National Energy Technology Laboratory.

DNV and PSE report on ship carbon capture & storage, Det Norske Veritas, Oslo and London, 2013, http://www.psenterprise.com/news/data/130211_dnv_ccs.pdf .

Ethan J. N., Evyatar S., Zachary S. F., Lisa D. P., and Menachem E., 2016. Low-Temperature Carbon Capture Using Aqueous Ammonia and Organic Solvents, Environ. Sci. Technol. Lett. 2016, 3, 291−296, DOI: 10.1021/acs.estlett.6b00253.

European Commission, 2012. Commission Staff Working Paper: Analysis of options beyond 20% GHG emission reductions: Member State results. Brussels, Feb 2012. http://ec.europa.eu/clima/policies/strategies/2020/docs/swd_2012_5_en.pdf

Fresh Water and Seawater Properties, International Towing Tank Conference (ITTC), 2011, page 8.

FutureGen 2.0 Project, Final Environmental Impact Statement, U.S. Department of Energy, USA, October, 2013. http://energy.gov/sites/prod/files/2013/10/f4/EIS-0460-FEIS-Volume_II_Part_1-2013.pdf

Gao, M.S., Wang, S.H., Wang, X.M. & Guo, M.C., 2011. CFD Simulation of Flow in Random Packing Columns with Seawater Desulfurisation, Advanced Materials Research Vols. 347-353 (2012) pp 364-371, doi:10.4028/www.scientific.net/AMR.347-353.364.

Global CCS Institute 2012, the Global Status of CCS: 2012, Canberra, Australia. ISBN 978-0-9871863-1-7. http://decarboni.se/sites/default/files/publications/47936/global-status-ccs-2012.pdf

Gong, W.Y., Cai, Z.H. & Jiang, L.X., 2008. Enhancing the Performance of Differential Evolution Using Orthogonal Design Method, Applied Mathematics and Computation 206 (2008) 56–69, doi:10.1016/j.amc.2008.08.053.

Gorgon Carbon Dioxide Injection Project, Chevron Australia, Australia, 2015. http://www.chevronaustralia.com/docs/default-source/default-document-library/fact-sheet-gorgon-c02-injection-project.pdf?sfvrsn=8

Hessabi, M., 2009. An Overview of Lime Slaking and Factors that Affect the Process, Chemco Systems, L.P. http://chemcoequipment.com/Files/Admin/Publications/AN_OVERVIEW_OF_LIME_SLAKING.pdf .

HiMSEN Engine, IMO Tier II Program 2012, Marine & Offshore GenSets, Marine Propulsion System Stationary GenSets, Hyundai Energy & Machinery Heavy Industries CO. LTD.

Hjertager, L.K., Hjertager, B.H., & Solberg, T., 2002. CFD Modeling of Fast Chemical Reactions in Turbulent Liquid Flows, Computers & Chemical Engineering, Volume 26, Issues 4–5, 15 May 2002, Pages 507–515. doi:10.1016/S0098-1354(01)00799-2

Hong, Z.N., Liu, C.B., & Li, J.H., 2012. Parameter Optimisation for Machined Round Parts by Using Grey Relational Analysis, J. Luo (Ed.): Affective Computing and Intelligent Interaction, AISC 137, pp. 441–448.

Horvath, A., Jordan, C., Lukasser, M., Kuttner, C., Makaruk, A., & Harasek, M., 2009, CFD Simulation of Bubble Columns using the VOF Model: Comparison of commercial and Open Source Solvers with an Experiment, Chemical Engineering Transactions, Volume 18 (2009), DOI: 10.3303/CET0918098. http://www.aidic.it/cet/09/18/098.pdf .

Houghton, J.T., 2004. Global Warming: The Complete Briefing. Chapter 3, Greenhouse Gases, Cambridge University Press.

Information Reference Document, 2008. Prepared and adopted by EU Climate Change Expert Group 'EG Science', Final Version, Version 9.1, 9th July 2008,

IPCC, 2005: IPCC Special Report on Carbon Dioxide Capture and Storage. Prepared by Working Group III of the Intergovernmental Panel on Climate Change [Metz, B., O. Davidson, H. C. de Coninck, M. Loos, & L. A. Meyer (eds.)]. Cambridge University Press, Cambridge, United Kingdom and New York, NY, USA, 442 pp.

IPCC, 2007: Climate Change 2007: Mitigation. Contribution of Working Group III to the Fourth Assessment Report of the Inter-governmental Panel on Climate Change [B. Metz, O.R. Davidson, P.R. Bosch, R. Dave, L.A. Meyer (eds)], Cambridge University Press, Cambridge, United Kingdom and New York, NY, USA., 851 pp.

Jiyuan, T., Guan-Heng, Y., & Chaoqun, L., 2013. Chapter 6 - Practical Guidelines for CFD Simulation and Analysis, In Computational Fluid Dynamics (Second Edition), edited by Jiyuan TuGuan-Heng YeohChaoqun Liu, Butterworth-Heinemann, 2013, Pages 219-273, ISBN 9780080982434, http://dx.doi.org/10.1016/B978-0-08-098243-4.00006-8.

Joshuah K. S., David W. K. and Gregory V. L., 2008. Carbon Dioxide Capture from Atmospheric Air Using Sodium Hydroxide Spray, Environmental Science & Technology / Vol. 42, No. 8, 2728–2735, 2008.

Kim, S.J., Cho, Y.G., Oh, C.S., Kim, D.E., Moon M.B., & Han, H.N., 2009. Development of a Dual Phase Steel Using Orthogonal Design Method, Materials and Design 30 (2009) 1251–1257, doi:10.1016/j.matdes.2008.06.017.

Klemas, L., & Bonilla, J. A., 2000. Packed column: Design and Performance, Distillation, Academic Press, 2000.

Lin, C.C., & Chen, B.C., 2007. Carbon Dioxide Absorption into NaOH Solution in a Cross-flow Rotating Packed Bed, Journal of Industrial and Engineering Chemistry, Vol. 13, No. 7, 1083-1090.

Littman, F.E., & Gaspari, H.J., 1956. Causticisation of Carbonate Solutions, Industrial and Engineering Chemistry, Vol 48, No. 3, page 408-410.

Melzer, L.S., 2012. Carbon Dioxide Enhanced Oil Recovery (CO2 EOR): Factors Involved in Adding Carbon Capture, Utilisation and Storage (CCUS) to Enhanced Oil Recovery.

Mahmoudkhani, M., & Keith, D.W., 2009. Low-energy sodium hydroxide recovery for CO2 capture from atmospheric air—Thermodynamic analysis, Energy and Environmental System Group, Institute for Sustainable Energy, Environment, Economy, University of Calgary, Canada.

Maloney, J.O., 2008. Perry's Chemical Engineers' Handbook, 8th edition, DOI: 10.1036/0071511245.

MARPOL Annex VI, Chapter IV, MEPC, 2011.

Massey, B. S., & Ward-Smith, A. J., 2012. Mechanics of fluids. London; New York, NY, Spon Press.

MEPC 60/WP.6, Prevention of Air Pollution from Ships, Communication with IPCC on CO2 Conversion Factors, Marine Environment Protection Committee, IMO, 2010

Mohammad, I., & Mohammad, A.K., 2011. Investigation of Bubble Column Hydrodynamics Using CFD Simulation (2d and 3d) and Experimental Validation, Petroleum and Coal 53 (2) 146-158 (2011), http://www.vurup.sk/sites/default/files/downloads/pc_2_2001_irani_111.pdf

Pflug, I.J., & Angelini, P., Dewey, D.H., 1957. Fundamentals of Carbon Dioxide Absorption as They Apply to Controlled-atmosphere Storage, Department of Agricultural Engineering and Horticulture.

Project Guide of MAN Diesel Engine: MAN B&W: S70MC-C7, 4th Edition, 2009, branch of MAN Diesel SE, Germany.

Qiu, M., Yan J.F., Zhao, B.H., Chen, L., & Bai, Y.X., 2011. A Finite-Element Analysis of the Connecting Bolts of Slewing Bearings Based on the Orthogonal Method, Journal of Mechanical Science and Technology 26 (3) (2012) 883~887, DOI 10.1007/s12206-011-1203-4.

Ronald, A.F., 1971. The Design of Experiments, Hafner Publishing Company, New York, 1971.

Rogner, H.-H., Zhou, D., Bradley, R., Crabbé, P., Edenhofer, O., Hare, B. (Australia), Kuijpers, L., & Yamaguchi, M., 2007: Introduction. In Climate Change 2007: Mitigation. Contribution of Working Group III to the Fourth Assessment Report of the Intergovernmental Panel on Climate Change [B. Metz, O.R. Davidson, P.R. Bosch, R. Dave, L.A. Meyer (eds)], Cambridge University Press, Cambridge, United Kingdom and New York, NY, USA.

Safe Handling of Caustic Soda (Sodium Hydroxide), 2006. Japan Soda Industry Association.

Second IMO GHG Study 2009, International Maritime Organisation (IMO) London, UK, April 2009; Buhaug, Ø., Corbett, J.J., Endresen, Ø., Eyring, V., Faber, J., Hanayama, S., Lee, D.S., Lee, D., Lindstad, H., Markowska, A.Z., Mjelde, A., Nelissen, D., Nilsen, J., Pålsson, C., Winebrake, J.J., Wu, W., & Yoshida, K.

Significant Ships of 2011: HYUNDAI TRUST: 180,000dwt Cape sized bulk carrier from Sungdong, p48-49.

Shipping, World Trade and the Reduction of CO2 Emissions, United Nations Framework Convention on Climate Change (UNFCCC), International Chamber of Shipping (ICS), Representing the Global Shipping Industry, London, UK, 2014. http://www.ics-shipping.org/docs/default-source/resources/environmental-protection/shipping-world-trade-and-the-reduction-of-co2-emissions.pdf?sfvrsn=6 .

Souto, E.C.S., Damasceno, J.J.R., & Hori, C.E., 2008. Study of Operational Conditions for the Precipitated Calcium Carbonate Production, in: Materials Science Forum Vols. 591-593 (2008), pp 526-530.

Teleken, J.G., Werle, L.O., Marangoni, C., Quadri, M.B., & Machado, R.A.F., 2009. CFD Simulation of Multiphase Flow in a Sieve Tray of a Distillation Column, Brazilian Journal of Petroleum and Gas, vol 3, page 93-102, 2009. ISSN 1982-0593.

Third IMO GHG Study 2014, International Maritime Organisation, Suffolk, United Kingdom, April, 2014. http://www.imo.org/en/OurWork/Environment/PollutionPrevention/AirPollution/Documents/Third%20Greenhouse%20Gas%20Study/GHG3%20Executive%20Summary%20and%20Report.pdf

Wilson, R., Luckow, P., Biewald, B., Ackerman, F., & Hausman, E., 2012. 2012 Carbon Dioxide Price Forecast, Synapse, Energy Economics Inc..

Witkowski, A., & Majkut, M., 2012. The Impact of CO2 Compression Systems on the Compressor Power Required for a Pulverized Coal-fired Power Plant in Post-combustion Carbon Dioxide Sequestration, the Archive of Mechanical Engineering VOL. LIX, page 343-360.

World Resources Institute (WRI), 2002. The US Greenhouse Gas Reduction Targets, Thomas Damassa, Mengpin Ge, And Taryn Fransen: https://www.wri.org/sites/default/files/WRI14_Fact_Sheet_US_GHG_singles.pdf

World Resources Institute (WRI). CCS Guidelines: Guidelines for Carbon Dioxide Capture, Transport, and Storage. Washington, DC: WRI, 2008. ISBN 978-1-56973-701-9. http://pdf.wri.org/ccs_guidelines.pdf

Web reference

AceChemPack Tower Packing Co. Ltd, Packed Column Design: http://www.tower-packing.com/Dir_column_packing.htm

Alibaba.com: http://www.alibaba.com/product-gs/445114514/Caustic_Soda.html;http://www.alibaba.com/product-

tp/113123860/QUICK_LIME .html; http://www.alibaba.com/product-gs/594411302/light_calcium_CaCO3.html?s=p. 12/12/2013

B., Wischnewski. Peace Software: http://www.peacesoftware.de/einigewerte/co2_e.html . 12/11/2013

Global Climate Change, NASA: http://climate.nasa.gov/effects/

Global Trends in Carbon and Sulfur Emissions, 2011. http://stochastictrend.blogspot.co.uk/2011/03/global-trends-in-carbon-and-sulfur.html

International ocean freight rate statistics, China Commodity Marketplace (CCM), 2013, http://www.chinaccm.com/40/20131206/402204_1576181.shtml . 22/11/2013

NASA, 2016. The consequences of climate change: http://climate.nasa.gov/effects/

National Geographic, Greenhouse effect, http://environment.nationalgeographic.com/environment/global-warming/gw-overview-interactive/

Slaking and Causticising, Metso Fiber Karlstad AB, 2011: http://www.metso.com/pulpandpaper/MPwFiber.nsf/WebWID/WTB-101115-2256F-DE839?OpenDocument&mid=71967A486FAB2F29C22575B00048DEBB#.Ud0_7aXs5CA . 18/7/2013

The International Volcanic Health Hazard Network-Carbon Dioxide: http://www.ivhhn.org/index.php?option=com_content&view=article&id=84. 13/09/2016

The Physics Hypertextbook: http://physics.info/heat-latent/. 12/12/2013

Understanding CCS, What is CCS how does it work and why is it important, Global Carbon Capture and Storage Institute: http://www.globalccsinstitute.com/understanding-ccs/the-climate-change-challenge . 5/12/2012

PUBLICATIONS

International Journal

1. Zhou, P., & Wang, H., 2014. Carbon capture and storage— Solidification and storage of carbon dioxide captured on ships, Ocean Engineering 91 (2014) 172–180, http://dx.doi.org/10.1016/j.oceaneng.2014.09.006 .
2. Wang, H., Zhou, P.L., & Wang, Z.C., 2016. Experimental and Numerical Analysis on Controllable Factors of CO2 Absorption Efficiency of Carbon Solidification System, Journal of Ocean Engineering, Volume 113, Pages 133–143 (2016), http://dx.doi.org/10.1016/j.oceaneng.2015.12.036
3. Wang, H., & Zhou, P.L., 2016. Reviews on Current Carbon Emission Reduction Technologies and Projects and their Feasibilities on Ships, Journal of Marine Science and Application (submitted)

International Conference

1. Wang, H., & Zhou, P.L., 2013. Carbon capture and storage—solidification and storage of CO2 captured on ships, Developments in Maritime Transportation and Exploitation of Sea Resources, the 15th International Maritime Association of the Mediterranean Congress, A Coruna, Spain, October 14 to 17, 2013, ISBN 978-1-138-00124-4.
2. Zhou, P., & Wang, H., 2014. CFD Simulations of Absorption Reaction in Carbon Solidification Processes, 18th International Conference. Transport Means, October 14 to 16, 2014.
3. Zhou, P., & Wang, H., 2015. Analysis on Numerical Simulations of CO2 Absorption Process of Carbon Solidification System, the 6th International Conference on Experiments/Process/System Modelling/Simulation/ Optimisation, Athens, Greece, from July 8 to 11, 2015.

4. Zhou, P., & Wang, H., 2015. A Case Ship Study on Practical Design and Installation of Carbon Absorption and Solidification System, Technologies, Operations, Logistics And Policies Towards Meeting 2050 Emission Targets, International Conference On Shipping In Changing Climates, Glasgow, United Kingdom, November 24-26, 2015.
5. Wang, H., Zhou, P.L., & Wang, Z.C., 2016. Solidification and Storage of CO2 Captured on Ships - Feasibility Analysis through Experiment, Simulation and Case Studies, International Conference on Marine Technology 2016 Harbin (submitted)
6. Zhou, P., & Wang, H., 2016. Education programme and marine engineering research in the Department of Naval Architecture, Ocean and Marine Engineering, ICMPTE, 2016 Shanghai (submitted)

APPENDIX 1. FLOW CHART FOR EXPERIMENT PROCESSES

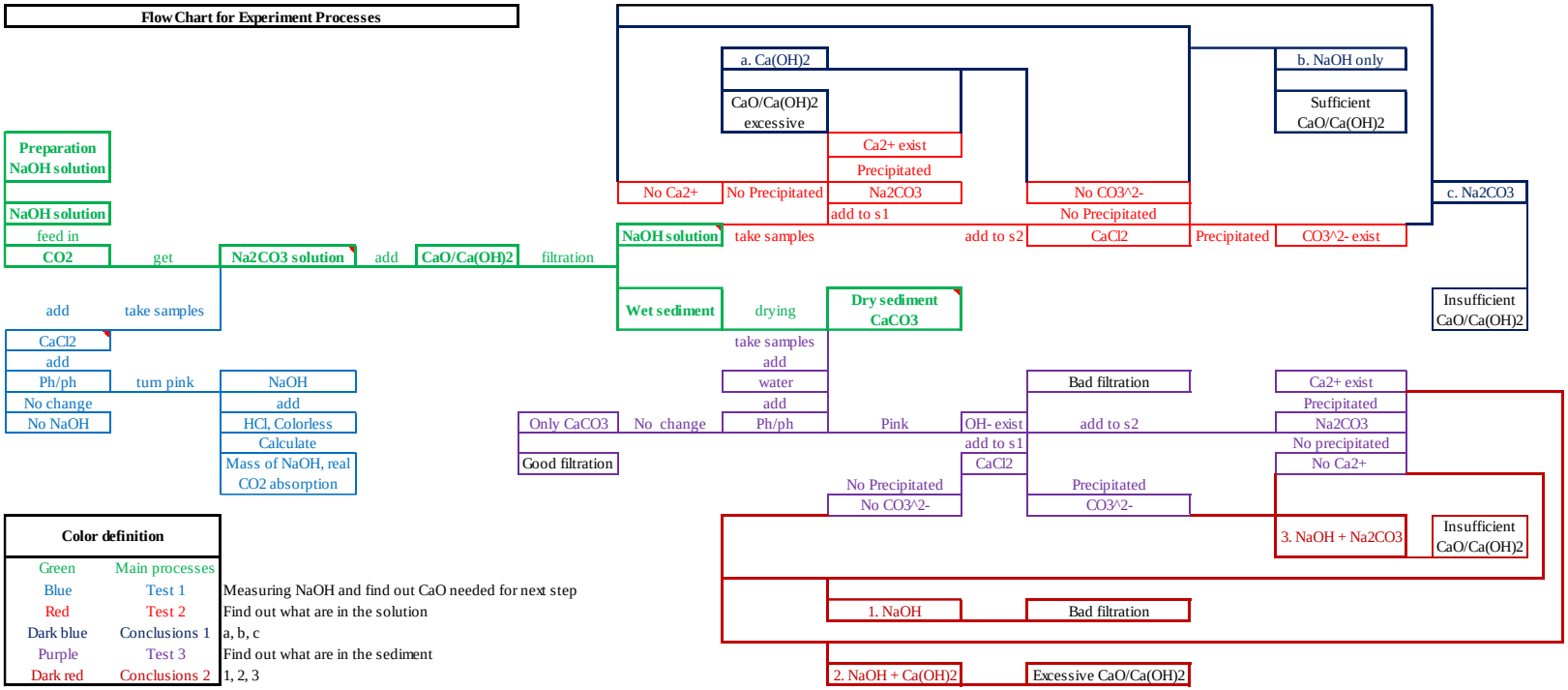

APP 1: Operations in laboratory experiment, including, absorption, filtration, and products testing

APPENDIX 2. EXPERIMENTAL RESULTS

Experiments Results Data																		
Processes	Items	CODE	10/06/2013	11/06/2013	12/06/2013	26/06/2013	27/06/2013	27/06/2013	28/06/2013	02/07/2013	03/07/2013	04/07/2013	04/07/2013	04/07/2013	05/07/2013	16/07/2013	17/07/2013	Units
	Containers		1L MC	1L MC	1L MC	1L MC	1L MC	1L MC	1L MC	1L B	2L MC	2L MC	1L MC	2L MC	1L MC	1L MC	1L MC	
CO_2 Absorption	Container+Diffuser+Pipe	A1	690.6	695.1	695	475	472.9	474.1	473.3	286.6	927	927.4	472.5	927.7	473.2	472.5	430	g
	A+NaOH Solution	A2	1644.7	1729.8	1536	1470.5	1471	1506.5	1500	1193	1967.7	2128.2	831.9	1562.1	1090.7	1405.6	1397.5	g
	NaOH Solution without Cylinder	B1	954.1	1034.7	841	995.5	998.1	1032.4	1026.7	906.4	1040.7	1200.8	359.4	634.4	617.5	933.1	967.5	g
	NaOH Concentration	r1	14%	14%	14%	14%	14%	14%	14%	14%	14%	14%	14%	14%	14%	14%	14%	99%
	NaOH Solute in Solution	B2	131.9536711	143.5108206	116.3204029	137.6896089	138.0492202	142.7933222	142.0049437	125.3660086	143.9413119	166.0850652	49.70933747	87.74514104	85.40766802	129.0589393	133.8168726	g
	CO_2 Need	B3	72.57451908	78.93095133	63.97622161	75.72928491	75.92707109	78.53632721	78.10271905	68.95130471	79.16772155	91.34678586	27.34013561	48.25982757	46.97421741	70.98241663	73.59927991	g
	Cylinder Weight Target	B4'	1717.274519	1808.730951	1599.976222	1546.229285	1558.927071	1585.036327	1578.102719	1261.951305	2046.867722	2219.546786	859.2401356	1610.359828	1137.674217	1476.582417	1471.09928	g
	A1+Na2CO3 solution when stop feeding	B4	1715	1805.1	1577.34	1590.5	1593.2	1581.9	1571.3	1252.8	2041	2205.5	852.9	1603	1135.1	1468.9	1464.3	g
	CO_2 Feed in	B5	70.3	75.3	41.34	75.72928491	49.7	75.4	71.3	59.8	73.3	77.3	21	40.9	44.4	63.3	66.8	g
	Room Temp.	T	20	24	23	25.5	22	23	22	21	21	23	25	25	24	24	26	°C
	Outlet Pressure of Regulator	P	1	1	1	1	1	1	1	1	1	1	1	1	1	1	1	Bar
	CO_2 Density	ρ	1.815	1.789	1.7955	1.77925	1.802	1.7955	1.802	1.8085	1.8085	1.7955	1.7825	1.7825	1.789	1.789	1.776	kg/m3
	CO_2 Used	B6	101.8215	101.95511	70.0245	89	90	101.9276855	93.88076297	112.1204541	98.17245499	96.957	30	64.37538032	63.48127782	83	86	g
	CO_2 Absorption Rate	r2	69%	74%	59%	85%	55%	74%	76%	53%	75%	80%	53.8%	64%	70%	76%	78%	
	Na_2CO_3 Solution without Cylinder	B7	1024.4	1110	882.34	1115.5	1120.3	1107.8	1098	966.2	1212	1278.1	482.765	763.8	661.9	996.4	1034.3	g
Filtration Preparation	Mass of Cooling Pool	C1	78.89	82	77.96	77.85	77.88	77.88	80.9	78.5	78.5	78.5	75.92	78.2	77.5	78.6	75.02	g
	C1+Na_2CO_3 Solution	C2	1099	1190.1	957.3	1071.7	1116.1	1184.4	1177	1043.4	1181	1207.7	452.6	751.5	736.4	1072.6	1063	g
	Na_2CO_3 without Pool	C3	1020.11	1108.1	879.34	993.85	1038.22	1106.52	1096.1	964.9	1102.5	1129.2	376.68	673.3	658.9	994	987.98	g
	Na_2CO_3 Rate	r3	100%	100%	100%	89%	93%	100%	100%	91%	91%	88%	78%	88%	100%	100%	96%	
	Maximum Na_2CO_3 from NaOH	C4	174.8386141	190.1518373	154.1245339	182.4387318	182.9152167	189.2011519	188.1565504	166.1099614	190.7222383	194.7945151	65.86487214	116.2623119	113.1651601	171.0030946	196.1651618	g
	Real Na_2CO_3 Get (Na_2CO_3 Solute in Pool)	C5	174.106422	189.8263522	153.6005028	162.5430154	169.5137341	188.9825407	187.8309608	151.8661187	173.491145	194.2097532	51.39142241	102.4867957	112.6522496	170.5912044	187.3801185	g
	Take a Sample of Na_2CO_3	D1'	48.84	41.9	35.9	39.13	31.22	25.83	31.312	37	29.2	31.72	40.4	49.8	42	37.3	30.65	g
	Test Tube	D1	13.99	13.9	14.1	13.76	13.76	13.62	13.735	13.7	13.63	13.73	13.76	13.73	13.78	13.72	13.75	g
	Na_2CO_3 Solute in Sample	D2	5.947994634	4.796622923	3.807959334	4.149234089	2.85075398	2.085345789	3.012047074	3.667199261	2.450119843	3.094078515	3.634563802	5.49041842	4.824778394	4.046821528	3.205251121	g
	$Ca(OH)_2$ Need	D3	4.152373612	3.348585814	2.658386705	2.896635119	1.990149005	1.455807438	2.102749844	2.560120239	1.710461023	2.160017077	2.537336994	3.832933614	3.36824152	2.825139557	2.237628141	g
Filtration	Filtered Solution	E1	498.4	467.1	299.2	296.9	480.5	281.6	310.9	311.3	311.1	297.7	300.4	401.9	295.3	312.9	319	g
	Flask	E2	353.2	310.1	241.6	241.6	240.4	241	240.3	240.7	240.3	240.4	240.46	352.3	240.8	240	240.5	g
	Expected NaOH in Sample	E6	4.489052554	3.620092772	2.873931573	3.131497426	2.151512438	1.573845878	2.273243075	2.767697555	1.849147052	2.335153596	2.74306702	4.143712015	3.641342184	3.054204927	2.41905745	g
	NaOH Fraction in Sample	r4	3%	2%	5%	6%	2%	4%	3%	4%	3%	4%	5%	8%	7%	4%	3%	g
	Take a Sample of Filtered Solution	E3	34.54	34.7	35.7	24.65	29.2	24	24.1	24.1	24.36	23.84	23.71	23.73	24.77	24.24	30.05	g
	Test Tube	E4	13.99	14.3	13.9	13.76	13.78	13.62	13.8	13.8	13.7	13.82	13.71	13.73	13.76	13.76	13.77	g
	Volume	E5	20	20	20	10	15	10	10	10	10	10	8	8.75	11	10.5	16.25	mL
	ICP Na+ Fraction	E7	16876.66667	9946	27993.93939	34720	8484	19190	14050	21050	14050	20670	29460	50150	34570	21100	14520	mg/L
	Real NaOH in Sample	E8	0.587014493	0.345947826	0.97370224	0.603826087	0.221321739	0.33373913	0.244347826	0.366086957	0.244347826	0.359478261	0.409878261	0.763152174	0.66133913	0.385304348	0.410347826	g
	NaOH Recycle Rate	r5	92%	74%	90%	98%	64%	83%	74%	91%	88%	88%	90%	91%	90%	88%	82%	
	Dried Sediment With Funnels, Papers and Trays	F1	80	112.4	82.7	43.82	84.2	42.69	44.93	43.81	44.89	45.52	46.9	46.6	47.6	44.42	45.206	g
	No of Funnels		2	3	2	1	2	1	1	1	1	1	1	1	1	1	1	
	No. of Papers		2	2	2	1	2	1	1	1	1	1	1	1	1	1	1	
	No. of Trays		1	1	2	1	2	1	1	1	1	1	1	1	1	1	1	
	Mass of Funnel		32.75	32.75	32.75	32.75	32.75	32.75	33.25	32.75	34.6	34.77	34.78	32.81	34.46	33.25	34.78	g
	Mass of Paper		1.07	0.65	0.65	1.16	1.16	1.16	1.18	1.16	1.15	1.35	1.14	1.14	1.165	1.164	1.15	g
	Mass of Trays		6.39	6.4	6.39	6.39	6.39	6.45	6.7	6.4	6.35	6.78	6.45	6.44	6.44	6.43	6.42	g
	Dried Sediment	F2	5.97	5.38	3.12	3.52	3.6	2.33	3.8	3.5	2.79	2.62	4.53	6.21	5.535	3.576	2.856	g
	$CaCO_3$ Expected	F3	5.611315692	4.525115965	3.592414466	3.914371782	2.689390547	1.967307348	2.841553843	3.459621944	2.311433814	2.918941995	3.428833776	5.179640019	4.55167773	3.817756159	3.023821812	g
Sediment Contents Test	Take a Sample of Sediment	F4	14	13.96	13.92	0.06	13.82	13.857	13.81	13.77	13.79	13.9949	13.76	13.93	13.905	13.755	13.963	g
	Volume	F5	20	31	21	20	15	20	16	10	10	26	17	17	21	20	20.2	mL
	ICP Na+ Fraction	F6	185.7	150.8	383.9	19.8	88.5	70.8	65.3	98.9	34.1	52	101	189	136	37.5	28.2	mg/L
	ICP Ca2+ Fraction	F7	330.7	775.1	550.5	773.2	854.4	710.4	574.8	945.1	1174	420.6	500.3	837	969.8	917.35	1066	mg/L
	Real NaOH in Sample	F8	0.192805043	0.364498899	0.014020696	0.040403478	0.083113043	0.05362503	0.069047652	0.1204	0.027576522	0.041765542	0.270539478	0.49572	0.18960072	0.038869565	0.025038736	g
	Real $Ca(OH)_2$ in Sample	F9	0.365241615	1.992930661	0.021386925	1.678359467	0.8535456	0.572369944	1.29307008	1.2239045	1.0099335	0.359354937	1.425539811	2.335283807	1.438211728	1.01147011	1.006839075	g
	$CaCO_3$ in Sediment	F10	5.411953342	3.022570441	3.084592379	1.801237055	2.663341357	1.704005026	2.437882268	2.1556955	1.752489978	2.218879521	2.833920711	3.378996193	3.907187552	2.525660325	1.824122189	g
	$CaCO_3$ Production Rate	r6	96%	67%	86%	46%	99%	87%	86%	62%	76%	76%	83%	65%	86%	66%	60%	

APP 2: Experiment intermedium and final results

APPENDIX 3. SOLUTION PROPERTIES UNDER DIFFERENT CONCENTRATIONS

Properties of sodium hydroxide **NaOH**

	State 1			State 2		
	ϑ_1 =	25	°	ϑ_2 =	25	°
	c_1 =	15	Weight%	c_2 =	20	Weight%
	c_1 =	173.9	g/l	c_2 =	242.8	g/l
	c_1 =	4.347	mol/l	c_2 =	6.07	mol/l
Saturation pressure	$p_{S,1}$ =	2620	Pa	$p_{S,2}$ =	2300	Pa
Properties:						
Density	ρ_1 =	1156	kg/m3	ρ_2 =	1211	kg/m3
Specific heat capacity	cp_1 =	3707	J/(kg·K	cp_2 =	3629	J/(kg·K
Thermal conductivity	λ_1 =	.644	W/(m·K	λ_2 =	.6505	W/(m·K
Dynamic viscosity	η_1 =	2.5	mPa·	η_2 =	3.938	mPa·
Kinematic viscosity	ν_1 =	0.000002	m2/s	ν_2 =	0.000003	m2/s
Prandtl number	Pr_1 =	14.39	-	Pr_2 =	21.97	-
Coeff.o.thermal expansion	β_1 =	.0004637	1/K	β_2 =	.0004955	1/K
Thermal diffusivity	a_1 =	1.503E-7	m2/s	a_2 =	1.48E-07	m2/s

M = 39.997 g/mol

Validity range: 20 < ϑ < 100 0 wt-% < c < 50 wt-%

1 NaOH | 1 Temperature 1 25 °C

APP 3: 15% and 20% NaOH solutions properties

Properties of sodium hydroxide **NaOH**

	State 1		State 2	
	ϑ_1 = 25	°	ϑ_2 = 25	°
	c_1 = 25	Weight%	c_2 = 30	Weight%
	c_1 = 317	g/l	c_2 = 396.3	g/l
	c_1 = 7.926	mol/l	c_2 = 9.908	mol/l
Saturation pressure	$p_{S,1}$ = 1900	Pa	$p_{S,2}$ = 1450	Pa
Properties:				
Density	ρ_1 = 1265	kg/m3	ρ_2 = 1318	kg/m3
Specific heat capacity	cp_1 = 3582	J/(kg·K	cp_2 = 3536	J/(kg·K
Thermal conductivity	λ_1 = .6535	W/(m·K	λ_2 = .6555	W/(m·K
Dynamic viscosity	η_1 = 6.377	mPa·	η_2 = 10.33	mPa·
Kinematic viscosity	ν_1 = 0.000005	m2/s	ν_2 = 0.000008	m2/s
Prandtl number	Pr_1 = 34.96	-	Pr_2 = 55.71	-
Coeff.o.thermal expansion	β_1 = .0004744	1/K	β_2 = .0004553	1/K
Thermal diffusivity	a_1 = 1.442E-7	m2/s	a_2 = 1.407E-7	m2/s

M = 39.997 g/mol

Validity range: 20 < ϑ < 100 0 wt-% < c < 50 wt-%

1 NaOH | 1 Temperature 1 25 °C

APP 4: 25% and 30% NaOH solutions properties

Properties of sodium hydroxide **NaOH**

	State 1		State 2	
	ϑ_1 = 25	°	ϑ_2 = 25	°
	c_1 = 18.76	Weight%	c_2 = 18.82	Weight%
	c_1 = 225.7	g/l	c_2 = 226.5	g/l
	c_1 = 5.643	mol/l	c_2 = 5.663	mol/l
Saturation pressure	$p_{S,1}$ = 2376	Pa	$p_{S,2}$ = 2372	Pa
Properties:				
Density	ρ_1 = 1197	kg/m3	ρ_2 = 1198	kg/m3
Specific heat capacity	cp_1 = 3648	J/(kg·K	cp_2 = 3647	J/(kg·K
Thermal conductivity	λ_1 = .6489	W/(m·K	λ_2 = .649	W/(m·K
Dynamic viscosity	η_1 = 3.519	mPa·	η_2 = 3.538	mPa·
Kinematic viscosity	ν_1 = 0.000003	m2/s	ν_2 = 0.000003	m2/s
Prandtl number	Pr_1 = 19.78	-	Pr_2 = 19.88	-
Coeff.o.thermal expansion	β_1 = .0004878	1/K	β_2 = .0004882	1/K
Thermal diffusivity	a_1 = 1.486E-7	m2/s	a_2 = 1.485E-7	m2/s

M = 39.997 g/mol

Validity range: 20 < ϑ < 100 0 wt-% < c < 50 wt-%

1 NaOH | 1 Temperature 1 25 °C

APP 5: 18.82% NaOH solutions properties

This page is left for blank